AD NUMBER

AD849738

LIMITATION CHANGES

TO:

Approved for public release; distribution is unlimited.

FROM:

Distribution authorized to U.S. Gov't. agencies and their contractors; Critical Technology; JAN 1969. Other requests shall be referred to Air Force Materials Laboratory, Metals and Ceramics Division, MAMS, Wright-Patterson AFB, OH 45433. This document contains export-controlled technical data.

AUTHORITY

afml ltr, 7 dec 1972

AFML-TR-68-63
Volume II

PHASE COMPATIBILITY STUDIES ON NICKEL-CHROMIUM-SILICON-CARBON BASE ALLOYS

Volume II. The Chromium-Silicon-Carbon and Nickel-Silicon-Carbon Systems

C. E. Brukl

Aerojet-General Corporation

TECHNICAL REPORT AFML-TR-68-63 VOLUME II

JANUARY 1969

AIR FORCE MATERIALS LABORATORY
AIR FORCE SYSTEMS COMMAND
WRIGHT-PATTERSON AIR FORCE BASE, OHIO

NOTICES

When Government drawings, specifications, or other data are used for any purpose other than in connection with a definitely related Government procurement operation, the United States Government thereby incurs no responsibility nor any obligation, whatsoever, and the fact that the Government may have formulated, furnished, or in any way supplied the said drawings, specifications, or other data, is not to be regarded by implication or otherwise as in any manner licensing the holder of any other person or corporation, or conveying any rights or permission to manufacture, use, or sell any patented invention that may in any way be related thereto. This document is subject to special export controls, and each transmittal to foreign governments or foreign nationals may be made only with prior approval of the Metals and Ceramics Division (MAMS), Air Force Materials Laboratory, Wright-Patterson AFB, Ohio 45433. The distribution of this report is limited because the protection of technology relating to critical materials is restricted by the Export Control Act.

Copies of this report should not be returned unless return is required by security consideration, contractual obligations, or notice on a specific document.

PHASE COMPATIBILITY STUDIES ON NICKEL-CHROMIUM-SILICON-CARBON BASE ALLOYS

Volume II. The Chromium-Silicon-Carbon and Nickel-Silicon-Carbon Systems

C. E. Brukl

FOREWORD

The work described in this technical report was carried out at the Materials Research Laboratory, Aerojet-General Corporation, Sacramento, California. The principal investigator for this project is Dr. E. Rudy, under USAF Contract F33615-67-C-1286. This contract was initiated under Project No. 7353, "Characterization of Solid Phase and Interphase Phenomena In Crystalline Substances", 735306, "Fundamentals of Composites", during the period April 1967 through November 1968. Funds for this project are supplied to the AF Materials Laboratory by the Office of Aerospace Research. The work was administered by the Advanced Metallurgical Studies Branch of the Metals and Ceramics Division, Air Force Materials Laboratory, Wright-Patterson AFB, Ohio under the direction of Capt. W. J. Meyerer.

The author wishes to thank Dr. E. Rudy for his advice and help during the course of this investigation, He further wishes to thank P. Booker, J. Pomodoro, R. Taylor, J. R. Hoffman, E. Spencer, and R. Cobb for their valuable help in the various aspects of the experimental investigation. A portion of the experimental work was done by Dr. Y. A. Chang.

Chemical analyses of the prepared alloys were carried out under the supervision of Mr. W. E. Trahan, Metals and Plastics Testing Laboratory, Aerojet-General Corporation.

Finally, the author wishes to acknowledge the following persons for their help in the preparation of this manuscript: Mr. R. Cristoni and Miss B. Barnes for the preparation of the drawings and the final typing.

The manuscript of this report was released by the author in November 1968 for publication as a Technical Report.

The other report issued under USAF Contract F33615-67-C-1286 was Volume I: The Cr-Si System.

This technical report has been reviewed and is approved.

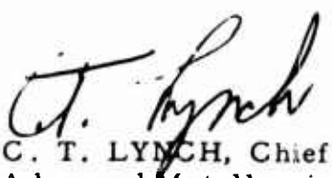

C. T. LYNCH, Chief
Advanced Metallurgical Studies Branch
Metals and Ceramics Division
AF Materials Laboratory

ABSTRACT

The high temperature phase equilibria of the Cr-Si-C and Ni-Si-C ternary systems have been investigated by means of melting point, differential thermal analytical, X-ray, and metallographic techniques. Cursory investigations were also made in the Ni-Si and Ni-C binary systems.

In the Cr-Si-C system, a ternary $D8_8$-type phase, which forms two-phase equilibria with most of the other respective binary phases is present. The high temperature phase equilibria include eleven, four-phase reactions of which seven are ternary eutectics. Seven pseudo-binary eutectics also occur.

The Ni-Si-C system has simple solid-state equilibria governed by the occurring binary phases. The high temperature phase equilibria of this system include seven four-phase reactions of which five are ternary eutectics and four pseudo-binary eutectics.

Isothermal sections into the melting range as well as three-dimensional space models are presented for both ternary systems.

TABLE OF CONTENTS

TABLE OF CONTENTS (Cont'd)

TABLE OF CONTENTS (Cont'd)

LIST OF ILLUSTRATIONS

LIST OF ILLUSTRATIONS (Cont'd)

LIST OF ILLUSTRATIONS (Cont'd)

LIST OF ILLUSTRATIONS (Cont'd)

LIST OF ILLUSTRATIONS (Cont'd)

LIST OF ILLUSTRATIONS (Cont'd)

LIST OF TABLES

LIST OF TABLES (Cont'd)

BLANK PAGE

I. INTRODUCTION AND SUMMARY

A. INTRODUCTION

Recent interest in developing high-strength, reinforced composite bodies has focused our attention on the high modulus and light weight refractory materials such as silicon carbide as potential fiber candidate materials. Since these materials are inherently brittle, it is essential to use binder materials having low moduli. The success of such composite bodies depends on the mechanical and chemical compatibilities between the fiber and binder materials. Apart from strength considerations, mechanical compatibility also implies the match of coefficients of thermal expansion; if this match is absent, cracks will develop in a temperature gradient field or under thermal cycling conditions and eventually cause failure of the composite.

Before one considers the mechanical compatibility of the fiber and binder materials, it is absolutely essential to study the chemical stability of these materials under environments of interest. Chemical compatibility implies no interaction between the two materials at any temperature of interest and hence offers a truly stable two-phase composite system.

Although in principle, one can predict the compatibility of any pair of materials such as the reinforcing and binder components in a composite system from the principles of chemical thermodynamics, the lack of pertinent data often makes these calculations impossible. Therefore, the best way to obtain compatibility data is to systematically investigate the phase equilibria of the materials of interest from solid state through the melting ranges. Such investigations not only yield precise and defined compatibility data, but will also lead to a complete mapping of the relative stabilities of alloy phases and thus greatly increases the predictive potential of thermodynamic approaches. Moreover, since the appearance of a liquid interface is associated with the

immediate failure of composite body, phase diagram data provide a direct criterion for the upper temperature service limit for the particular composite system.

The objective of the present work was to investigate the stabilities of silicon carbide, a potential fiber candidate material, in the presence of chromium and nickel, since both metals are inherently ductile and may be used as binder materials for developing a metal-silicon carbide composite. Accordingly, cursory phase equilibria investigations in the binary Ni-Si and Ni-C systems with detailed investigations in the Cr-Si, Cr-Si-C, and Ni-Si-C systems have been made.

The detailed descriptions of the investigations in chromium-silicon system have been previously submitted as a separate entity and are not included in this report.

B. SUMMARY

The high temperature phase equilibria of both the chromium-silicon-carbon and nickel-silicon-carbon systems have been investigated by means of X-ray, D.T.A., metallographic, and melting point techniques. In addition, cursory investigations confirming the melting temperatures in the binary systems Ni-C and Ni-Si were performed. A minor correction to the already submitted report on the chromium-silicon system is included.

1. Binary Systems

a. The Chromium-Silicon System

Additional D.T.A. experiments with the Cr_5Si_3 compound have shown that there is no allotropic α - β transformation in this phase at 1505°C. The corrected constitution diagram is presented in Figure 15.

b. The Nickel-Silicon System

Results of the experiments to determine the melting points of several alloys in this system showed excellent agreement with the solidus temperatures published in the literature (Table XX). The crystal structures of most of the phases occurring as well as most of the isothermal reactions in the nickel-silicon system were verified.

The high temperature form of Ni_2Si was not able to be retained by quenching, but strong metallographic evidence was observed to indicate its presence. The investigations were not able to confirm the reported, but in some cases also denied, presence of the low temperature allotropic modifications of the Ni_3Si phase. No indication of a reported high temperature allotrope of $NiSi_2$ was observed.

c. The Nickel-Carbon System

Melting point experiments to check the eutectic temperature of the nickel-graphite eutectic yielded a value of 1322°C; this is in excellent accord with the literature value of 1318°C.

2. Ternary Systems

a. The Chromium-Silicon-Carbon System

The primary feature of this system is the occurrence of a congruently melting, ternary $D8_8$-type phase in a small homogeneous range about the composition $Cr_{55}Si_{36.5}C_{8.5}$. This ternary phase is in equilibrium with most of the binary phases at 1100°C as shown in Figure 1.

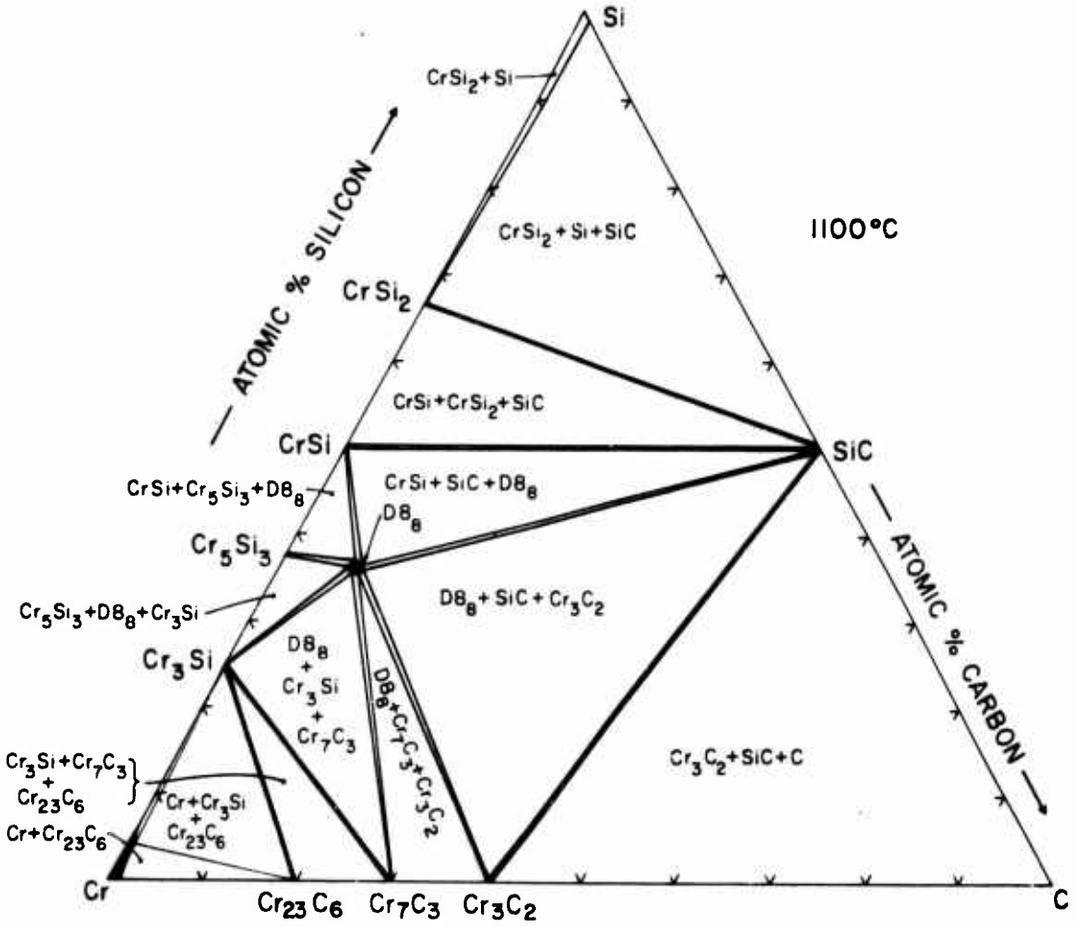

Figure 1. Cr-Si-C: Phase Equilibria at 1100°C.

At 1100°C and also at higher temperatures, there is no mutual solubility in either the carbides or silicides.

The following pseudo-binary eutectic reaction isotherms (limiting tie lines) were observed:

(1) The Cr_3C_2-$D8_8$ Pair

The reaction proceeding at 1530°C is represented by:

$$\text{Liquid} \underset{T \geq 1530°C}{\overset{T \leq 1530°C}{\rightleftharpoons}} Cr_3C_2 + D8_8 \text{ Phase}$$

The equilibrium compositions of the partaking phases are given in Table I.

Table I. Approximate Equilibrium Compositions of Phases Partaking of the Pseudo-Binary Eutectic Reaction L $\longrightarrow Cr_3C_2 + D8_8$ at 1530°C.

Phase	Concentration, At.%		
	Cr	Si	C
Liquid	57	19	24
Cr_3C_2	~60	<< 1	~40
$D8_8$	55	36.5	8.5

(2) The Cr_7C_3-$D8_8$ Pair

The pseudo-binary eutectic reaction at 1540°C is given by:

$$\text{Liquid} \underset{T \geq 1540°C}{\overset{T \leq 1540°C}{\rightleftharpoons}} Cr_7C_3 + D8_8 \text{ Phase}$$

The equilibrium compositions of the partaking phases are presented in Table II.

Table II. Approximate Equilibrium Compositions of Phases Partaking of the Pseudo-Binary Eutectic Reaction L $\longrightarrow Cr_7C_3 + D8_8$ at 1540°C.

Phase	Composition, At.%		
	Cr	Si	C
Liquid	71	11.5	17.5
Cr_3Si	~75	~25	<<1
Cr_7C_3	~70	<<1	~30

(3) The Cr_7C_3-Cr_3Si Pair

The pseudo-binary eutectic reaction at 1528 °C along this section is represented by:

$$\text{Liquid} \underset{T \geq 1528°C}{\overset{T \leq 1528°C}{\rightleftharpoons}} Cr_7C_3 + Cr_3Si$$

The equilibrium concentrations of the reacting phases are given in Table III.

Table III. Approximate Equilibrium Compositions of Phases Partaking of the Pseudo-Binary Eutectic Reaction, $L \longrightarrow Cr_7C_3 + Cr_3Si$ at 1528 °C.

Phase	Composition, At.%		
	Cr	Si	C
Liquid	71	11.5	17.5
Cr_3Si	~75	~25	<<1
Cr_7C_3	~70	<<1	~30

(4) The Cr_3Si-$D8_8$ Pair

This pseudo-binary eutectic reaction takes place at 1515 °C:

$$\text{Liquid} \underset{T \geq 1515°C}{\overset{T \leq 1515°C}{\rightleftharpoons}} Cr_3Si + D8_8 \text{ Phase}$$

The compositions of the reacting components are given in Table IV.

Table IV. Approximate Equilibrium Compositions of the Phases Partaking of the Pseudo-Binary Eutectic Reaction, L $\longrightarrow$ Cr_3Si at 1515°C.

Phase	Composition, At.%		
	Cr	Si	C
Liquid	66.5	29.5	4
Cr_3Si	~75	~25	<<1
$D8_8$ Phase	55	36.5	8.5

(5) The $D8_8$-SiC Pair

The pseudo-binary eutectic reaction proceeding at 1635°C along this section is given by:

$$\text{Liquid} \underset{T \geq 1635°C}{\overset{T \leq 1635°C}{\rightleftharpoons}} D8_8 \text{ Phase} + SiC$$

The equilibrium concentrations of the reacting phases are given in Table V.

Table V. Approximate Compositions of Phases Partaking of the Pseudo-Binary-Eutectic Reaction at 1635°C.

Phase	Composition, At.%		
	Cr	Si	C
Liquid	51	37.5	11.5
$D8_8$ Phase	55	36.5	8.5
SiC	0	50	50

(6) The Cr_5Si_3-$D8_8$ Pair

The pseudo-binary eutectic reaction at about 1510°C along this section is described by:

$$\text{Liquid} \underset{T \geq 1510^\circ C}{\overset{T \leq 1510^\circ C}{\rightleftharpoons}} Cr_5Si_3 + D8_8 \text{ Phase}$$

Table VI contains the equilibrium concentrations of the reacting phases.

Table VI. Approximate Equilibrium Concentrations of Phases Partaking of the Pseudo-Binary Eutectic Reaction, $L \longrightarrow Cr_5Si_3 + D8_8$ at 1510°C.

Phase	Compositions, At.%		
	Cr	Si	C
Liquid	58.5	37	4.5
Cr_5Si_3	62.5	37.5	<<1
$D8_8$	55	36.5	8.5

(7) The following four-phase reactions occur in the ternary Cr-Si-C system:

(a) The ternary eutectic in the metal-rich portion of the ternary system is described by a Class I reaction at 1460°C:

$$\text{Liquid} \underset{T \geq 1460^\circ C}{\overset{T \leq 1460^\circ C}{\rightleftharpoons}} Cr_3Si + Cr_{ss} + Cr_{23}C_6$$

The equilibrium concentrations of the phases partaking of this four-phase reaction are given in Table VII.

Table VII. Equilibrium Concentrations of Phases Partaking of the Four-Phase Ternary Eutectic Reaction at 1460°C.

Phase	Composition, At.%		
	Cr	Si	C
Liquid	79	10	11
Cr_3Si	~75	~25	<<1
$Cr_{23}C_6$	79.3	1	20.7
Cr	~94.5	~5	~0.5

(b) A Class II reaction at 1510°C in the metal-rich portion of the system is represented by:

$$\text{Liquid} + Cr_7C_3 \underset{T \geq 1510°C}{\overset{T \leq 1510°C}{\rightleftharpoons}} Cr_{23}C_6 + Cr_3Si$$

The equilibrium concentrations of the phases partaking of this Class II, four-phase reaction at 1510°C are given in Table VIII.

Table VIII. Approximate Equilibrium Concentrations of Phases Partaking of a Class II, Four-Phase Reaction, $L + Cr_7C_3 \longrightarrow Cr_{23}C_6 + Cr_3Si$ at 1510°C.

Phase	Composition, At.%		
	Cr	Si	C
Liquid	77.5	11.5	11
Cr_7C_3	~70	<<1	~30
$Cr_{23}C_6$	~79.3	<<1	~20.7
Cr_3Si	~75	~25	<<1

(c) The ternary eutectic among Cr_7C_3, Cr_3Si, and the $D8_8$ phase is represented by a Class I, four-phase reaction at about 1510°C:

$$\text{Liquid} \underset{T \geq 1510°C}{\overset{T \leq 1510°C}{\rightleftharpoons}} Cr_3Si + Cr_7C_3 + D8_8 \text{ Phase}$$

The equilibrium concentrations of these phases are given in Table IX.

Table IX. Approximate Equilibrium Concentrations of the Phases Partaking of the Four-Phase Ternary Eutectic Reaction at 1510°C.

Phase	Composition, At.%		
	Cr	Si	C
Liquid	70	11.5	18.5
Cr_3Si	~75	~25	<<1
C	~70	<<1	~30
[illegible]	55	36.5	8.5

(d) Another ternary eutectic among Cr_7C_3, $D8_8$ phase, and Cr_3C_2 is also described by a Class I, four-phase reaction at 1520°C.

$$\text{Liquid} \underset{T \geq 1520°C}{\overset{T \leq 1520°C}{\rightleftharpoons}} Cr_3C_2 + Cr_7C_3 + D8_8 \text{ Phase}$$

The equilibrium concentrations of the phases partaking of this Class I reaction are given in Table X.

Table X. Approximate Equilibrium Concentrations of the Phases Partaking of the Class I, Four-Phase Ternary Eutectic Reaction at 1520°C.

Phase	Composition, At.%		
	Cr	Si	C
Liquid	60	18.5	21.5
Cr_7C_3	70	<<1	30
Cr_3C_2	60	<<1	40
$D8_8$ Phase	55	36.5	8.5

(e) A Class II, four-phase reaction at 1410°C occurs in the vicinity of the CrSi phase:

$$\text{Liquid}+Cr_5Si_3 \underset{T\geq 1410°C}{\overset{T\leq 1410°C}{\rightleftharpoons}} CrSi+D8_8 \text{ Phase}$$

The equilibrium concentrations of these reacting phases are given in Table XI.

Table XI. Approximate Equilibrium Concentrations of the Phases Partaking of the Class I, Four-Phase Ternary Eutectic Reaction $L+Cr_5Si_3 \longrightarrow CrSi+D8_8$ at 1410°C.

Phase	Composition, At.%		
	Cr	Si	C
Liquid	~50	~46.5	~3.5
Cr_5Si_3	62.5	37.5	<<1
CrSi	50	50	<<1
$D8_8$	55	36.5	8.5

(f) Another Class II, four-phase reaction occurs in the vicinity of the CrSi phase as liquid replaces the solid-state equilibrium at 1400°C:

$$\text{Liquid}+D8_8 \text{ Phase} \underset{T\geq 1400°C}{\overset{T\leq 1400°C}{\rightleftharpoons}} CrSi+SiC$$

The equilibrium concentrations of the phases partaking of this Class II reaction are given in Table XII:

Table XII. Approximate Equilibrium Concentrations of the Phase Partaking of the Class II, Four-Phase Ternary Eutectic Reaction $L+D8_8$ Phase $\longrightarrow$ CrSi+SiC at 1400°C.

Phase	Composition, At.%		
	Cr	Si	C
Liquid	46	51.5	2.5
$D8_3$ Phase	55	36.5	8.5
CrSi	50	50	<<1
SiC	0	50	50

(8) The following four-phase reactions and one pseudo-binary eutectic reaction were not detected, but are presumed to occur in the ternary Chromium-Silicon-Carbon system:

	Type	Approximate Temperature °C	Remarks
Liquid+C $\longrightarrow$ Cr_3C_2+SiC	Class II	1790	Disappearance of SiC-Cr_3C_2 Solid-State Equilibrium
Liquid $\longrightarrow$ $D8_8$+Cr_3C_2+SiC	Class I	1630	Ternary Eutectic
Liquid $\longrightarrow$ Cr_5Si_3+$D8_8$+Cr_3Si	Class I	1505	Ternary Eutectic
Liquid $\longrightarrow$ $CrSi_2$+CrSi+SiC	Class I	1380	Ternary Eutectic
Liquid $\longrightarrow$ $CrSi_2$+Si+SiC	Class I	1300	Ternary Eutectic
Liquid $\longrightarrow$ $CrSi_2$+SiC	Limiting Tie Line	1480	Pseudo-Binary Eutectic

(9) Using all experimental results and isothermal sections (Figures 54 through 66), a three-dimensional space model of the chromium-silicon-carbon system was established (Figure 2).

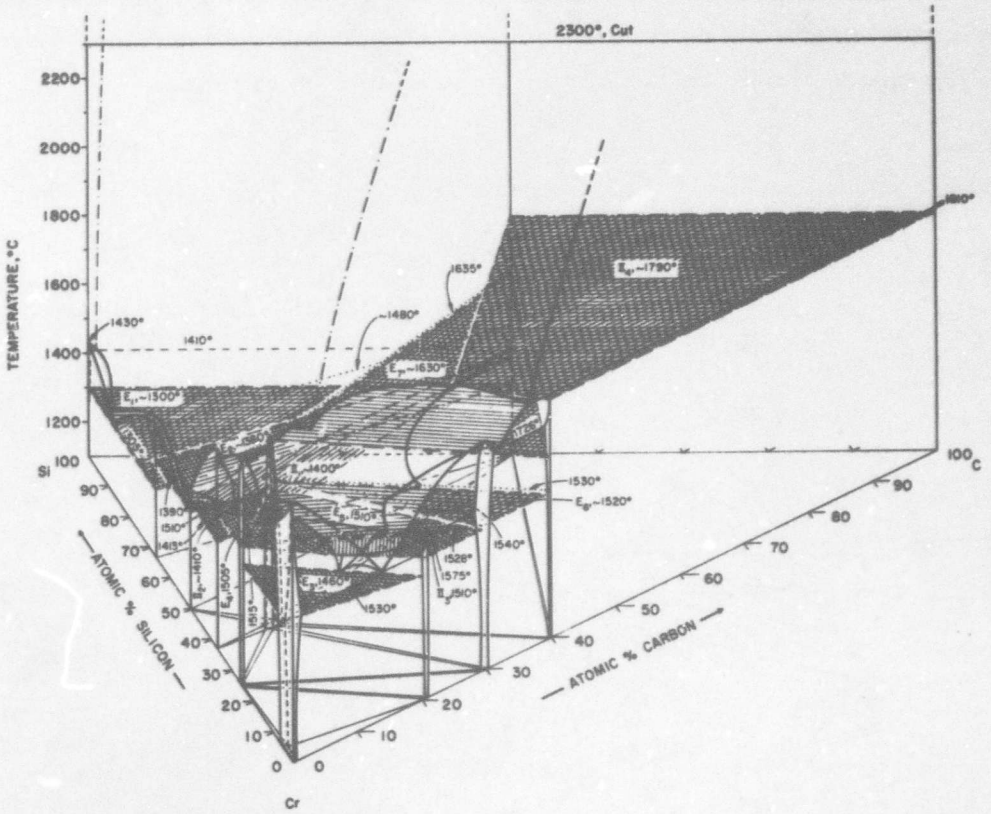

Figure 2. The Chromium-Silicon-Carbon System.

(10) Qualitative Kinetic Studies

Special D.T.A. experiments performed with mixtures of chromium metal and silicon carbide powders indicated that at all temperatures above about 1330°C, a strong exothermic reaction occurs between these materials as more stable ternary equilibrium are formed.

b. The Nickel-Silicon-Carbon System

There are no ternary phases formed in this three-component system; the solid-state phase equilibria is governed solely by the respective binary phases. Figure 3 portrays the solid-state equilibrium at 800°C where it is seen that the binary nickel silicides form narrow two-phase fields with either silicon carbide or graphite.

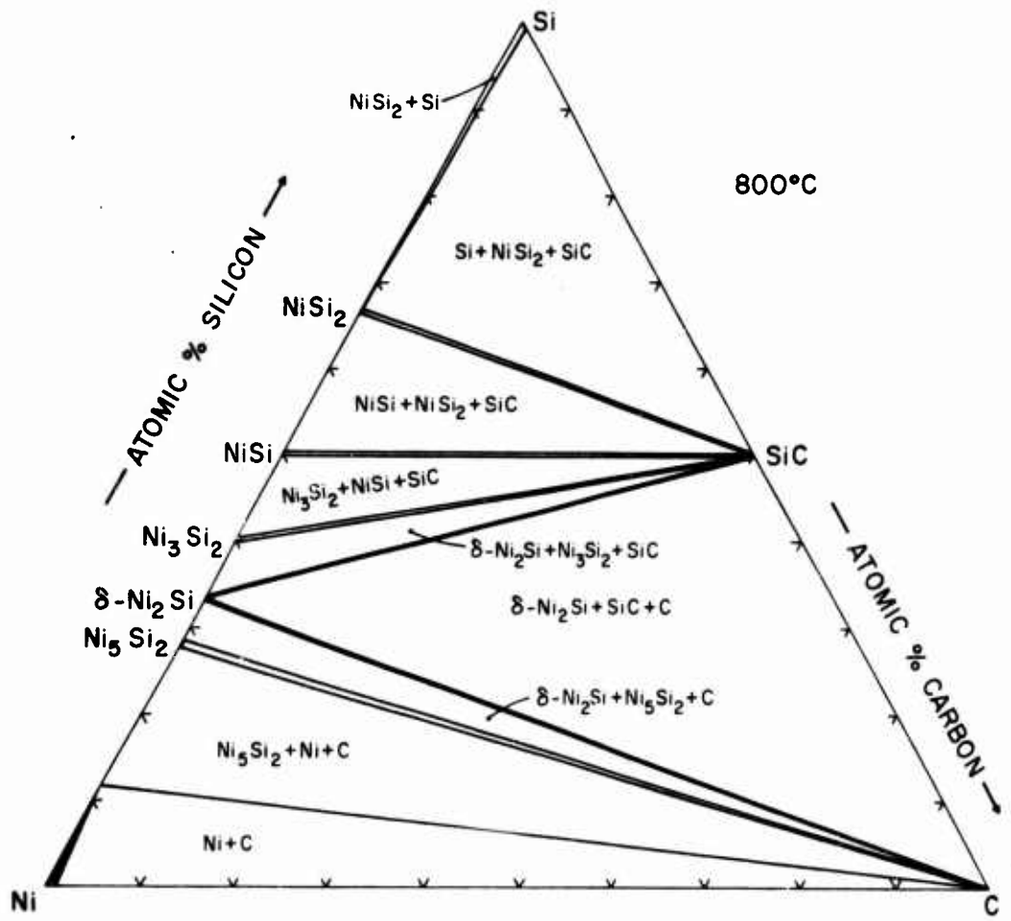

Figure 3. Ni-Si-C: Phase Equilibria at 800°C.

At 800°C and also at higher temperatures, neither silicon carbide nor any of the binary nickel silicides show any mutual solubility among themselves or with graphite.

The following pseudo-binary eutectic reaction isotherms (limiting tie lines) were observed:

(1) The Ni_5Si_2-C Pair

The reaction proceeding at 1270°C is represented by:

$$\text{Liquid} \underset{T \geq 1270°C}{\overset{T \leq 1270°C}{\rightleftharpoons}} Ni_5Si_2 + C$$

The equilibrium concentrations of the partaking phases are given in Table XIII.

Table XIII. Approximate Equilibrium Concentrations of the Phases Partaking of the Pseudo-Binary Eutectic Reaction $L \longrightarrow Ni_5Si_2 + C$ at 1270°C.

Phase	Composition, At.%		
	Ni	Si	C
Liquid	~71	28	~1
Ni_5Si_2	~71.4	~28.6	<<1
C	0	0	100

(2) The θ-Ni_2Si-C Pair

The pseudo-binary eutectic reaction at 1282°C is given by:

$$\text{Liquid} \underset{T \geq 1282^\circ C}{\overset{T \leq 1282^\circ C}{\rightleftharpoons}} \theta\text{-}Ni_2Si + C$$

The equilibrium concentrations of the partaking phases are given in Table XIV.

Table XIV. Approximate Equilibrium Concentrations of the Phases Partaking of the Pseudo-Binary Eutectic Reaction $L \longrightarrow \theta\text{-}Ni_2Si + C$ at 1282°C.

Phase	Composition, At.%		
	Ni	Si	C
Liquid	~65.5	~32	<<2.5
θ-Ni_2Si	~67.7	~33.3	<<1
C	0	0	100

(3) The following four-phase reactions were observed in the ternary Ni-Si-C system:

(a) A ternary eutectic in the metal-rich portion of the ternary system is described by a Class I reaction at 1145°C:

$$\text{Liquid} \underset{T \geq 1145^\circ C}{\overset{T \leq 1145^\circ C}{\rightleftharpoons}} Ni_{ss} + C + Ni_3Si$$

The equilibrium concentrations of the phases partaking of this four-phase reaction are given in Table XV.

Table XV. Equilibrium Concentrations of the Phases Partaking of the Four-Phase Ternary Eutectic Reaction at 1145°C.
$L \longrightarrow Ni_{ss} + C + Ni_3Si$

Phase	Composition, At.%		
	Ni	Si	C
Liquid	78	19	3
Ni_{ss}	~82.2	~17.5	~0.3
C	0	0	100
Ni_3Si	~75	~25	<<1

(b) Another four-phase reaction in the metal-rich portion of the ternary Ni-Si-C system is described by a Class II, four-phase reaction at about 1160°C:

$$\text{Liquid} + Ni_5Si_2 \underset{T \geq 1160°C}{\overset{T \leq 1160°C}{\rightleftharpoons}} Ni_3Si + C$$

The equilibrium concentrations of the phases partaking of this four-phase reaction are given in Table XVI.

Table XVI. Equilibrium Concentrations of Phases Partaking of the Class II, Four-Phase Reaction $L + Ni_5Si_2 \longrightarrow Ni_3Si + C$ at ~1160°C.

Phase	Composition, At.%		
	Ni	Si	C
Liquid	76.5	~21	~2.5
Ni_5Si_2	~71.4	~28.6	<<1
Ni_3Si	~75	~25	<<1
C	0	0	100

(c) A Class II, four-phase reaction at about 993°C in the region near $NiSi_2$ is described by:

$$\text{Liquid} + \text{Si} \underset{T \geq \sim 993^\circ C}{\overset{T \leq \sim 993^\circ C}{\rightleftharpoons}} NiSi_2 + SiC$$

The equilibrium concentrations of the phases partaking of this four-phase reaction at about 993°C are given in Table XVII.

Table XVII. Equilibrium Concentrations of the Phases Partaking of the Four-Phase Reaction, Liquid + Si $\longrightarrow$ $NiSi_2$ + SiC at About 993°C.

Phase	Composition, At.%		
	Ni	Si	C
Liquid	~49.5	~50	~0.5
$NiSi_2$	~33.3	~66.7	<<1
Si	0	99	~1
	0	50	50

(4) The following four-phase and pseudo-binary reactions were not detected, but are presumed to occur in the ternary Nickel-Silicon-Carbon system:

Reaction	Type	Approximate Temperature °C	Remarks
Liquid $\longrightarrow Ni_5Si_2 + \theta\text{-}Ni_2Si + C$	Class I	1260	Ternary Eutectic
Liquid $\longrightarrow \theta\text{-}Ni_2Si + SiC + C$	Class I	1280	Ternary Eutectic
Liquid $\longrightarrow NiSi + \theta\text{-}Ni_2Si + SiC$	Class I	964	Ternary Eutectic
Liquid $\longrightarrow NiSi_2 + NiSi + SiC$	Class I	966	Ternary Eutectic
Liquid $\longrightarrow NiSi + SiC$	Limiting Tie Line	992	Pseudo-Binary Eutectic
Liquid $\longrightarrow \theta\text{-}Ni_2Si + SiC$	Limiting Tie Line	1300	Pseudo-Binary Eutectic

(5) Using all experimental results and isothermal sections (Figures 92 through 102), a three-dimensional space model of the Nickel-Silicon-Carbon system was established (Figure 4).

(6) Qualitative Kinetic Studies

Special D.T.A. experiments performed with mixtures of nickel metal and silicon carbide powders indicated that at all temperatures above about 1000°C, a strong exothermic reaction occurs between these materials as more stable nickel silicide-graphite, ternary equilibria are formed.

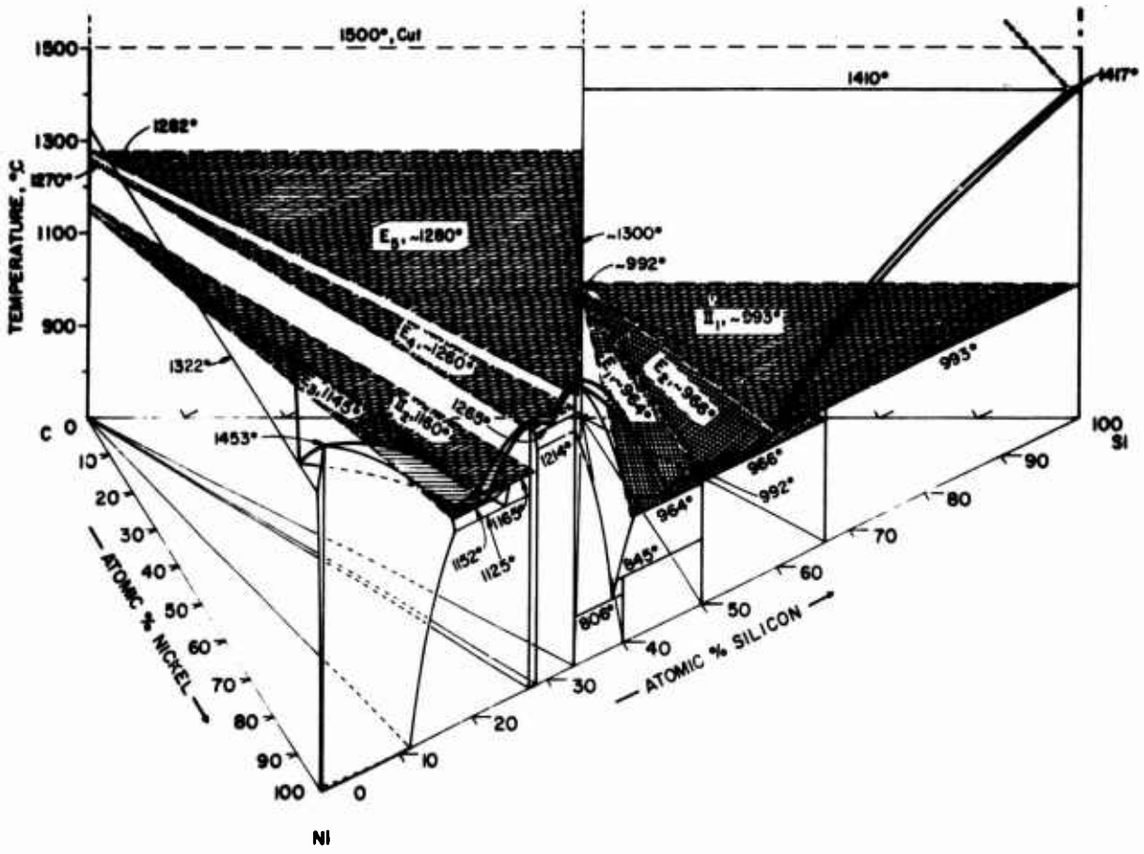

Figure 4. The Nickel-Silicon-Carbon System.

II. LITERATURE REVIEW

A. BINARY SYSTEMS

1. The Chromium-Silicon System

The final report on the chromium-silicon system, a part of this overall program, has been previously submitted as a separate entity; the detailed literature review presented therein need not be repeated here.

2. The Nickel-Silicon System

The earliest investigations in this system go back as far as 1906; for detailed information regarding this early work, the reader is referred to the compilation in M. Hansen's Constitution of Binary Alloys[1].

The first complete investigation of the constitution of this system in more recent times was by Iwase and Okamoto[2] in 1936. These authors found six intermediate compounds: Ni_5Si_2, Ni_2Si, NiSi, Ni_3Si, Ni_3Si_2, and $NiSi_2$; the first three melt congruently and while Ni_3Si and $NiSi_2$ decompose peritecticly, and Ni_3Si_2 forms in a peritectoid reaction. These authors also report an allotropic transformation in the $NiSi_2$ compound at 981°C. A. Osawa and M. Okamoto[3] performed X-ray analyses on the Ni-Si intermediate compounds and determined the crystal structures of the following compounds: β_1-Ni_3Si, Ni_5Si_2, δ-Ni_2Si, θ-Ni_2Si, Ni_3Si_2, NiSi, and two forms of $NiSi_2$. In addition, they found three allotropic modifications of Ni_3Si. K. Ruttewit and G. Masing[4] investigated the nickel-rich portion of the nickel silicon system and confirmed the results of Iwase and Okamoto[2] and some of the results of Osawa and Okamoto[3]. They could not, however, confirm the θ-δ-Ni_2Si transformation temperature from Iwase and Okamoto, nor were they able to confirm the transformation temperatures of the allotropic modifications of Ni_3Si. They reported instead a eutectoid decomposition of the Ni_3Si phase at 1126°C.

Schubert and Pfisterer[5][6] ascertained that the crystal structure of $NiSi_2$ is of the C-1 (CaF_2) type; this contradicted the earlier findings of Osawa and Okamoto[3]. They further stated that Ni_2Si had the NiAs (B8)-type structure. In 1951-3 K. Toman[7][9] determined the crystal structures of NiSi, δ-Ni_2Si, and θ-Ni_2Si; NiSi is orthorhombic and related to NiAs; δ-Ni_2Si was also found to be orthorhombic, while θ-Ni_2Si was hexagonal. The lattice parameters of θ-Ni_2Si differed only slightly from those reported by Osawa and Okamoto[3]. Work by A. Wittmann, K. Burger, and H. Nowotny[10] has refuted the reported structure by B. Boren[11] and confirmed the studies of K. Toman[7] by stating that the compound NiSi has an orthorhombic (B-31) structure. According to Gunvor Pilstrom[8], Ni_3Si_2 is orthorhombic in contrast to the reports of Owawa and Okamoto[3]; in addition, Pilstrom reports a trigonal unit cell for Ni_5Si_2 although Osawa and Okamoto[3] reported an orthohexagonal cell. G. Saini[18] later confirmed the crystal structure of Ni_5Si_2 as reported by Pilstrom[8].

Several publications have appeared describing studies on the solubility of silicon in nickel[12, 13, 14, 15, 16, 17, 19]; at room temperature the solubility is about 10 At% silicon, while at 900° and 1150°C the solubilities are reported to be 12.7 and 17.6 At.% silicon respectively. The solubility of nickel in silicon is reported to be very small[5, 11].

Table XVIII shows the intermediate phases occurring in the Nickel-Silicon system with their crystal structures and lattice parameters. Figure 5 depicts the composite phase diagram as drawn by M. Hansen[1].

Table XVIII. Nickel-Silicon Intermediate Phases and Crystal Structures.

Phase	Crystal Structure	Lattice Parameter	Literature
β_1-Ni_3Si	Cubic (Cu_3Au Type)	a = 3.507Å	16
β_2-Ni_3Si	Unknown	---	15
β_3-Ni_3Si	Unknown	---	15
Ni_5Si_2	Hexagonal (trigonal symmetry)	a = 6.670Å c = 12.267-12.332Å	8, 18
θ-Ni_2Si	Hexagonal	a = 3.805, c = 4.890Å	9, 3
δ-Ni_2Si	Orthorhombic	a = 7.06, b = 4.99, c = 3.73Å	9
Ni_3Si_2	Orthorhombic	a = 12.229, b = 10.805, c = 6.924Å	7
NiSi	Orthorhombic (Deformed NiAs Type)	a = 5.62, b = 5.18, c = 3.34Å	7
$NiSi_2$	Cubic (CaF_2 Type)	a = 5.406Å	5, 6

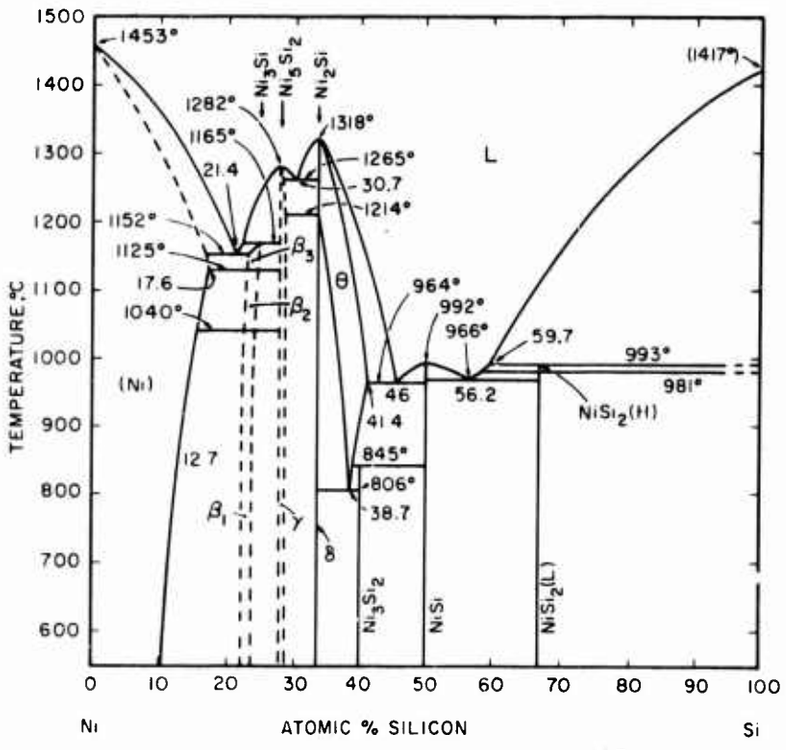

Figure 5. Ni-Si: Composite Constitution Diagram[1].

3. The Chromium-Carbon System

Extensive investigations on the constitution of the Chromium-Carbon system were done by A. Westgren et al[20], E. Friemann, and F. Scurwald[21], K. Hatsuta[22], and D. Bloom and N. Grant[23]. These authors established the constitution diagram and showed that only three compounds $Cr_{23}C_6$, Cr_7C_3, and Cr_3C_2 exist in this sytem. The crystal structures of these three compounds were firmly established by a long list of investigators[24-31]. $Cr_{23}C_6$[20-23, 27, 30, 31], formerly identified as Cr_4C, crystallizes in a complex face centered cubic type[24] while Cr_7C_3 has a hexagonal structure[28] with a trigonal unit cell; Cr_3C_2 crystallizes in an orthorhombic type structure[29]. Table XIX shows the Chromium-Carbon intermediate phases and their crystal structures.

Table XIX. Chromium-Carbon Intermediate Phases and Their Crystal Structures.

Phase	Crystal Structure	Lattice Parameter	Literature
$Cr_{23}C_6$	Cubic ($D8_4$ Type)	a = 10.659Å	24
Cr_7C_3	Hexagonal (trigonal)	a = 14.01, c = 4.532Å	28
Cr_3C_2	Orthorhombic ($D5_{10}$ Type)	a = 5.53, b = 2.827, c = 11.48Å	29

Recent, unpublished investigations in this laboratory by E. Rudy[32] who employed melting point, metallographic and X-ray techniques have led to a revision of the Chromium-Carbon system where the major change is the disclosure that Cr_7C_3 melts congruently and not peritecticly as previously reported. Figure 6 shows a reproduction of this phase diagram.

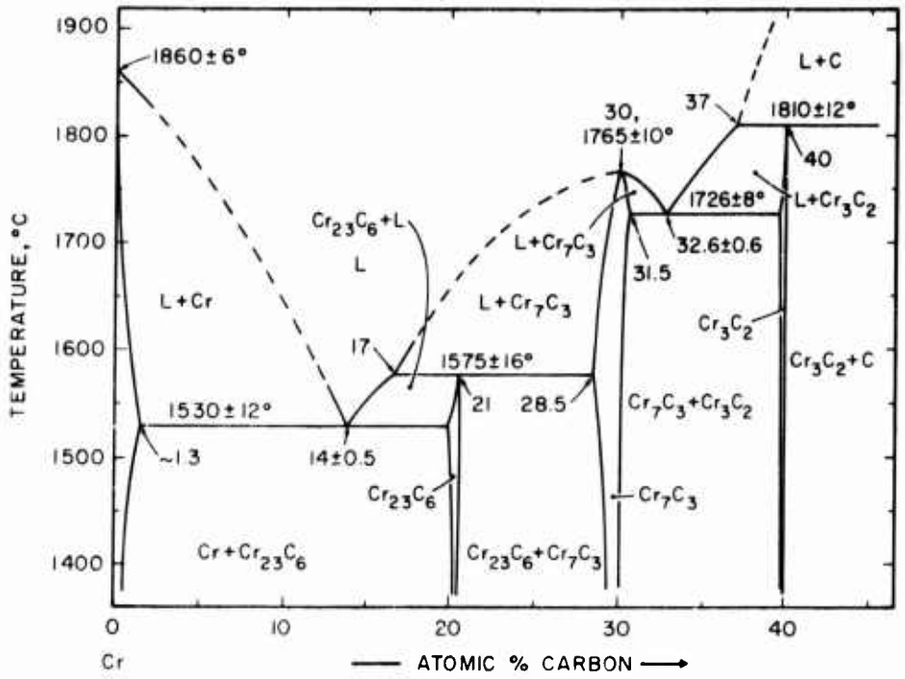

Figure 6. The Chromium-Carbon System[32].

4. The Nickel-Carbon System

The nickel-carbon system has been the object of many investigations, primarily in regard to the presence, absence, and stability of a carbide, Ni_3C. The solidus and liquidus temperatures have been determined by several investigators[33-41]. Figure 7 shows a composite partial diagram drawn by M. Hansen[42]. This phase diagram does not show the results of many conflicting reports[39, 40, 43, 44, 45, 52] concerning the presence of an apparently metastable[46] carbide, Ni_3C. There are reports that this Ni_3C phase is only obtained in very rapidly quenched, superheated melts; there are also many reports that the Ni_3C phase is only stable below about 400°C. Several authors[46, 47, 48] have also reported that a Ni_3C has a close packed hexagonal structure with lattice parameters of a = 2.628 and c = 4.306Å[51]. There is a recent publication describing a Ni_3C with a rhombohedral structure[51].

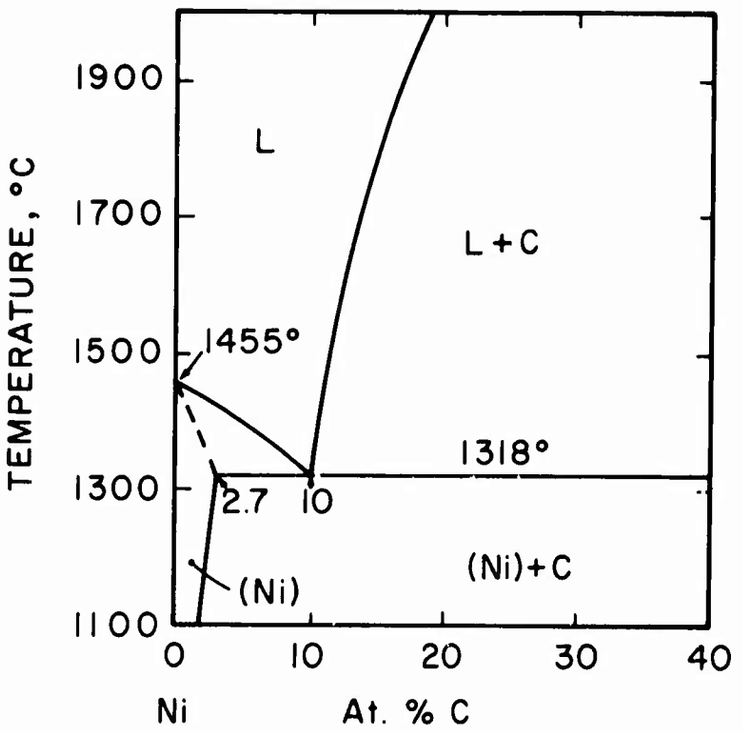

Figure 7. The Nickel-Carbon System[42].

The solubility of carbon in nickel has also been investigated numerous times[33-35, 37, 38, 49, 50]. The majority of the data is in very good agreement; the solubility is about 3 At.% carbon at 1318°, 2 At.% at 1200°C, and 1.1 At% at 1000°C.

The nickel-graphite eutectic, which is located very close to 10 At.% graphite has been reported to melt at 1314°C (Fe contaminated[36]), 1312°C[37], 1313°C[38], and 1326°C[39].

5. The Silicon-Carbon System

In spite of the fact that silicon monocarbide is the basis of many commercial abrasive items by virtue of its high hardness, as well as being used in many high temperature applications, the constitution diagram of the silicon carbon-system has never been completely established.

Many different, but closely related, crystal polymorphs of SiC, (apparently the only intermediate compound found in this system) have been observed, isolated, and their crystal structures determined[53]. The so-called α-forms have either hexagonal or rhombohedral symmetry, and the various polymorphs are based on different atom stacking sequences[54].

A lengthy listing of the many works is given in Constitution of Binary Alloys[53]. A face-centered cubic form, the β-SiC (B3-type), a low temperature modification with a lattice parameter of 4.349Å has also been observed[54].

H. Nowotny and co-workers[55] performed exploratory investigations in the silicon-carbon system using X-ray, chemical, and thermal analyses. On the basis of these experiments, two possible phase diagrams for the silicon-carbon systems were developed; one possibility is a version containing a peritectic-similar reaction involving liquid silicon (with carbon in solution), solid SiC, and vapor. The other version proposes a eutectic-similar decomposition of liquid silicon (with carbon in solution) into solid SiC and vapor. Due to the small temperature difference between the melting point of pure silicon and silicon-carbon alloys lying between Si and SiC, it was not possible to determine whether a eutectic or peritectic reaction is present at lower temperatures. Both proposed diagrams display the decomposition of SiC into graphite and vapor at about 2700°C. The decomposition temperature of SiC has also been independently reported by O. Ruff[56].

Recently, R. Scarce and G. Slack[57] as well as R. Dolloff[58] have investigated the silicon-carbon system and have concluded that SiC decomposes peritecticly into liquid Si and graphite. There is, however, a vast discrepancy in the reported peritectic decomposition temperatures. Scarce[57] reports 2830°C while Dolloff[58] reports 2540°C; the latter author further reports

that silicon and SiC form a eutectic at .75 At.% C and 1402°C. In a new study on the ternary Silicon-Carbon-Nitrogen system, E. Gugel, P. Ettmayer, and A. Schmidt[59] have presented a modified, composite phase diagram of Silicon-Carbon system based primarily on the work of H. Nowotny and co-workers[55], but including newer results by Brokhin and Funke[60] as well as by Knippenberg[61]. This picture is reproduced in Figure 8.

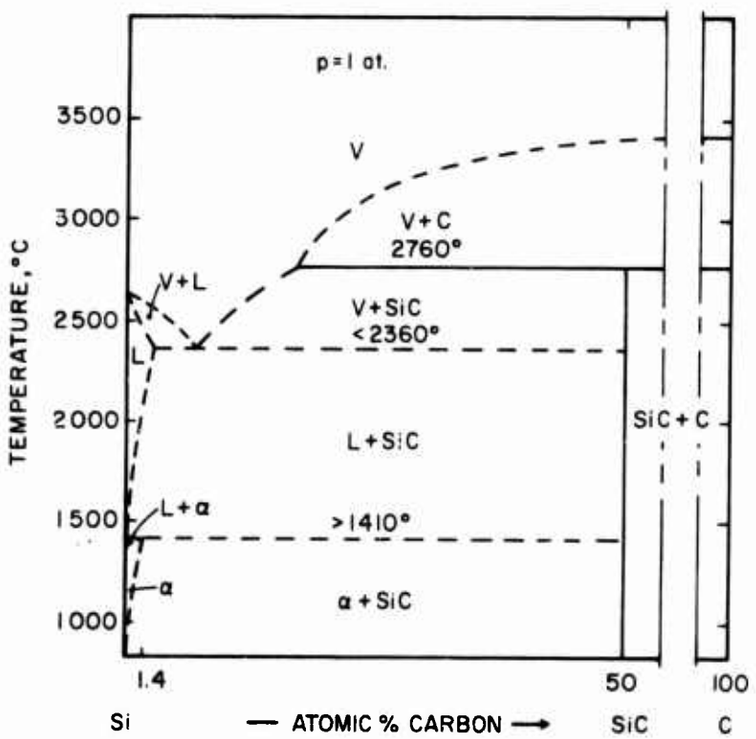

Figure 8. The Silicon-Carbon System[59].

It seems quite apparent that the exact constitution of the Silicon-Carbon-diagram—excluding the many crystallographic modifications of SiC—is still not definitely known.

B. TERNARY SYSTEMS

1. The Chromium-Silicon-Carbon System

In 1955, E. Parthe, H. Schachner, and H. Nowotny[62] reported a ternary phase, $Cr_{5-x}Si_{3-y}C_{x+y}$ with the $D8_8$-type structure in the Chromium-Silicon-Carbon system. The lattice parameters of this hexagonal phase were: $a = 6.97_9$ and $c = 4.71_6$kX.

L. B. Griffiths and A. I. Mlavsky[63] reported that they had grown single crystals of α-SiC from a chromium solution and indicated that the pseudo-binary system Cr-SiC forms a simple eutectic whose temperature is ~1600°C.

2. The Nickel-Silicon-Carbon System

No mention was found in the available literature of any investigations concerning this ternary system.

BLANK PAGE

III. EXPERIMENTAL PROCEDURES

A. STARTING MATERIALS

The starting materials for all parts of these investigations were either the elemental powders and/or pre-prepared silicides.

The chromium powder was supplied by the Shieldalloy Corporation from the Stark Company in Berlin. The chromium powder was sized between 74 and 44 micrometers and had the following vendor's analysis (in ppm): Fe - 200, Mg - 1000, and 0 - 250. An "in-house" analysis by the Aerojet Chemicals and Plastics Division yielded a value of 480 ppm in oxygen content. A Debye-Scherrer powder photograph of this material yielded only the cubic A-2 type structure pattern with a lattice parameter of $a = 2.88_5 \text{Å}$.

The silicon powder, which was purchased from Var-Lac-Oid Chemical Company, Elizabeth, New Jersey had a particle size of less than 44 micrometers. The vendor's analysis of impurities (in ppm) was: Al <1, Ca <1, Co <30, Cr <1, Cu <1, Fe <100, Mn <1, O- <30, Ti <1, and all others <10. Only the diamond type structure pattern was seen on X-ray powder photograph of this material; the lattice parameter was $a = 5.429_7 \text{Å}$.

The nickel powder was also supplied by Var-Lac-Oid of Elizabeth, New Jersey. This powder was sized smaller than 74 micrometers and had the following impurities as listed by the vendor (in ppm): C-80, Co-600, Cu-60, Fe-100, and S-150. An X-ray powder photograph of this material showed only the face centered cubic pattern of nickel; the lattice parameter was $a = 3.52_4 \text{Å}$.

The graphite powder used was supplied by the National Carbon Company and had the following typical impurities (in ppm): S-110, Si-46, Ca-44, Fe-40, Al-8, Ti-4, Mg-2, V-trace, and ash 800 max. Ninety-nine percent of this graphite had a particle size

smaller than 44 micrometers. Highly overexposed X-ray films of the graphite powder showed no traces of any impurities.

The pre-prepared materials were $CrSi_2$, Ni_2Si, and SiC. Since the exothermic reaction resulting from the union of chromium and silicon is relatively mild, weighed powders were mixed in proportion to give the disilicide. A small amount of camphor in ether was added to serve as a binder in cold pressing bricketts. The bricketts were placed under a vacuum of 30 inches of mercury at a temperature of 110°C for 12 hours to remove the camphor. The compacts were subsequently reacted in a molybdenum muffle furnace at 1200°C under hydrogen; an additional sintering under these same conditions lasted four hours. The reacted compacts were crushed in an agate mortar and sieved to a size smaller than 74 micrometers. A Debye-Scherrer powder photograph of this material showed an overwhelming majority of the hexagonal C-40 pattern of $CrSi_2$ with trace amounts of Si and CrSi; the lattice parameters of the $CrSi_2$ phase were $a = 4.42_4$ and $c = 6.36_5$Å. A silicon analysis taken on this preparation gave a value of 52.18 Wt.% (66.9 At.%) silicon.

The preparation of the silicon carbide master alloy followed the steps outlined above for the preparation of the discilicide, but it was sintered at 1350°C for 1 hour. An X-ray film of this silicon carbide showed only the pattern of the cubic β-SiC; the lattice parameter was 4.35_8Å; a carbon analysis showed 47.4 At.% carbon present in the SiC.

The preparation of the nickel silicide initially presented problems which were ultimately overcome by careful observance of the reaction process in the furnace. In the three attempts to prepare a sizeable quantity of a starting nickel silicide, the initial steps followed in mixing, pressing, and camphor-evaporation were the same as those used with $CrSi_2$ and SiC. Due to the relatively high reaction temperatures of nickel-silicon mixtures in relation to the rather low melting points in the nickel-silicon binary system (~750-800° vs. 964°C), coupled with

the rather large exothermic heat of reaction; the first two attempts at preparing $NiSi_2$ failed when the nickel-silicon mixture melted completely, segregating the low melting eutectics and reacting with the container in the hydrogen muffle furnace at approximately 800°C.

A preparation of Ni_2Si was ultimately achieved by reacting small, well mixed batches of nickel and silicon powders at this concentration by immediately moving the pressed brickett to a cold part of the hydrogen muffle furnace at the onset of the exothermic reaction; in this manner, melting was held to a minimum. The Ni_2Si prepared was ground and sieved in the same way as the $CrSi_2$ and SiC. A silicon analysis yielded a total silicon amount of 19.87 Wt.% or 34.2 At.%. The Debye-Scherrer powder photograph of this material showed primarily the pattern of the low temperature form (δ) of Ni_2Si with trace amount of Ni_3Si_2. The lattice parameters of the δ-Ni_2Si, having an orthorhombic structure were $a = 7.05_1$, $b = 5.00_1$, and $c = 3.72_7$ Å.

B. ALLOY PREPARATION AND HEAT TREATMENTS

Initial melting point samples in the binary Nickel-Silicon system were made by cold pressing the elemental powders; although the samples were heat treated at 825°C prior to the melting point runs, homogenization had not occurred, and the melting point measurements were masked by the very rapid increase in temperature caused by the strong exothermic reaction of compound formation. These samples, as well as those in the ternary were successfully prepared and run in the melting point furnace by using the prepared Ni_2Si as a starting compound. The melting point samples, both binary and ternary, using the starting powders $CrSi_2$, SiC, and Ni_2Si respectively, were made by hot pressing in graphite dies. The excess graphite and adhering carbide layer were carefully removed by grinding, and after the center portion of the sample was reduced, a black body hole of 1 mm in diameter and at least 3 mm in depth was drilled. Figure 9 shows one of these melting point samples.

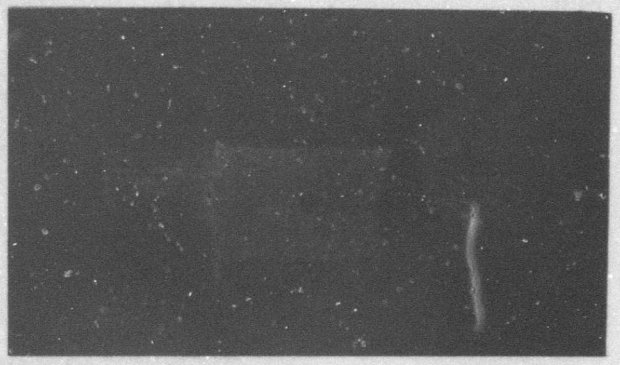

Figure 9. Typical Pirani Melting Point Sample. X210

In the nickel-silicon-carbon system, after the first group of melting point samples were made using Ni_2Si, Si, Ni, and graphite and the melting point results recorded; a second group of samples, using SiC as one of the starting components was made for it was suspected that the correct equilibria (i.e., formation of SiC) in the samples made with free Si and graphite had not been established prior to melting.

Metallographic specimens were prepared by arc melting unmelted portions of the melting point samples in a Zak tungsten electrode button arc melting furnace under helium. Considerable difficulty was experienced, as was expected, in obtaining non-porous metallographic specimens from the SiC-rich regions of both the Ni-Si-C and Cr-Si-C ternary systems by arc melting. Because of the great difference in melting points between the binary silicide systems and SiC, and the corresponding exceptionally steep rise in the liquidus curves toward the Si-C side of the ternary,

especially in the Ni-Si-C system, considerable silicon and graphite losses were experienced from not only the decomposition of SiC, but also from boiling and vaporization of the binary silicides. Fortunately, since most of the reactions of interest in these two ternary systems take place quite near to the metal-silicon binaries, the absence of decent metallographic specimens in the SiC-rich portion of the ternary presented no unbearable loss of experimental data.

The heat treated samples from the ternary regions were either unmelted portions of melting point samples, or pieces of sample material which had been arc melted. These specimens were contained in a tantalum can and heat treated in a Brew tungsten-mesh element furnace. Figures 10 and 11 show the compositional location and heat treatments of the ternary alloys in the Cr-Si-C and Ni-Si-C systems.

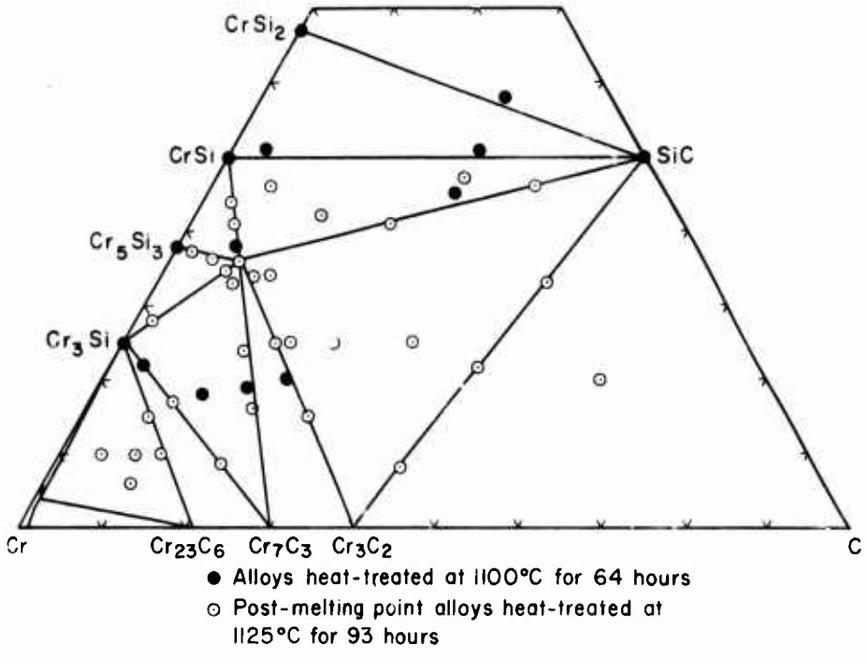

Figure 10. Cr-Si-C: Location and Heat Treatment of Ternary Alloys

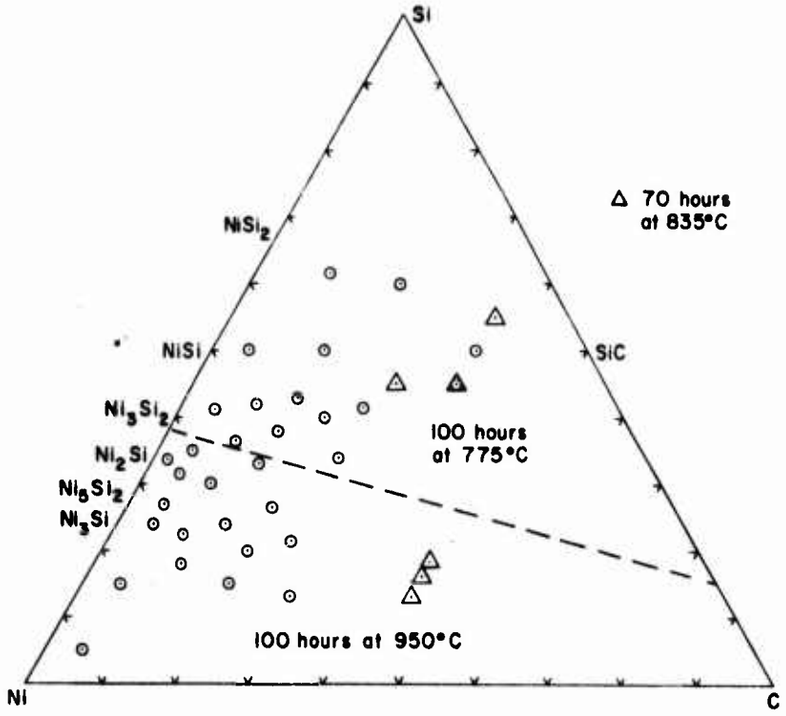

Figure 11. Ni-Si-C: Location and Heat Treatment of Ternary Alloys.

The main difficulty encountered in the heat treatments of the ternary alloys, in particular with the Ni-Si-C system, was with the conversion of free silicon and graphite to SiC and conversely the decomposition of SiC (when used as a starting material) to form the correct equilibria as dictated by the ternary phase equilibria. The heat treating temperatures employed had to be low enough to prevent melting of the binary silicides, yet in most cases, those temperatures do not favor the kinetics of either the formation of SiC or its decomposition even in long time heat treatment; the resulting heat treated samples showed nonequilibrium states; however, sufficient information was obtained to delineate the correct phase equilibria in the two ternary systems.

C. DETERMINATION OF MELTING POINTS

The melting point measurements were carried out in a special furnace employing the Pirani Black Body Hole technique by measuring the temperature of a solid-liquid phase change with a Bureau of Standards calibrated optical pyrometer. This method employs direct resistance heating across the sample; the details of the equipment used in this laboratory, the temperature corrections applied for absorption by the quartz glass viewing ports, and deviations due to non-black-body conditions have been reported in detail in other Air Force-sponsored reports[64][65] and need not be elaborated on here. The furnace was pressurized at each run with about 2-1/2 atmospheres of pure helium to suppress the vaporization of silicon. In addition, each sample was held for several minutes at sub-solidus temperatures to assure equilibration of the solid-state phases.

Little difficulty was encountered in the melting point determinations of ternary alloys in the chromium-silicon-carbon system except for those samples lying in two regions. High silicon containing alloys were difficult to measure in the Pirani furnace because of the nonmetallic, semiconductor properties of silicon; the electrical conductivity is too low to permit initial resistive heating and exceptionally high silicon containing samples were not able to be measured.

Samples from this ternary system which contained considerable amounts of SiC showed a behavior caused primarily by the large difference in melting points between SiC and the chromium silicides as well as the $D8_8$ ternary phase. The liquidus surfaces in the ternary system rise steeply toward the Si-C binary side, and since relatively little melt is formed with increasing temperature after the binary silicide or ternary phase containing portion has melted; the so-called collapsing temperature [64][65] (a valid guide for the approximation of the liquidus surface) of the Pirani specimen could not be reliably used, for increases in the temperature to

ranges where collapsing would normally occur led to superheating, possible boiling, vaporization, and certainly concentration shifts in the lower melting binary (and ternary) constituents.

The above mentioned effects were also observed with the Ni-Si-C melting point samples, and they were certainly more severe because the melting points in the nickel-silicon binary system are in general some 300 to 500°C lower than in the chromium-silicon system. In addition, an interesting effect was observed during melting point runs with ternary Ni-Si-C alloys. Regardless of whether the ternary samples showed equilibria with either graphite or silicon-carbide, the low melting silicides segregated completely from both the graphite and/or silicon carbide on melting, failing to wet the SiC or graphite grains. This visually observed effect was subsequently confirmed by Debye-Scherrer powder X-ray photographs of various portions of melted samples.

D. DIFFERENTIAL THERMAL ANALYSIS

The high temperature differential analysis equipment in use in this laboratory employs graphite heating elements and sample-dummy holders; it uses a cadmium sulfide photo cell which responds alternately to infrared radiation from the sample and the dummy.

Numerous details describing actual operation, electronic systems, power control, feedback systems, recording setup, and interpretation of results have been elaborately documented in other Air Force-sponsored reports[65][66] and need not be repeated here.

In the chromium-silicon-carbon system there is a strong interaction of virtually all chromium silicide-rich compositions with graphite, not only solid-state reactions, but also solid-liquid equilibria; the experimenter must be careful in his interpretation of the results which may be masked in a great part by the undesired interactions.

Several results, however, were able to be obtained when the temperatures used did not exceed the eutectic temperatures of silicide carbide, silicide-ternary phase, or carbide-ternary phase eutectics. Valuable information was obtained also in semi-quantitative kinetic experiments involving the reaction of chromium metal-silicon carbide mixtures by shielding the cold pressed powder compacts from the graphite holder with silicon carbide.

Identical experiments with nickel metal-silicon carbide mixtures were run in the same manner. Because of the much lower melting points in Nickel-Silicon and Nickel-Silicon-Carbon systems, the lower temperature limit (~1200°C) of the D.T.A. apparatus was exceeded and no reliable normal D.T.A. experiments were possible except for the experiment described above.

Figure 10 shows the location of D.T.A. samples in the Chromium-Silicon-Carbon system where experiments were made.

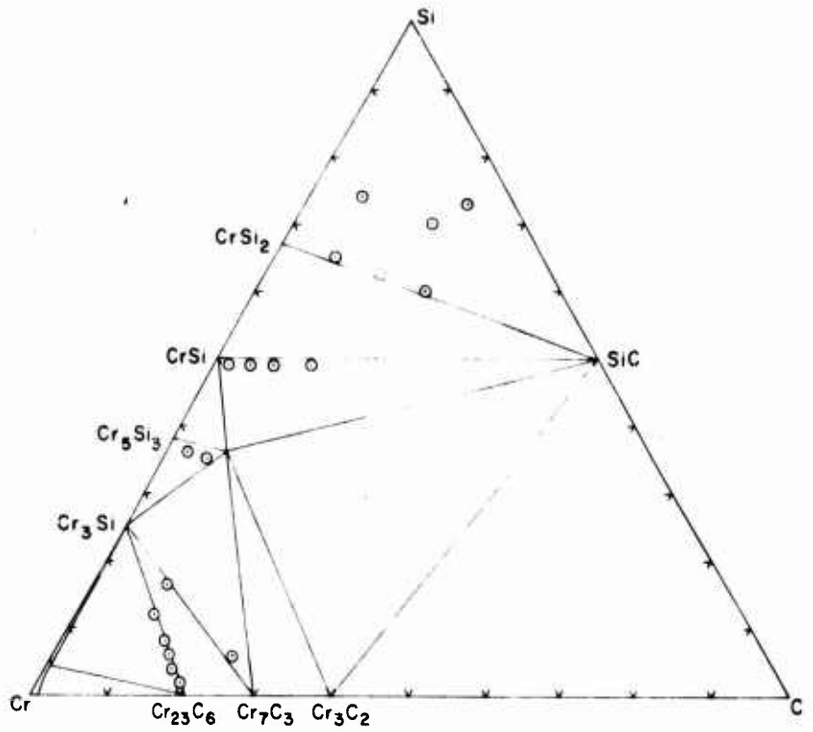

Figure 12. Cr-Si-C: Location of D.T.A. Samples.

E. METALLOGRAPHY

Figures 13 and 14 show the location of ternary (and some binary) Cr-Si-C and Ni-Si-C samples which were studied metallographically with a Zeiss Ultraphot II microscope. These samples were all arc melted pieces of melting point specimens, but in some cases separate hot pressed, cleaned and arc melted specimens were prepared separately for metallographic examination.

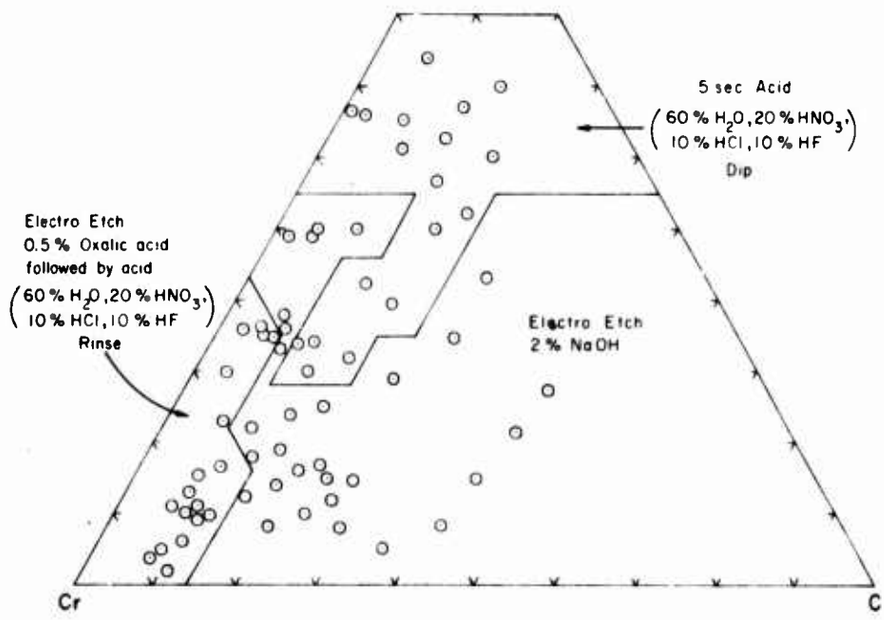

Figure 13. Cr-Si-C: Compositional Location and Etching Procedures of Ternary Alloys.

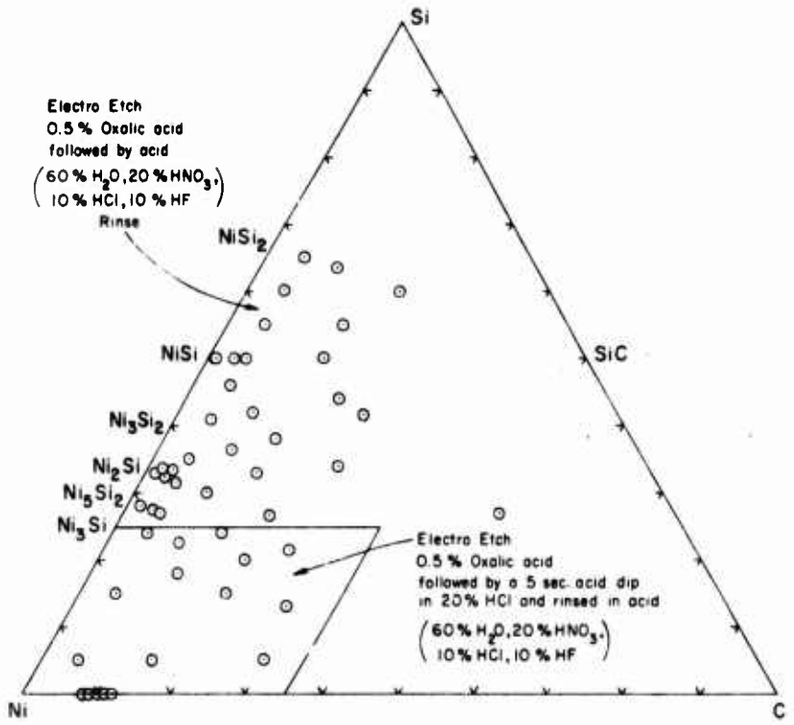

Figure 14. Ni-Si-C: Compositional Location and Etching Procedures of Ternary Alloys.

The samples were prepared by mounting the alloys in an electrically conductive mixture of diallyl-phthalate-lucite copper base mounting material. The samples were roughly ground on varying grit sizes of silicon carbide paper; the final polishing was performed on a microcloth using a suspension of 0.05 micrometer alumina in Murakami's solution. The final etching techniques used on the samples varied with the overall alloy composition.

The etchants used yielded satisfactory results, and phase differentiation was made without great difficulty.

F. X-RAY ANALYSIS

Debye-Scherrer X-ray powder photographs were made of all melting point, heat treated, arc melted, and D.T.A. samples.

In many cases, two or more X-rays were made of the segregated portions of the melting point samples. All sample material was irradiated with a Chromium K_α radiation using a Siemens II unit. The film strips were measured on a Siemens Kirem coincidence scale with a micrometer (0.01 mm scale divisions) attachment. All exposures were evaluated with respect to the nature of the phases present; many films were measured for lattice dimensions to determine binary homogeneous ranges and ternary solubilities.

The structures of all the phases occurring in the respective binary systems as well as the one Cr-Si-C ternary phase are well documented and therefore presented no particular interpretation difficulties.

On the other hand, there are some discrepancies in the publications concerning the nickel-silicon binary system—not so much in regard to the crystal structures (they seem well characterized), but rather in respect to the number of phases or allotropic modifications thereof. There appears some doubt as to whether there is a stable, high temperature modification of $NiSi_2$ as well as two low temperature forms of Ni_3Si.

G. CHEMICAL ANALYSIS

Chemical analyses for oxygen and nitrogen by a vacuum fusion method were made on some of the starting metal powders as a check on the vendor's analysis. The nitrogen contents were negligible and in one case (Cr), the oxygen content was somewhat higher (250 ppm vs. 480 ppm) than the vendor's reported value. It was felt, however, that this slight discrepancy was not serious enough to cause concern that the powder was unduly contaminated.

The starting silicides as well as some randomly picked post experimental alloys were checked for their silicon content* by fusing the sample in a sodium hydroxide-sodium peroxide

* The silicon analyses were performed under the direction of W. D. Trahan in the Aerojet-General's Metals and Plastics Chemical Testing Laboratory.

mixture, dissolving the melt in perchloric acid and volatizing the silicon as H_2SiF_6 with a hydrofluoric-sulfuric acid mixture.

Carbon analyses performed on some randomly chosen post-experimental alloys were made using the standard, direct combustion method by measuring the thermal conductivity of the combusted CO_2-O_2 gas mixture in a Leco carbon analyzer.

The analyses showed that the silicon losses, as expected, could be correlated to the high temperature and duration of exposure of these samples to high temperatures either in arc melting or in the melting point experiments. Some of the arc melted specimens, for example, in particular those containing large amounts of SiC or free silicon, showed losses as large as 10-15 At.%. The carbon losses, on the other hand, were minimal. These results were supported by the X-ray findings and taken account of in the interpretation of the experimental results.

BLANK PAGE

IV. RESULTS

A. THE CHROMIUM-SILICON SYSTEM

Although the investigations on the constitution of this binary system have been concluded and already submitted separately in final form as part of the requirements of this contract, the one open point has been clarified in recent additional studies. It was reported that the Cr_5Si_3 compound undergoes an α-β crystal structural change at 1505°C as evidenced by sharp exothermic peaks on cooling and pronounced endotherms in heating recorded in differential thermal analysis experiments. Concurrent with these experimental results, however, all attempts to isolate the high temperature form by rapid quenching in both an arc melter and tin bath quenching failed; nothing other than the known tetragonal, T-1 - type crystal structure for the Cr_5Si_3 phase was observed.

Under carefully controlled conditions, the differential thermal analysis experiments were repeated with the Cr_5Si_3 composition. The maximum temperature attained during the run was held to about 1515-1520°C. The D.T.A. trace showed the previously observed and reported endotherms and exotherms at 1505-1510°C. The sample, however, when removed from its graphite holder, showed definite signs of melting on surfaces which were in contact with the graphite holder although the melting point of the Cr_5Si_3 compound is some 160°C higher at 1680°C and that of the $D8_8$ carbon containing, ternary phase at 1649°C. (See Section IV-D-1-a below.) The conclusion is, therefore, that eutectic melting occurred on the Cr_5Si_3-graphite interface indicating a Cr_5Si_3-$D8_8$ pseudo-binary eutectic; the D.T.A. endotherms and exotherms are actual, but represent melting rather than an allotropic transformation.

Figure 15, presented below, reflects this minor change in the chromium-silicon system by the deletion of the previously proposed α-β transformation in Cr_5Si_3 at 1505°C.

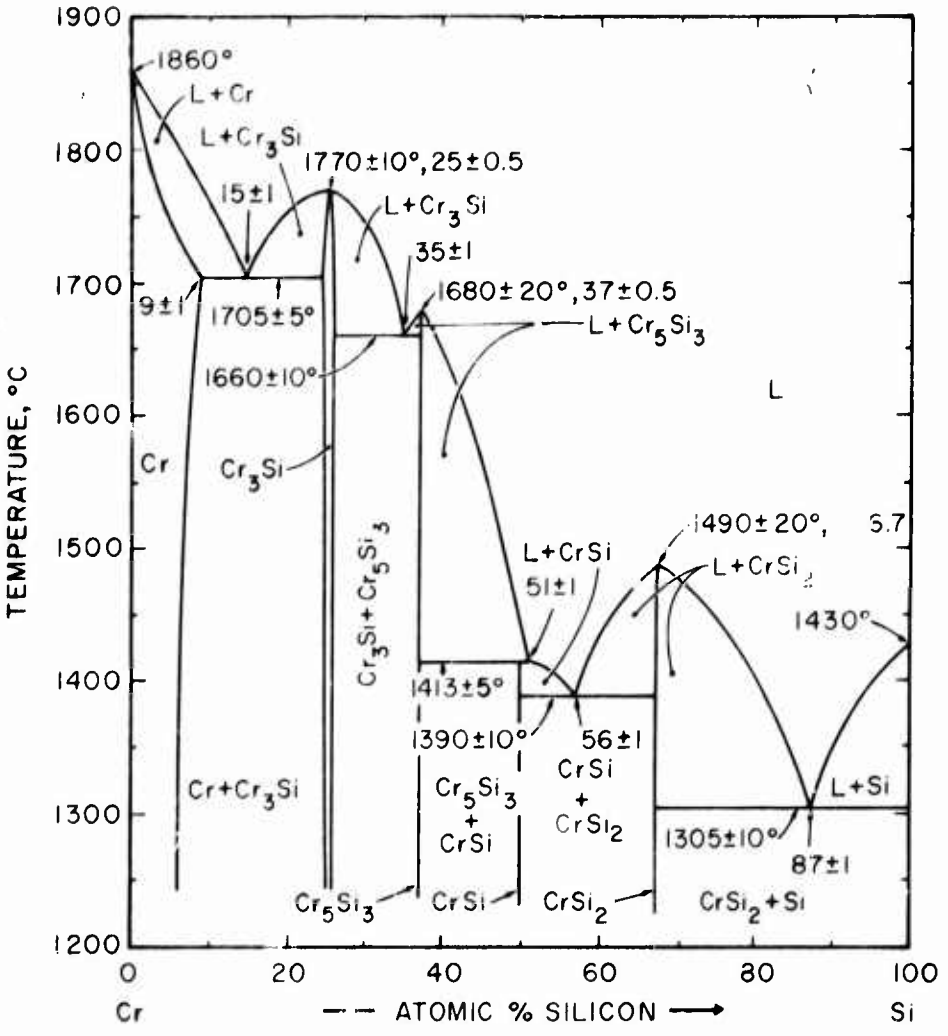

Figure 15. Cr-Si: Revised Constitution Diagram.

B. THE NICKEL-SILICON SYSTEM

Since it was not possible to run differential thermal analysis experiments in the high temperature apparatus available here, the confirming and checking investigations in this system were restricted to Pirani melting point determinations, Debye-Scherrer X-ray investigations, and metallographic studies which are presented as part of the detailed description of the Ni-Si-C system.

The melting point results, reported in the table below, are in very good agreement with those values reported by M. Hansen[1].

Table XX. Melting Point Results of Some Nickel-Silicon Alloys.

Composition Ni-Si(At.%)	Incipient Melting Point °C	Collapsing Temperature °C	M. Hansen[1] Literature Value Incipient Melting °C
96-4	1413	1428	1415
92-8	1357	1362	1353
88-12	1265	1286	1250
86-14	1250	1250	1220
84-16	1202	1202	1190
79-21	1167	1170	1152
71.2-28.8	1257	1268	1282
66-34	1287	1292	1318
54-46	985	985	964

The Debye-Scherrer X-ray patterns presented by the phases in the nickel-silicon system were confirmed with the exception of the θ-Ni_2Si phase, the high temperature form of $NiSi_2$, the β_3-Ni_3Si, and other reported structures of lower temperature allotropes of Ni_3Si.

In the concentration range of the θ-Ni_2Si phase (33.3-41.9 At.% Si) none of the X-ray patterns obtained from either melting point, arc melted, or heat treated samples showed sufficiently discernible amounts of this high temperature modification, both in binary Ni-Si and ternary Ni-Si-C samples; only bare trace amounts of what might be attributed to the θ-Ni_2Si phase were observed. Metallographic investigation of the samples in this region, however, (see Section IV-E-2-a below) always depicted signs of a transformation structure. It is apparent that under more severe quenching conditions, the θ-structure could indeed be retained.

The high temperature form of $NiSi_2$ was never observed either metallographically or in Debye-Scherrer X-ray films of samples prepared with the techniques and methods used in these investigations.

Considerable amounts of the peritecticly formed Ni_3Si were seen in X-ray films of both arc melted and melting point samples, although the X-ray patterns were never sharp enough to be measured or even compared to the published literature reports of the Cu_3Au structure[3][16][17]. There were never any indications of low temperature modifications of the Ni_3Si structure; in fact, heat treated samples from the ternary Ni-Si-C region near the Ni_3Si phase showed X-ray evidence that the Ni_3Si phase present in arc-melted and melting point samples had disappeared after heat treating at 950°C. These experimental facts tend to support the findings of other investigators[2, 4, 67] who state that the Ni_3Si phase is not stable below about 1100°C.

Table XXI shows the phases, crystal structures, and measured lattice parameters of the nickel-silicon compounds observed in this investigation.

Table XXI. Observed Nickel-Silicon Phases, Crystal Structures, and Lattice Parameters.

Phase	Crystal Structure	Lattice Parameter
Ni_3Si	---	---
Ni_5Si_2	Hexagonal	$a = 6.66_7$, $c = 12.28$Å
θ-Ni_2Si	---	---
δ-Ni_2Si	Orthorhombic	$a = 7.05_9$, $b = 4.98_6$ $c = 3.72_4$Å
Ni_3Si_2	Orthorhombic	$a = 12.21_8$, $b = 10.80_4$, $c = 6.91_7$Å
NiSi	Orthorhombic	$a = 5.62_6$, $b = 5.18_5$, $c = 3.325$Å
$NiSi_2$	Cubic	$a = 5.41_0$Å

Since the melting point results, X-ray comparisons, and lattice parameters as well as the metallographic findings (Section IV-E) were in excellent accord with the published literature on the NiSi system with the exceptions noted above, it was felt that the phase equilibrium information available is quite sufficient for the interpretation of the constitution of the Ni-Si-C ternary system, and no further investigations were undertaken in the Nickel-Silicon binary system.

C. THE NICKEL-CARBON SYSTEM

The brief investigations in this system were restricted to the determination of the eutectic melting temperature in this binary system. Metallographic studies were also made on arc melted portions of the five samples measured by the Pirani melting point technique. These are, however, not reproduced, for the structures observed contained agglomerated graphite with no truly representative eutectic structure. This occurrence has been observed several times in the past by other authors, and it is apparent that the eutectic structures are only obtained when rather rapid cooling rates, faster than those obtained in the arc melter used in these experiments, are employed.

Table XXII and Figure 16 show that the values obtained for the Ni-C eutectic temperature agree very well with the literature value[36-39] of 1318 °C.

Table XXII. Melting Temperature of Some Nickel-Carbon Alloys.

At.%		Temperatures, °C	
Ni	C	Incipient Melting	Collapsing
92	8	1325	1338
91	9	1322	1335
90	10	1324	1324
89	11	1320	1320
88	12	1320	1320

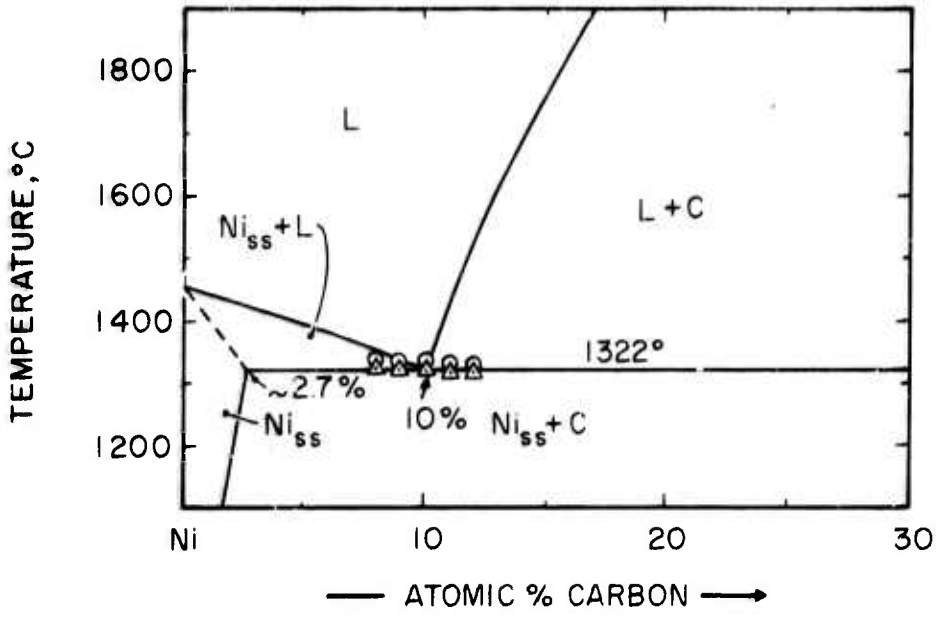

Figure 16. Ni-C: Low Temperature Portion of Constitution Diagram.

D. THE CHROMIUM-SILICON-CARBON SYSTEM

1. Solid-State Equilibria

The main feature of the ternary chromium-silicon-carbon system is the occurrence of a ternary phase with the $D8_8$-type structure; this compound belongs to the class of so-called Nowotny phases. In many other combinations, this phase is known to have sizeable homogeneous ranges; however, this is not the case with chromium-silicon-carbon system where the $D8_8$ phase has only a small homogeneous range about the composition $Cr_{55}Si_{36.5}C_{8.5}$. The measured lattice parameters ($a = 6.97_9$, and $c = 4.72_9$ Å) agree quite well with those given in the literature [62].

The primary information used in constructing the isotherm at 1100°C (Figure 18) for the Cr-Si-C system came from the X-ray evaluation of the alloys heat treated at 1100 and 1125°C under helium as shown by Figure 17.

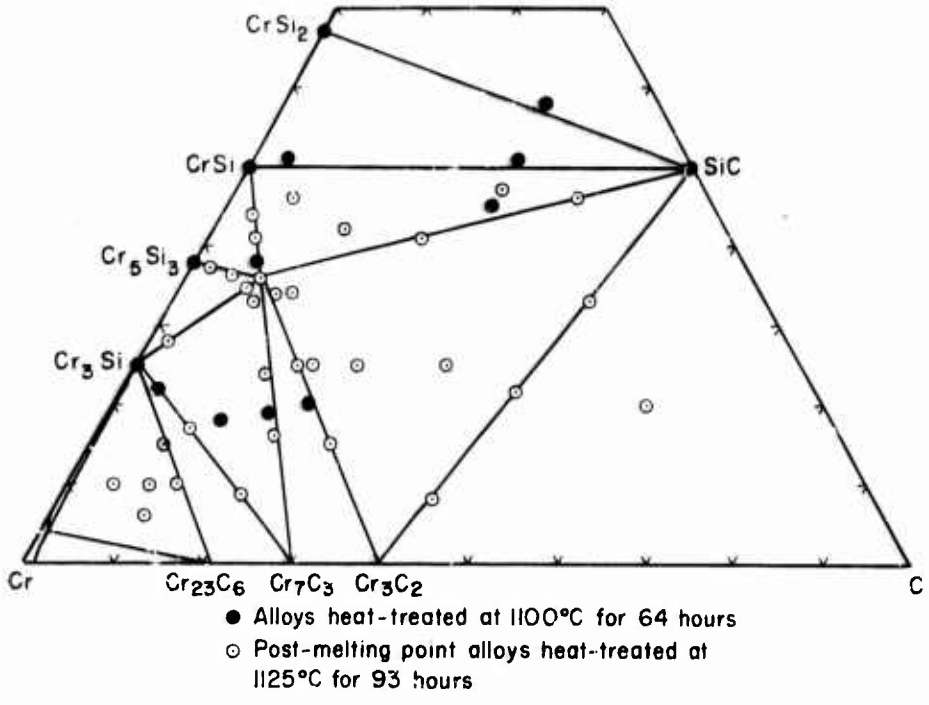

Figure 17. Cr-Si-C: Compositional Location and Conditions of Heat Treated Samples.

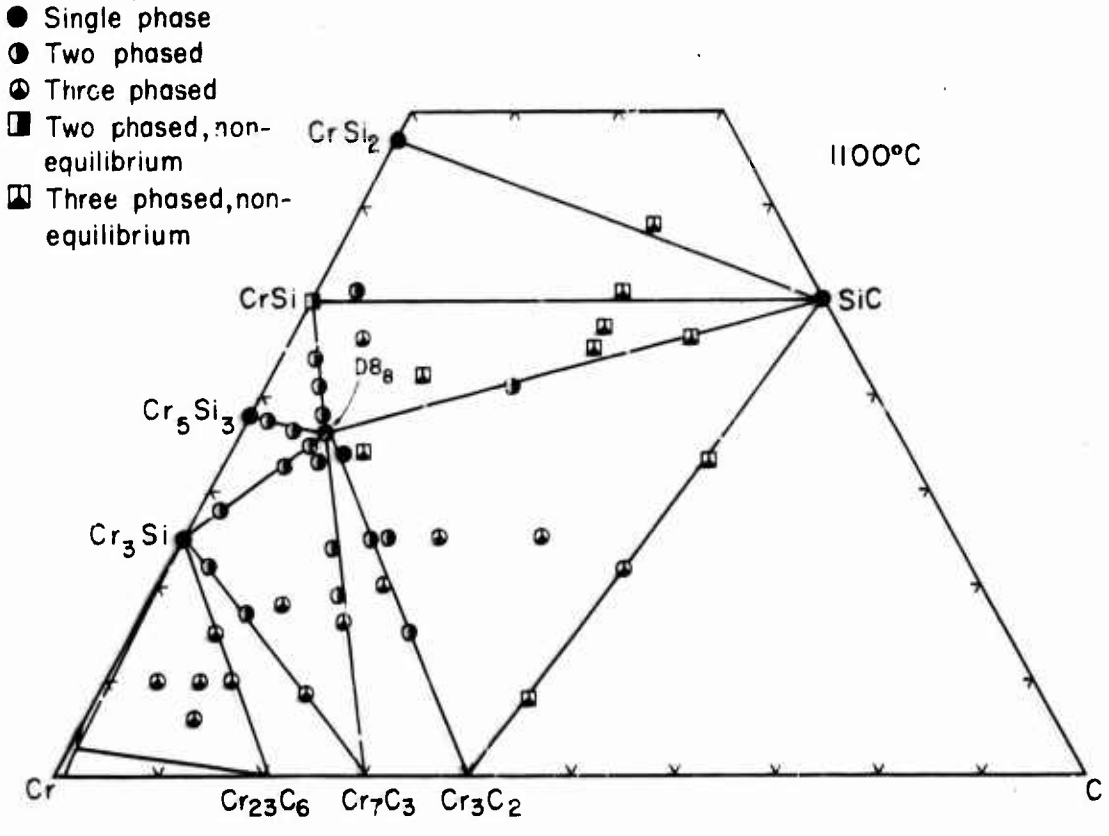

Figure 18. Cr-Si-C: Qualitative X-ray Evaluation of Heat Treated Alloys.

There are no other ternary phases in this ternary system, and the $D8_8$ phase forms two-phase equilibria with six other binary phases as shown in the 1100°C isotherm (Figure 18).

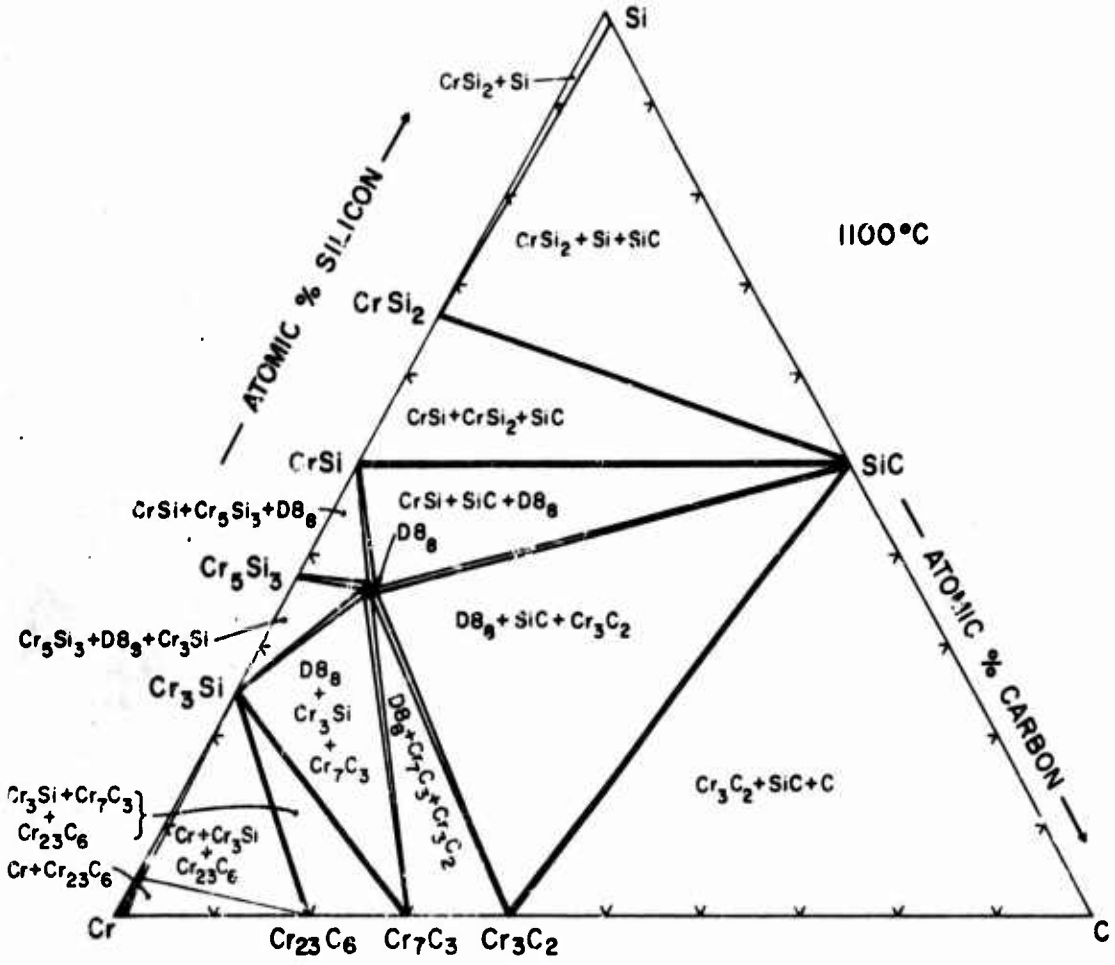

Figure 19. Cr-Si-C: Isotherm at 1100°C.

The samples indicated as being two or three-phased nonequilibrium in the X-ray evaluation diagram (Figure 17) have this designation due to incomplete reaction of the starting materials, primarily for the lack of complete formation of SiC from silicon and graphite.

Although some Cr-Si and Cr-C intermediate phases have small homogeneous ranges in their respective binary systems, there is no carbide-silicide mutual solubility into the ternary field as evidenced by the lack of change of lattice parameters of ternary alloys compared to the respective binary-phase constituents. The solubility of silicon and carbon in chromium in the ternary region was not specifically investigated, and there is no indication to believe that any unusual behavior occurs in the ternary region so that a mere joining of the solubilities shown in the respective binaries is permissible.

Silicon carbide, which, under the methods of preparation employed here, always occurred with the B-3 cubic type structure, did not show any tendency to take either silicides of carbides of this ternary system into solid solution; the same lattice parameter of $a = 4.35_8$ Å was observed in both ternary and binary alloys.

2. High Temperature Phase Equilibria

There are several pseudo-binary eutectic systems within the ternary Cr-Si-C region which were detected both metallographically and by analysis of melting point results as well as by D.T.A. in some cases; in addition, there are several ternary eutectics.

Figure 20 shows the compositional locations of the many melting point samples which were measured in the course of this investigation; Figure 21 portrays the locations of the samples which were examined metallographically, and Figure 12 depicts the positions of the D.T.A. samples investigated.

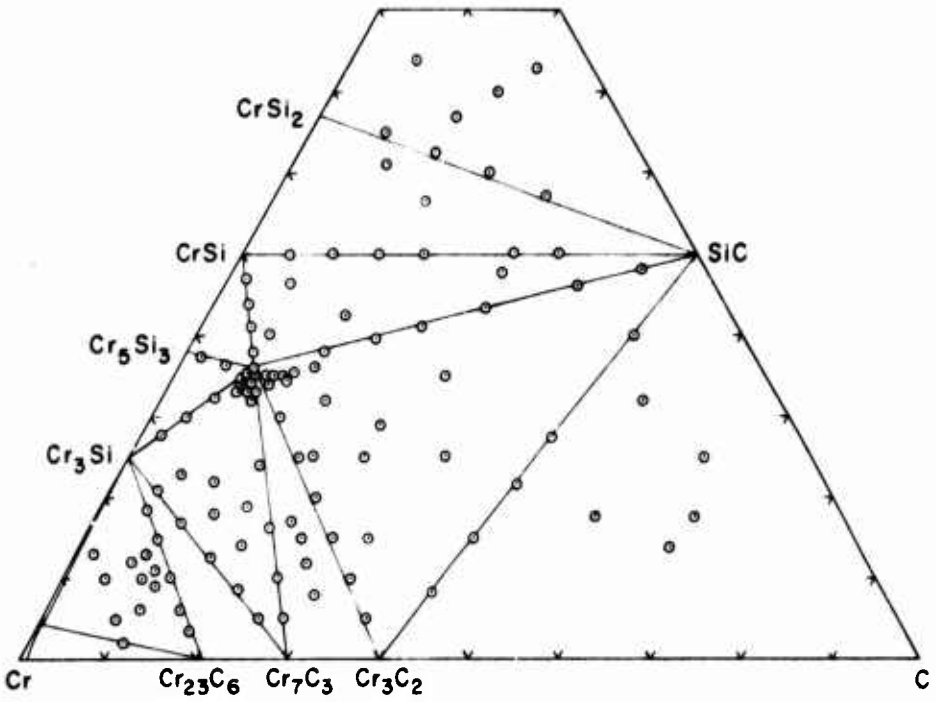

Figure 20. Cr-Si-C: Location of Melting Point Samples.

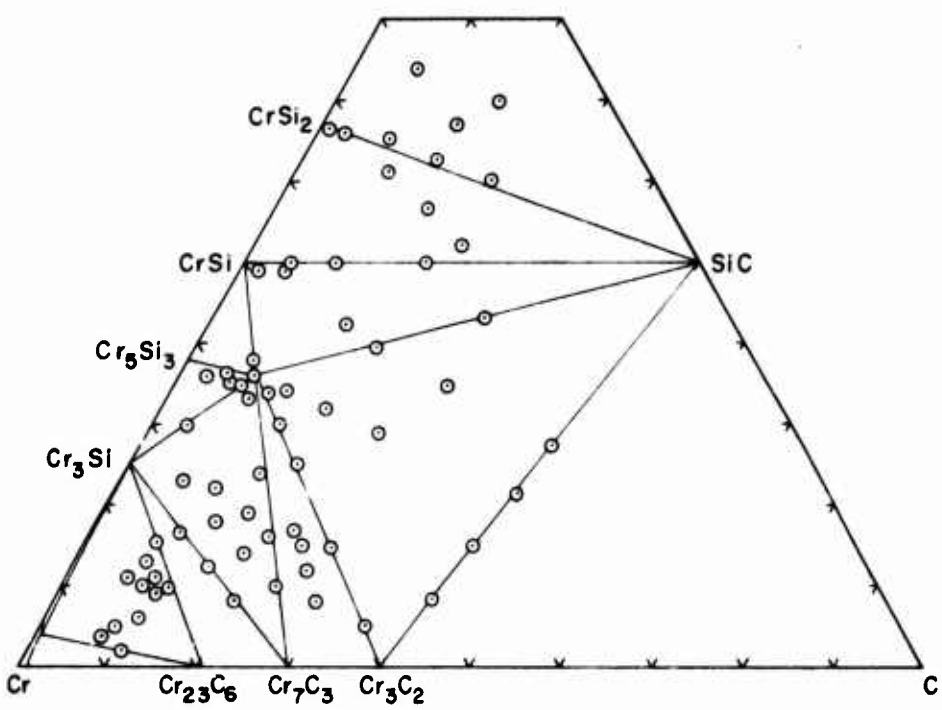

Figure 21. Cr-Si-C: Location of Metallographic Specimens.

a. The $D8_8$ Phase

The many melting point samples in the vicinity of the $D8_8$ phase have indicated that this phase melts congruently in a small range centering about the composition $Cr_{55}Si_{36.5}C_{8.5}$. The maximum melting temperature recorded was 1649°C. Even at temperatures near melting, the homogeneous range of this ternary compound is not very large. Figures 22 through 24 show representative metallographic photomicrographs of alloys from the $D8_8$ region.

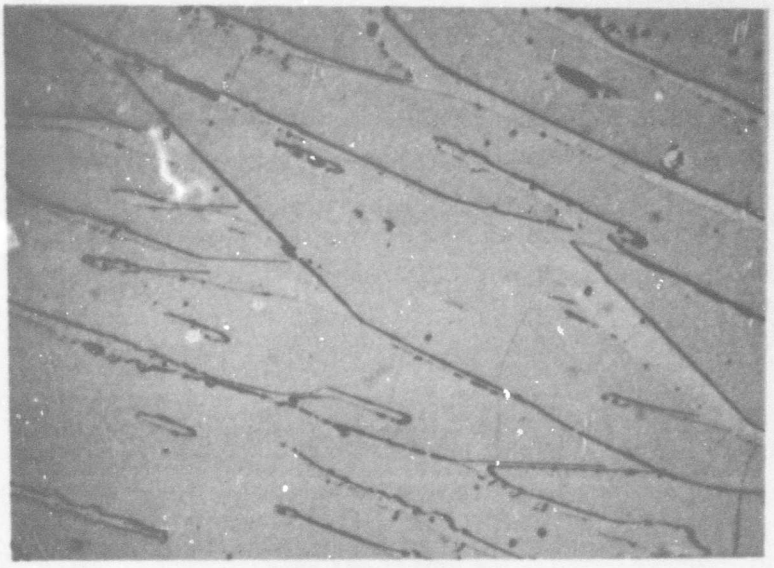

Figure 22. Cr-Si-C: 58.3/36.7/5, Photomicrograph of an Arc Melted Sample. X560

Large Angular Primary $D8_8$ Grains with Small Amounts of CrSi on Grain Boundaries.

X-ray: $D8_8$ with Traces of CrSi

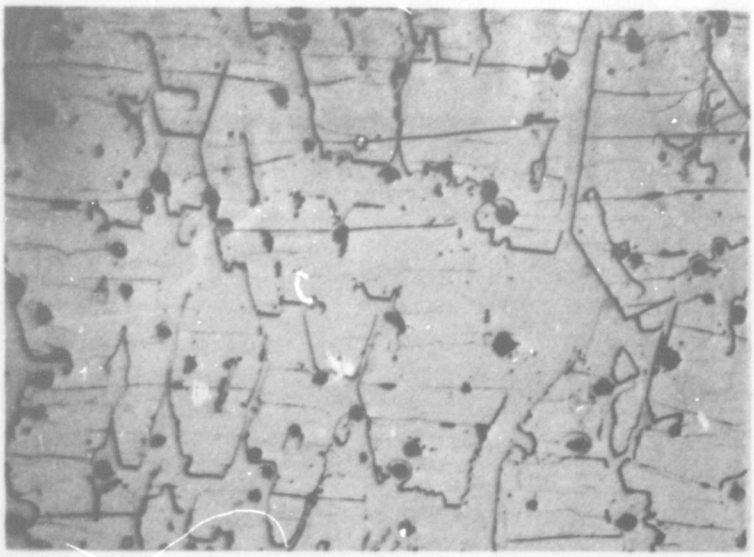

Figure 23. Cr-Si-C: 55/38/7, Photomicrograph of an Arc Melted Sample. X400

Primary $D8_8$ Grains with CrSi in Grain Boundaries; Black Spots are Pieces of Unreacted SiC.

X-ray: $D8_8$ + Little CrSi.

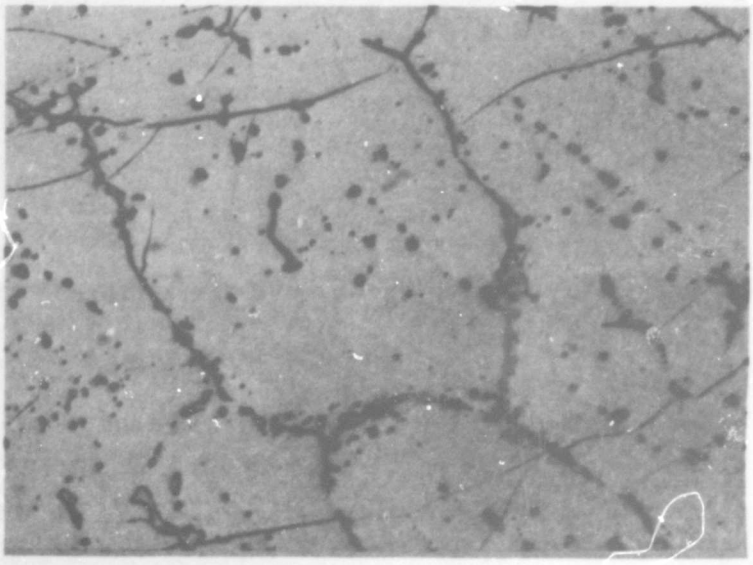

Figure 24. Cr-Si-C: 58/35/7, Photomicrograph of an Arc Melted Specimen. X320

Primary $D8_8$ Grains with Small Amounts of Cr_3Si on Grain Bounaries. Black Dots are Traces of Unreacted SiC.

X-ray: $D8_8$

b. The Cr_3C_2-$D8_8$ Section

This section contains a pseudo-binary eutectic located at about 48 Mole % $D8_8$-phase. The melting temperature, 1530°C, is indicated along with the experimentally determined melting points in Figure 25. The metallography of alloys along this section is shown in Figures 26 through 29.

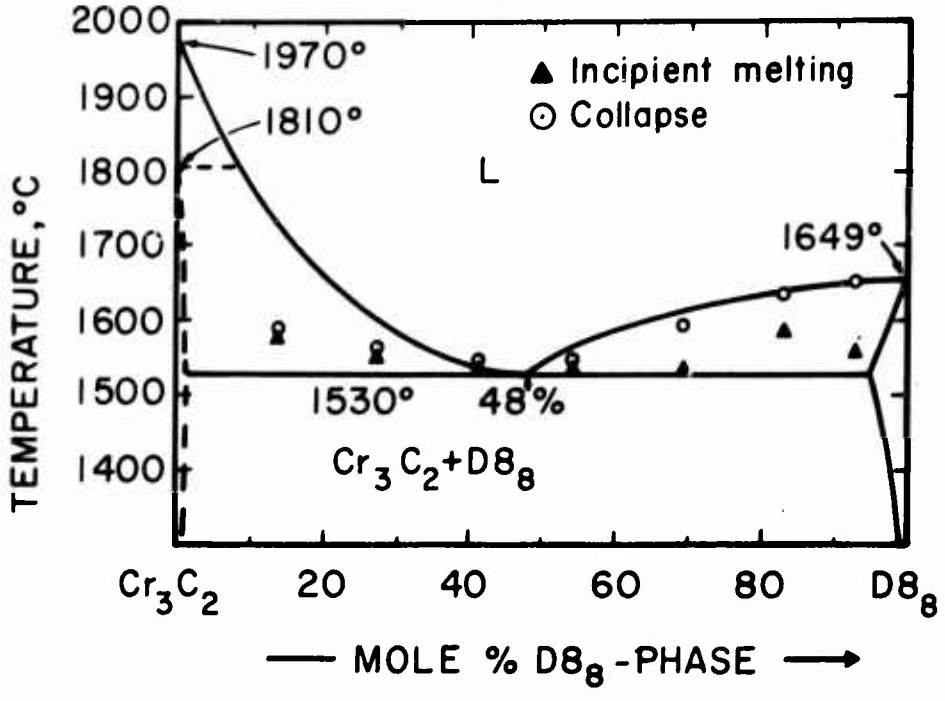

Figure 25. Cr-Si-C: The Cr_3C_2-$D8_8$ Pseudo-Binary Section

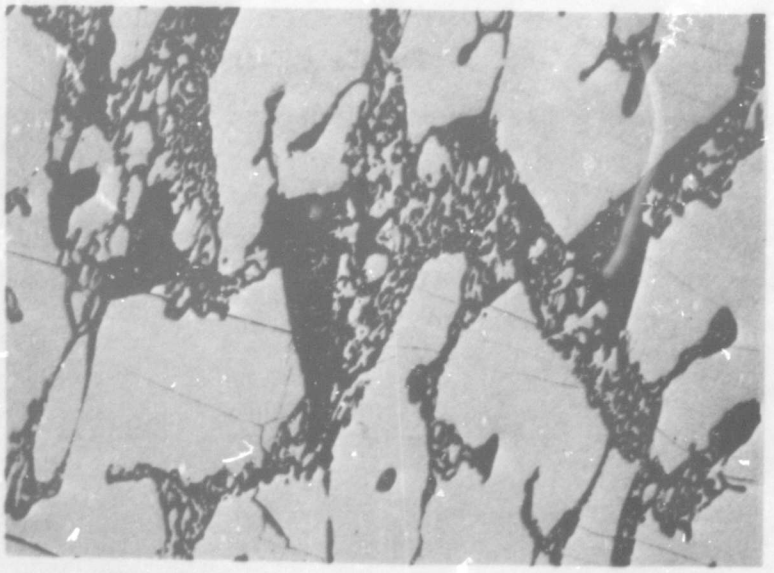

Figure 26. Cr-Si-C: 57/25/18, Photomicrograph of an Arc Melted Alloy. X560

Primary $D8_8$ Grains in $D8_8$-Cr_3C_2 Eutectic Matrix.

X-ray: $D8_8$ + Cr_3C_2

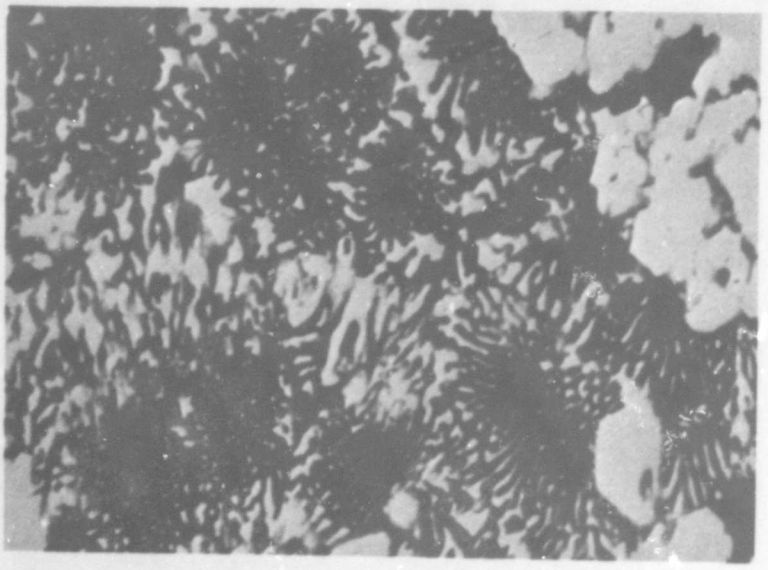

Figure 27. Cr-Si-C: 57/25/18, Photomicrograph of an Arc Melted Alloy. X2500

$D8_8$-Cr_3C_2 Eutectic Portion.

X-ray: $D8_8$ + Cr_3C_2

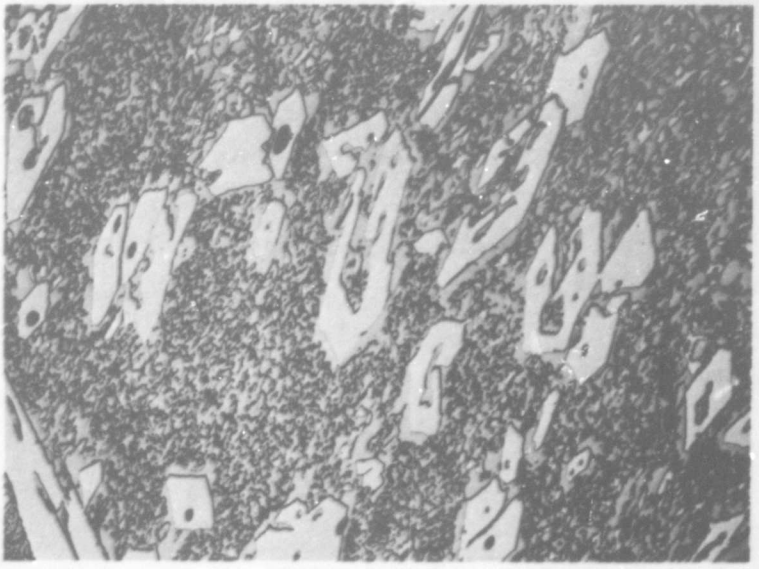

Figure 28. Cr-Si-C: 58/15/27, Photomicrograph of an Arc Melted Alloy. X480

Primary Cr_3C_2 in Partially Annealed and Divorced $D8_8$-Cr_3C_2 Eutectic.

X-ray: Cr_3C_2+$D8_8$

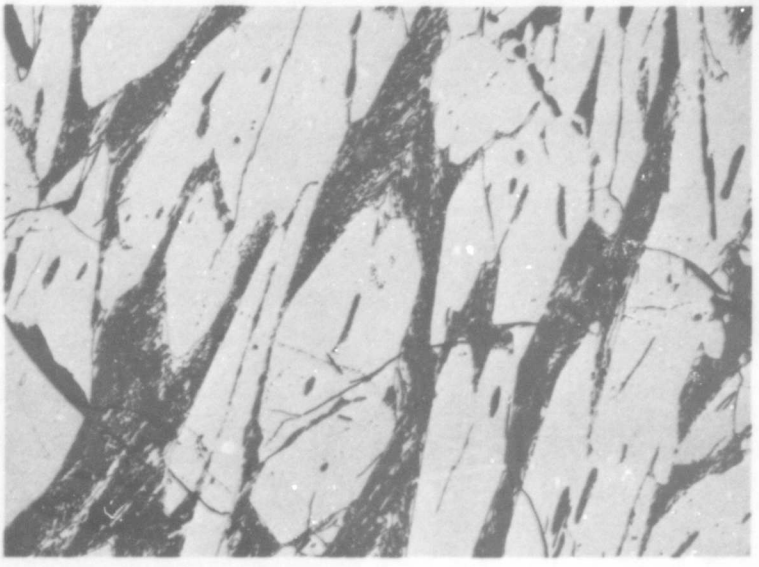

Figure 29. Cr-Si-C: 59/5/36, Photomicrograph of an Arc Melted Alloy. X325

Primary Cr_3C_2 in a $D8_8$-Cr_3C_2 Eutectic.

X-ray: Cr_3C_2 + Little $D8_8$

c. The Cr_7C_3-$D8_8$ Section

Experimental results, both melting point and metallographic, showed that a pseudo-binary eutectic system exists along this section. With the aid of metallography the eutectic was placed at about 48 Mole % $D8_8$ phase, while, as Figure 30 shows, the eutectic temperature is 1540°C. Figures 31 and 32 depict the metallographic findings along this section.

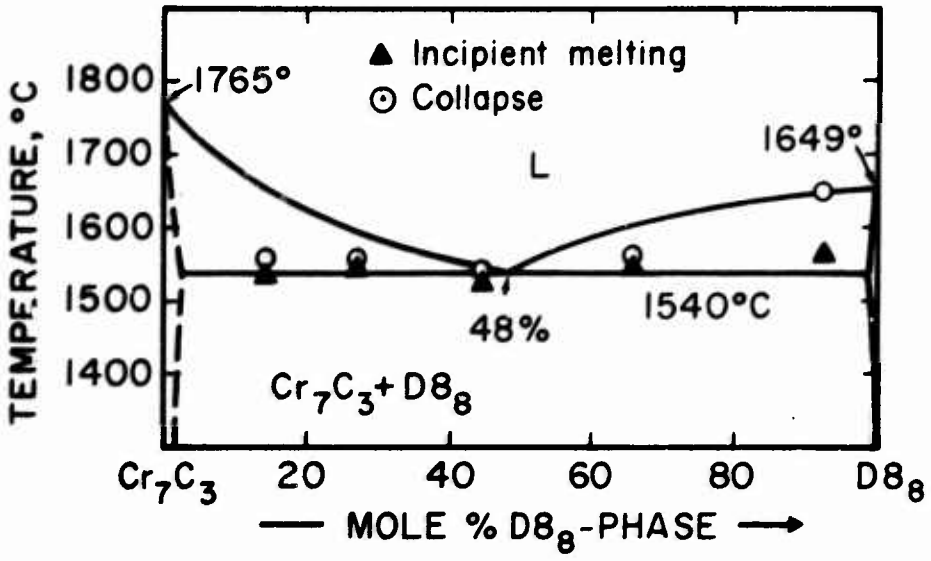

Figure 30. Cr-Si-C: The Cr_7C_3-$D8_8$ Pseudo-Binary Section.

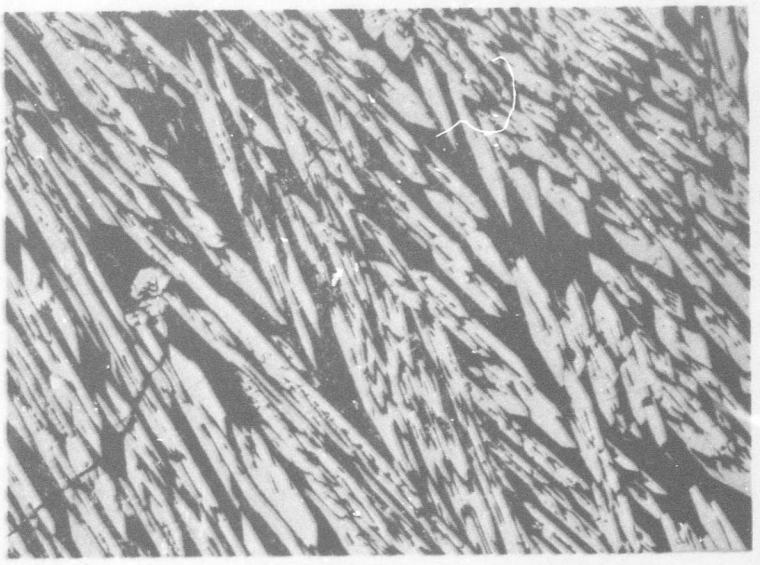

Figure 31. Cr-Si-C: 61/24/15, Photomicrograph of an Arc Melted Alloy. X90

Primary $D8_8$ Phase in a $D8_8$-Cr_7C_3 Eutectic Matrix.

X-ray: Cr_7C_3 + $D8_8$

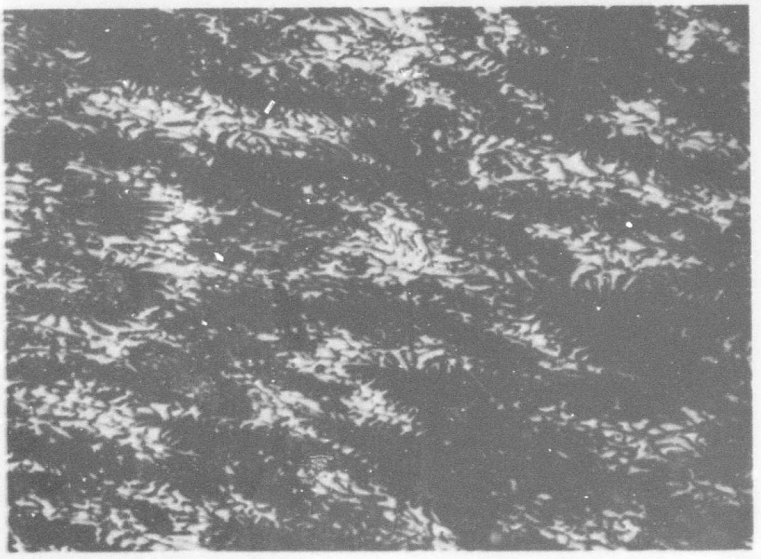

Figure 32. Cr-Si-C: 64/16/20, Photomicrograph of an Arc Melted Alloy. X920

$D8_8$-Cr_7C_3 Eutectic.

X-ray: $D8_8$ + Cr_7C_3

d. The Cr_7C_3-Cr_3Si Section

This pair of binary compounds also forms a pseudo-binary eutectic system. As shown in Figures 33 through 35, the eutectic point is located at 43 Mole % Cr_3Si, and the eutectic temperature is 1528°C.

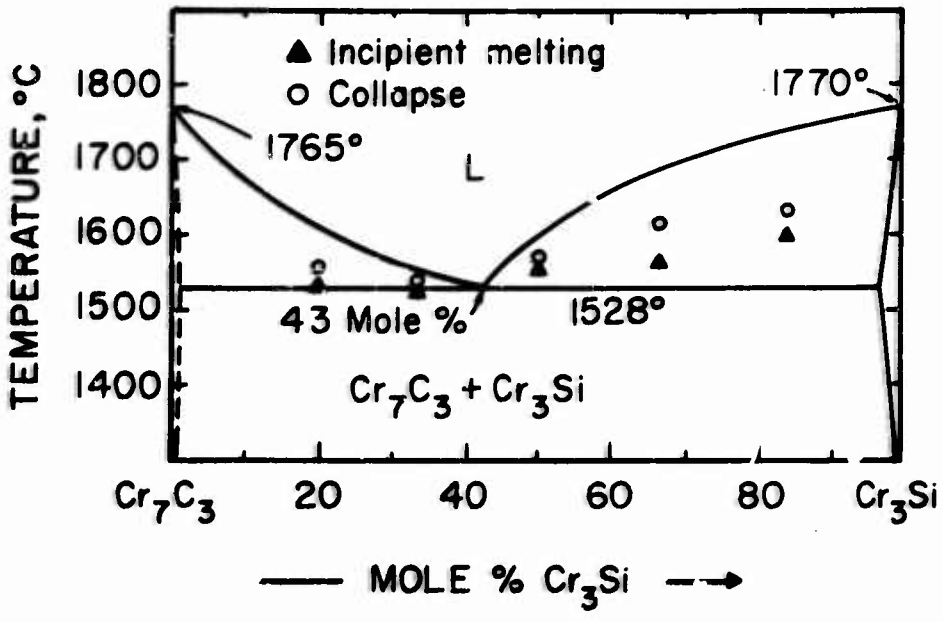

Figure 33. Cr-Si-C: The Cr_7C_3-Cr_3Si Pseudo-Binary Section.

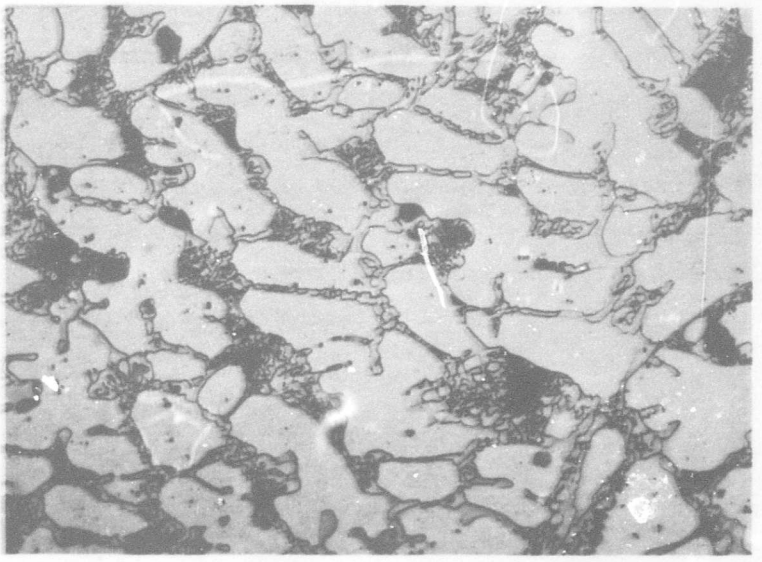

Figure 34. Cr-Si-C: 73.5/16.5/10, Photomicrograph of an Arc Melted Alloy. X520

Primary Cr_3Si in a Partially Annealed Cr_3Si-Cr_7C_3 Eutectic.

X-ray: $Cr_3Si + Cr_7C_3$

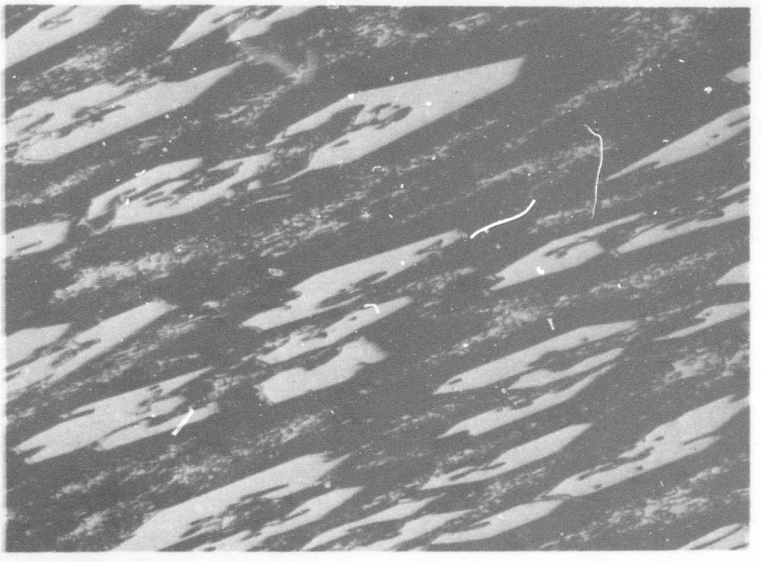

Figure 35. Cr-Si-C: 71.5/8.5/20, Photomicrograph of an Arc Melted Alloy. X270

Primary Cr_7C_3 in a Cr_7C_3-Cr_3Si Eutectic Matrix.

X-ray: $Cr_7C_3 + Cr_3Si$

e. The Cr_3Si-$D8_8$ Section

Cr_3Si and the ternary $D8_8$ phase form a pseudo-binary eutectic system; the eutectic point is located at 36 Mole % $D8_8$ phase, and the eutectic temperature is 1515°C. Figure 36 shows the experimentally determined melting points, and Figure 37 shows the typical eutectic structures found along this section.

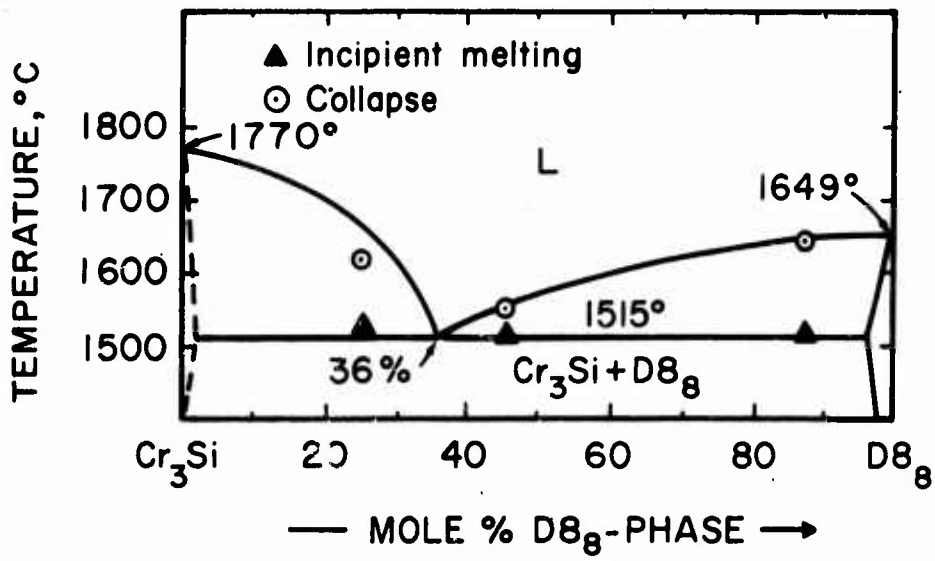

Figure 36. Cr-Si-C: The Cr_3Si-$D8_8$ Pseudo-Binary Section.

Figure 37. Cr-Si-C: 66/30/4, Photomicrograph of an Arc Melted Alloy. X275

Primary $D8_8$ Phase (Dark) in a Partially Annealed $D8_8$-Cr_3Si Eutectic Matrix.

X-ray: $Cr_3Si + D8_8$

f. The $D8_8$-SiC Section

This section also contains a pseudo-binary eutectic system. As is to be expected from the difference in melting points, the $D8_8$-SiC eutectic point lies quite close to the lower melting compound, the $D8_8$ phase; the eutectic is located at about 6 Mole % SiC, and the eutectic temperature is 1635°C.

Figure 38 shows the experimentally determined melting points, and Figures 39 through 41 depict the metallographic structures observed along or near this section.

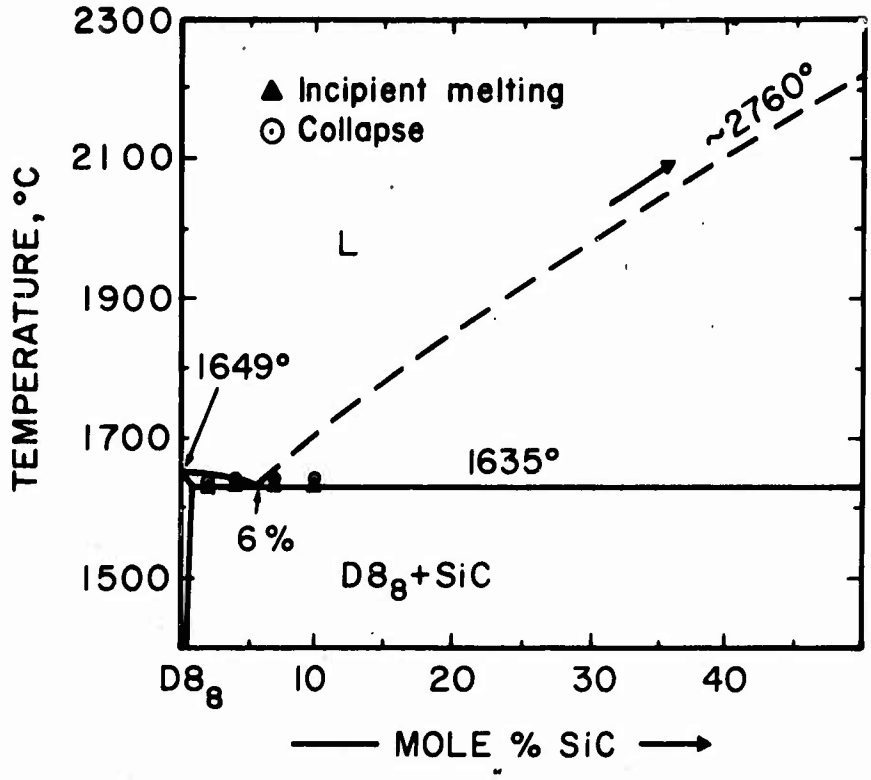

Figure 38. Cr-Si-C: The $D8_8$-SiC Pseudo-Binary Section.

To date, the chromium-silicon-carbon $D8_8$ phase-SiC eutectic appears to be the only fully documented pseudo-binary eutectic with SiC among the refractory metal (4a-6a groups) silicocarbide combinations, although H. Nowotny and co-workers[55] have alluded to the possibility of a molybdenum-$D8_8$ phase-SiC pseudo-binary eutectic in a diagram presented in a publication on the Mo-Si-C system.

Figure 39. Cr-Si-C: 55.5/33.5/11, Photomicrograph of an Arc Melted Alloy. X240

Primary $D8_8$ (Grey) in a Matrix of $D8_8$-SiC Eutectic. Traces of Third Phase (White), Probably Cr_3C_2, Present on Grain Boundaries.

X-ray: $D8_8$ + Little SiC

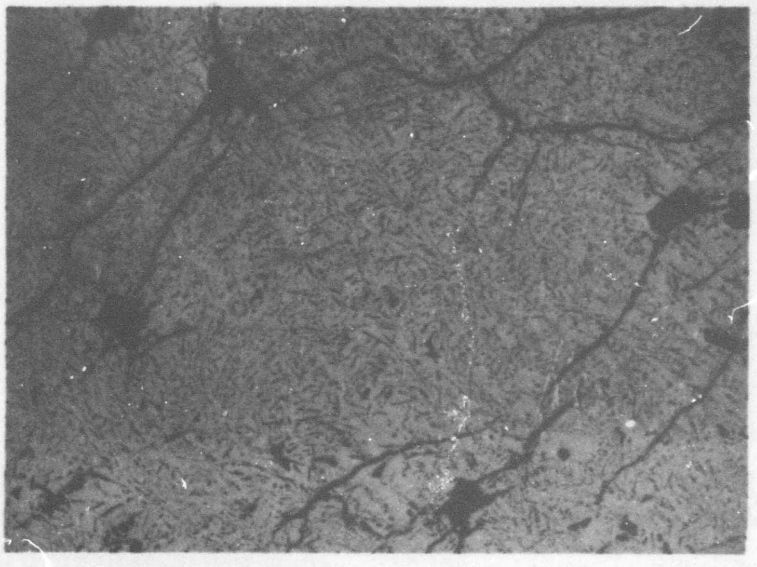

Figure 40. Cr-Si-C: 53/34/13, Photomicrograph of an Arc Melted Alloy. X175

$D8_8$-SiC Eutectic with Small Amounts of Unreacted SiC (Black Grains).

X-ray: $D8_8$ + Little SiC

Figure 39. Cr-Si-C: 55.5/33.5/11, Photomicrograph of an Arc Melted Alloy. X240

Primary $D8_8$ (Grey) in a Matrix of $D8_8$-SiC Eutectic. Traces of Third Phase (White), Probably Cr_3C_2, Present on Grain Boundaries.

X-ray: $D8_8$ + Little SiC

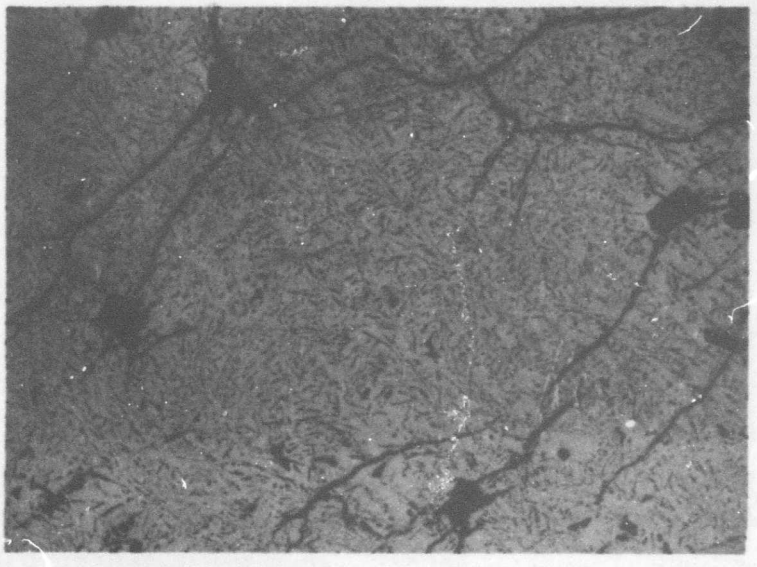

Figure 40. Cr-Si-C: 53/34/13, Photomicrograph of an Arc Melted Alloy. X175

$D8_8$-SiC Eutectic with Small Amounts of Unreacted SiC (Black Grains).

X-ray: $D8_8$ + Little SiC

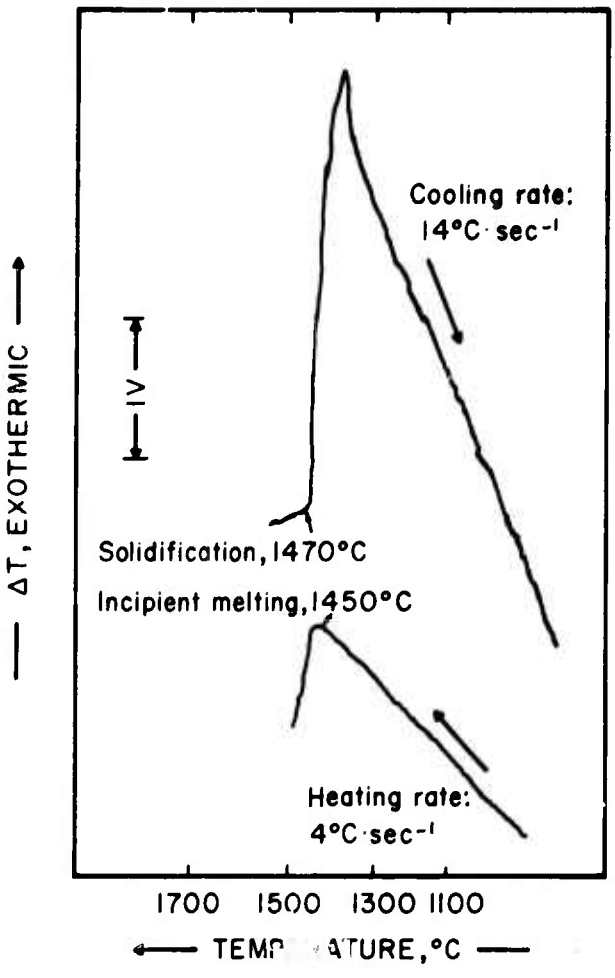

Figure 42. Cr-Si-C: 77.5/12/10.5

D.T.A. Thermogram Showing Ternary Eutectic Melting.

This ternary eutectic melting is described by a Class I, four-phase reaction (Figure 59).

$$\text{Liquid} \xrightarrow{1460^{\circ}C} Cr + Cr_3Si + Cr_{23}C_6$$

Figure 39. Cr-Si-C: 55.5/33.5/11, Photomicrograph of an Arc Melted Alloy. X240

Primary $D8_8$ (Grey) in a Matrix of $D8_8$-SiC Eutectic. Traces of Third Phase (White), Probably Cr_3C_2, Present on Grain Boundaries.

X-ray: $D8_8$ + Little SiC

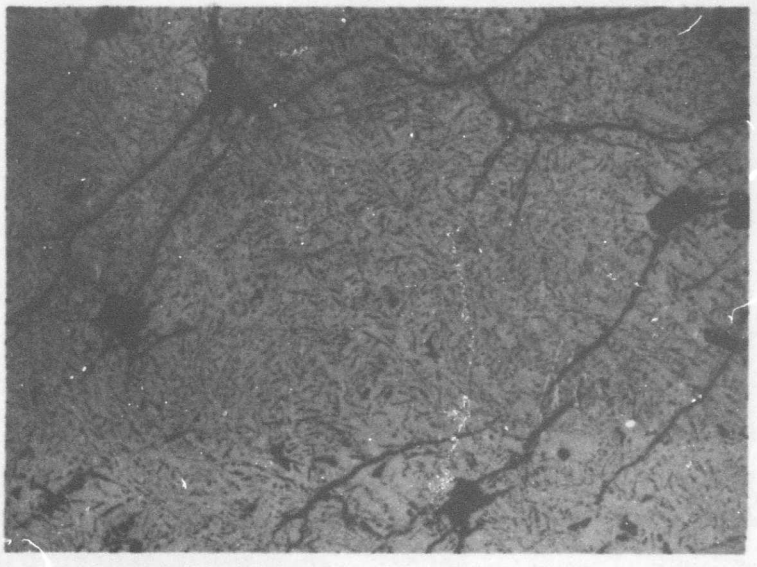

Figure 40. Cr-Si-C: 53/34/13, Photomicrograph of an Arc Melted Alloy. X175

$D8_8$-SiC Eutectic with Small Amounts of Unreacted SiC (Black Grains).

X-ray: $D8_8$ + Little SiC

Melting point results and also D.T.A. experiments on alloys near or on the $Cr_{23}C_6$-Cr_3Si section have shown that the peritectic decomposition temperature of the $Cr_{23}C_6$ is depressed in the ternary as a result of silicon additions in the form of Cr_3Si. The solid-solid phase equilibria of $Cr_{23}C_6$ in the ternary region is terminated at about 1510°C in a Class II, four-phase reaction:

$$\text{Liquid} + Cr_7C_3 \xrightarrow{\sim 1510°C} Cr_{23}C_6 + Cr_3Si$$

Figure 45 shows a representative D.T.A. trace of the alloys in this region. Since the peritectic reaction to $Cr_{23}C_6$ apparently takes place quite rapidly, no representative metallographic picture portraying the four phases partaking of this reaction was obtained.

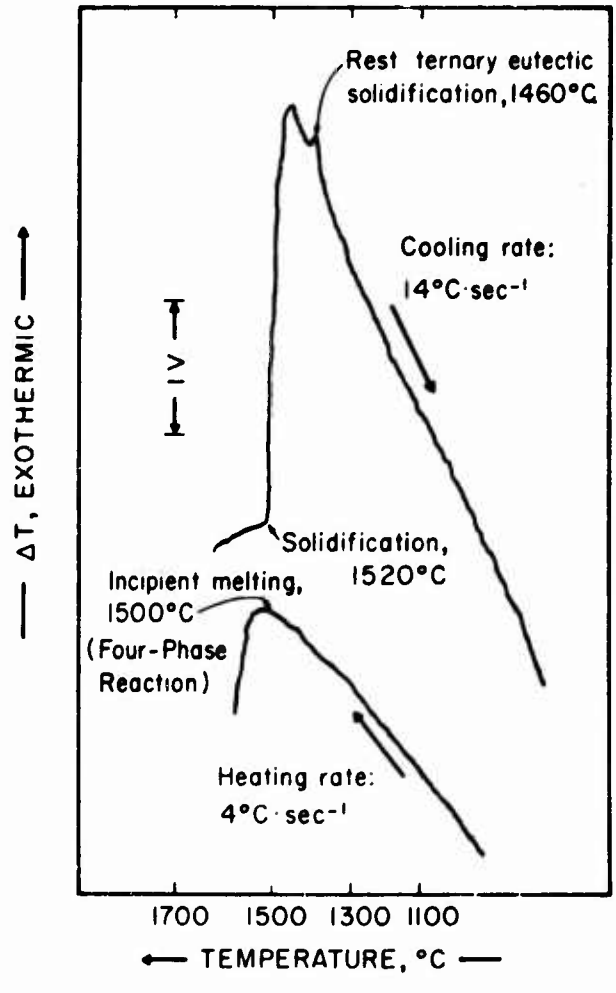

Figure 45. Cr-Si-C: 78/8/14, D.T.A. Thermogram of an Alloy Showing Four-Phase Melting and Rest Eutectic Solidification.

h. The Cr_7C_3-Cr_3Si-$D8_8$ Region

In this small three-phase area, another Class I, four-phase reaction was found to occur at about 1510°C. The three boundary phases partake of a ternary eutectic located at about $Cr_{70}Si_{11.5}C_{18.5}$. The Class I reaction is described by:

$$\text{Liquid} \xrightarrow{\sim 1510°C} Cr_3Si + Cr_7C_3 + D8_8 \text{ Phase} \quad \text{(Figure 60)}$$

Since the difference between the melting point of the ternary eutectic is quite close to the melting points of the pseudo-binary eutectics bounding this region, it was quite difficult to pinpoint the incipient melting point of the ternary eutectic. However, Figure 46 shows a typical photomicrograph of the alloys in this area.

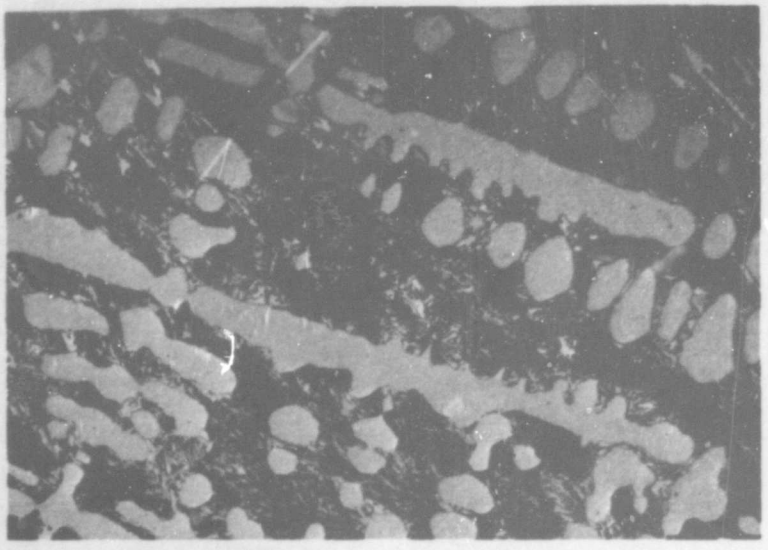

Figure 46. Cr-Si-C: 68/14/18, Photomicrograph of an Arc Melted Alloy. X500

Primary Cr_3Si in a Ternary Eutectic Matrix of Cr_3Si-$D8_8$ Phase-Cr_7C_3.

X-ray: $Cr_3Si + Cr_7C_3 + D8_8$

i. The Cr_7C_3-Cr_3C_2-$D8_8$ Region

These three phases also partake of a Class I, four-phase reaction, a ternary eutectic located at about $Cr_{60}Si_{18.5}C_{21.5}$. The exact melting temperature of the ternary eutectic was not able to be pinpointed exactly for the same reason as given in the preceding section. However, the Class I reaction occurs quite close to 1520°C.

$$\text{Liquid} \xrightarrow{1520°C} Cr_7C_3 + Cr_3C_2 + D8_8$$

Some of the metallographic photomicrographs which were used in locating this ternary eutectic are presented in the following figures:

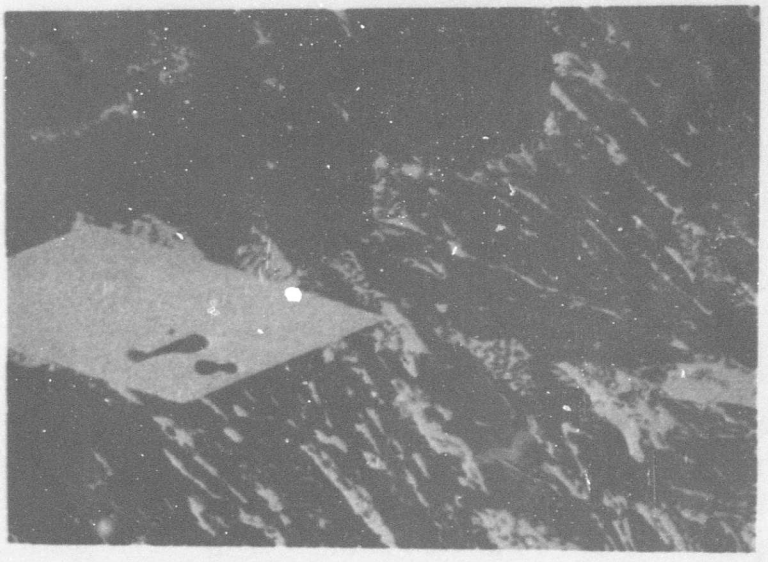

Figure 47. Cr-Si-C: 62/12/26, Photomicrograph of an Arc Melted Alloy. X1350

Primary Cr_7C_3 in a Ternary Eutectic Matrix of Cr_7C_3+Cr_3C_2 + $D8_8$ Phase.

X-ray: Cr_7C_3+Cr_3C_2+$D8_8$

i. The Cr_7C_3-Cr_3C_2-$D8_8$ Region

These three phases also partake of a Class I, four-phase reaction, a ternary eutectic located at about $Cr_{60}Si_{18.5}C_{21.5}$. The exact melting temperature of the ternary eutectic was not able to be pinpointed exactly for the same reason as given in the preceding section. However, the Class I reaction occurs quite close to 1520°C.

$$\text{Liquid} \xrightarrow{1520°C} Cr_7C_3 + Cr_3C_2 + D8_8$$

Some of the metallographic photomicrographs which were used in locating this ternary eutectic are presented in the following figures:

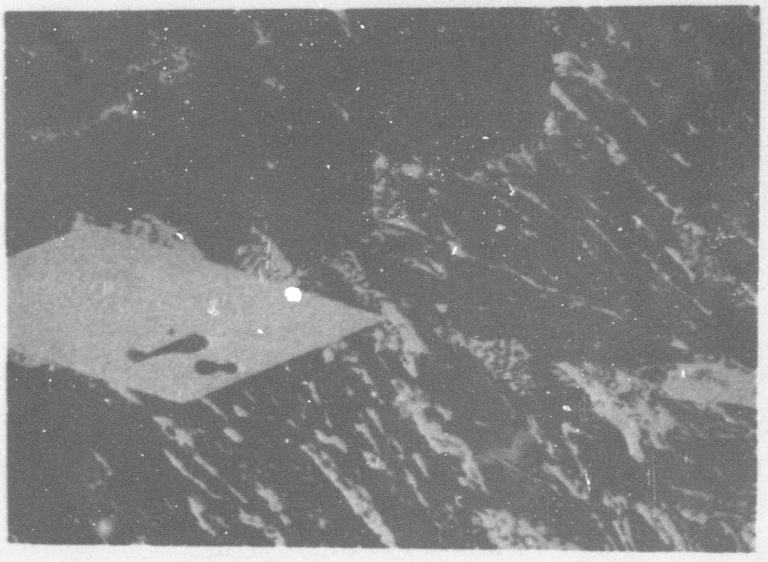

Figure 47. Cr-Si-C: 62/12/26, Photomicrograph of an Arc Melted Alloy. X1350

Primary Cr_7C_3 in a Ternary Eutectic Matrix of Cr_7C_3+Cr_3C_2 + $D8_8$ Phase.

X-ray: Cr_7C_3+Cr_3C_2+$D8_8$

Owing to the rather strong decomposition tendencies of the silicides and silicon carbide containing alloys in this area at higher temperatures near 1800-2000°C, as for example in arc melting; it was not possible to obtain melted samples suitable for metallographic examination and photographing.

k. The Cr_5Si_3-$D8_8$ Section

Although metallographic studies did not prove conclusively that a pseudo-binary eutectic exists between the binary compound Cr_5Si_3 and the ternary $D8_8$ phase, it can be stated with a reasonable amount of certainty that the D.T.A. results of experiment with Cr_5Si_3 (Figure 49) described in Section IV-A indicate the presence of eutectic melting at approximately 1510°C along this section. This pseudo binary eutectic is indicated in Figure 67.

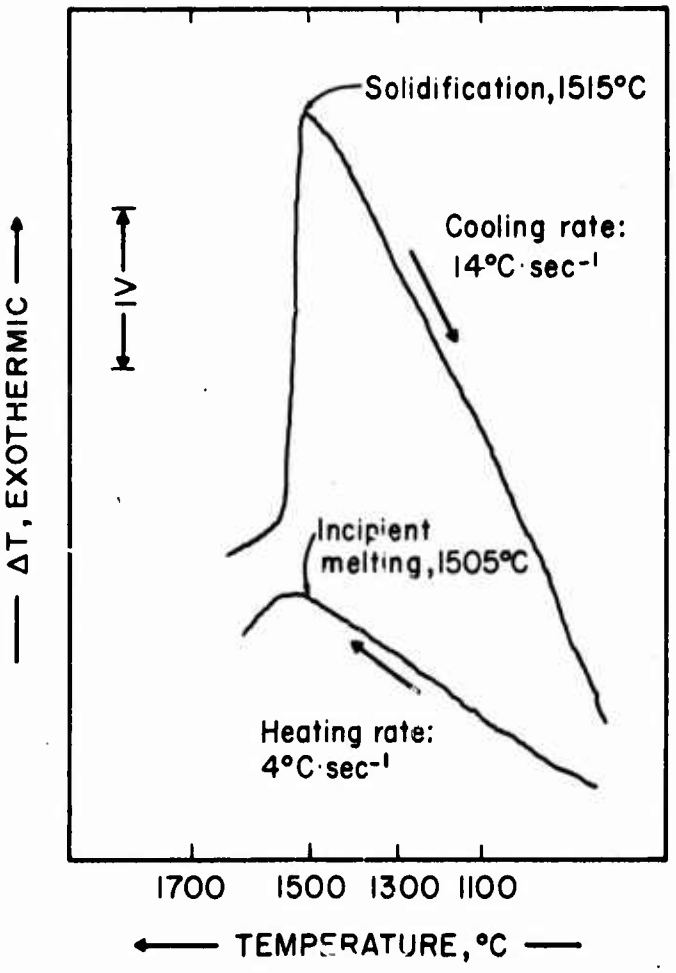

Figure 49. Cr-Si: 62.5/37.5, D.T.A.

Thermogram of a Carburized Cr_5Si_3 Alloy Indicating Probable Cr_5Si_3-$D8_8$ Pseudo-Binary Eutectic Melting.

1. The Cr_5Si_3-SiC-CrSi Region

In this region of the ternary system, there are two, Class II, four-phase reactions involving liquid and the peritecticly melting binary compound CrSi. The first of these is a simple two-over-two Class II reaction where melt and the $D8_8$ phase form a two-phase equilibria replacing the solid-state CrSi-SiC equilibrium at ~1400°C:

$$\text{Liquid} + D8_8 \text{ Phase} \xrightarrow{\sim 1400^\circ C} \text{CrSi} + \text{SiC}$$

The second Class II, four-phase reaction involves the disappearance of the CrSi-$D8_8$ solid-state equilibrium as a prelude to the vanishing of the peritectic melting CrSi in the chromium-silicon binary system:

$$\text{Liquid} + Cr_5Si_3 \xrightarrow{\sim 1410^\circ C} CrSi + D8_8 \text{ Phase}$$

Since these two, four-phase reactions occur in a very small temperature internal and within an almost equally small concentration range (Figures 56, 57, and 67), the differential thermal analysis experiments do not differentiate between the two reactions; the D.T.A. curves merely show that the peritectic decomposition point of the CrSi compound has been lowered slightly in the ternary region compared with its binary value of 1413°C.

Figure 50. Cr-Si-C: 46/49/5, Photomicrograph of an Arc Melted Alloy. X210

Four-Phase Reaction Mixture of SiC (Dark), CrSi (White), $CrSi_2$, $D8_8$, and Cr_5Si_3.

Co-crystallized CrSi and SiC in Eutectic-Like Matrix of $CrSi_2$-CrSi with Small Amounts of $D8_8$ and Cr_5Si_3.

X-ray: CrSi + Little $CrSi_2$ + Traces of SiC, $D8_8$, and Cr_5Si_3

m. The Ternary Area Near $CrSi_2$

Since a probable pseudo-binary eutectic, very rich in $CrSi_2$, exists between $CrSi_2$ and SiC as stated above, metallographic pictures of alloys lying further out on the ternary system toward SiC show co-crystallized SiC in a $CrSi_2$ matrix or, when somewhat silicon-richer, in a $CrSi_2$-Si eutectic matrix. This is illustrated by the following photomicrographs:

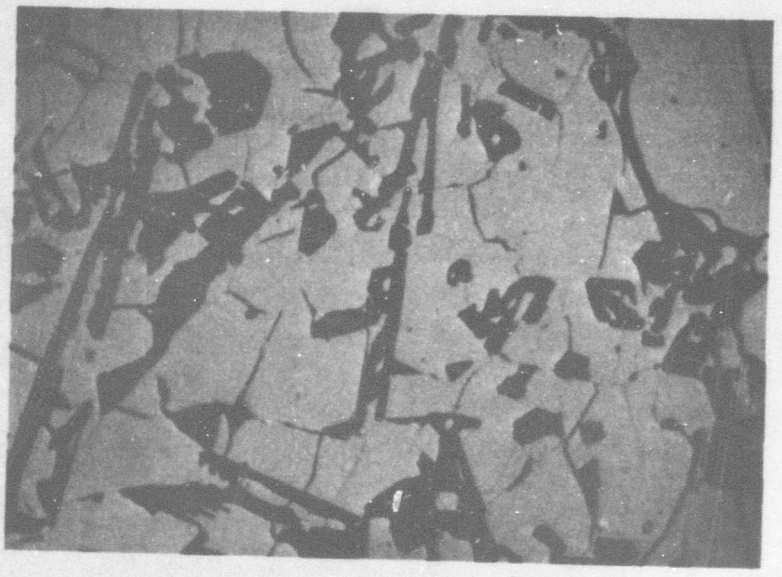

Figure 51. Cr-Si-C: 29/61/10, Photomicrograph of an Arc Melted Alloy. X400

Primary SiC (Dark) in a $CrSi_2$ Matrix.

X-ray: $CrSi_2$+SiC

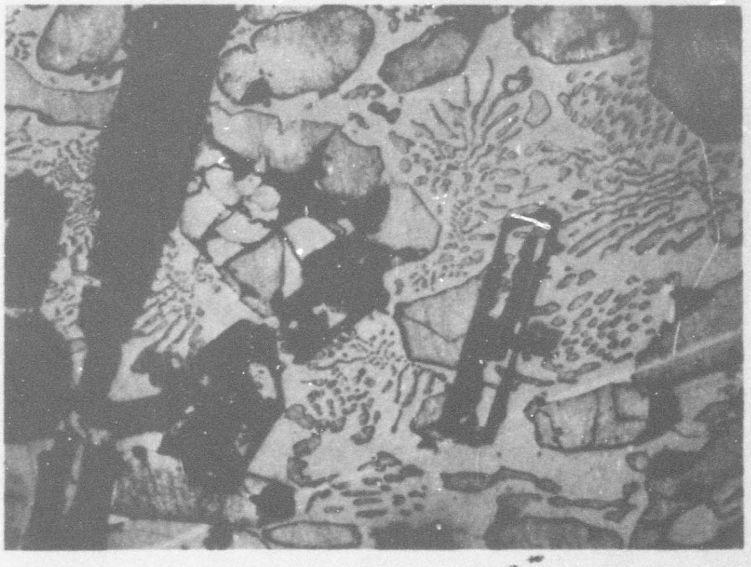

Figure 52. Cr-Si-C: 18/67/15, Photomicrograph of an Arc Melted Alloy. X560

Co-crystallized $CrSi_2$ and SiC in a $CrSi_2$-Si Eutectic Matrix.

X-ray: $CrSi_2$+Si+SiC

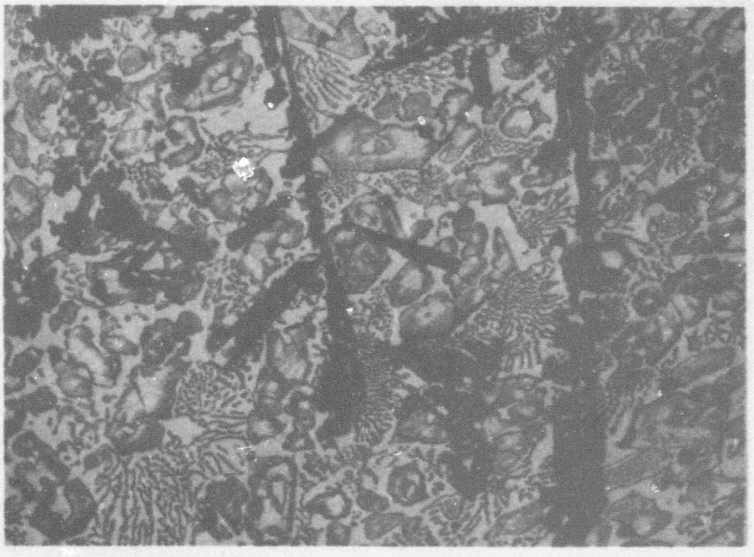

Figure 53. Cr-Si-C: 19/74/7, Photomicrograph of an Arc Melted Alloy. X210

Co-crystallized SiC (Dark) and $CrSi_2$ in a $CrSi_2$-Si Matrix.

X-ray: $CrSi_2$+Si+SiC

n. Other Four-Phase Reactions in the Cr-Si-C System

By nature of the experimentally documented pseudo-binary eutectics and, in part, by Class II, four-phase reactions with the resulting melting trough diagram; it becomes evident that for a consistent high temperature phase equilibria interpretation, certain solid-liquid reactions must also be present in some areas of the ternary system. These proposed four-phase reactions, or the physical evidence thereof, may often times go undetected primarily because of two common and interrelated facts. When the suspected four-phase reaction lies quite close to either a binary system or a ternary intermediate compound, the quantities of the more distant partaking phase are vanishingly small and often go unobserved; furthermore, the isothermal temperature of such four-phase reactions are usually so close to other isotherms in the close proximity that small differences are often not seen.

There are four such occurrences in the ternary Cr-Si-C system. These reactions are merely listed in a table below with the approximate temperature of occurrence and a brief description. It is seen (Figure 67) that each of these reactions lies close to the binary Cr-Si system or to the ternary $D8_8$ phase.

Table 23. Undetected Probable Additional Four-Phase Reactions in the Cr-Si-C System.

Reaction	Class	Approximate Temperature °C	Remarks
$L \longrightarrow D8_8 + Cr_3C_2 + SiC$	I	1630	Ternary Eutectic
$L \longrightarrow Cr_5Si_3 - D8_8 + Cr_3Si$	I	1505	Ternary Eutectic
$L \longrightarrow CrSi + CrSi_2 + SiC$	I	1380	Ternary Eutectic
$L \longrightarrow Si + CrSi_2 + SiC$	I	1300	Ternary Eutectic

In addition, for the same reasons noted above, a pseudo-binary, eutectic-type reaction isotherm is indicated to occur on the $CrSi_2$-SiC section at about 1480°C:

$$\text{Liquid} \xrightarrow{\sim 1480°C} CrSi_2 + SiC$$

o. Assembly of the Phase Diagram

With all the information obtained from metallographic studies, melting point experiments and D.T.A. runs, in particular the collapsing temperatures of the melting point samples, a series of ternary isotherms from 1100° to 2300°C were drawn to show the melting sequences and important four-phase reactions. These isotherms (Figures 54 through 66), in turn, formed the basis for the construction of the three-dimensional space model in Figure 2. As a final illustration, a drawing showing the melting troughs and isothermal solid-liquid reactions in the ternary Cr-Si-C system is presented in Figure 67. One trough arm of the probable ternary eutectic among $D8_8$, SiC, and Cr_3C_2 is drawn dashed to indicate that toward the silicon-carbon side of the ternary there are probably one or more complicated, four-phase reactions involving vapor as the characteristics of the silicon-carbon system change rapidly with increasing temperature.

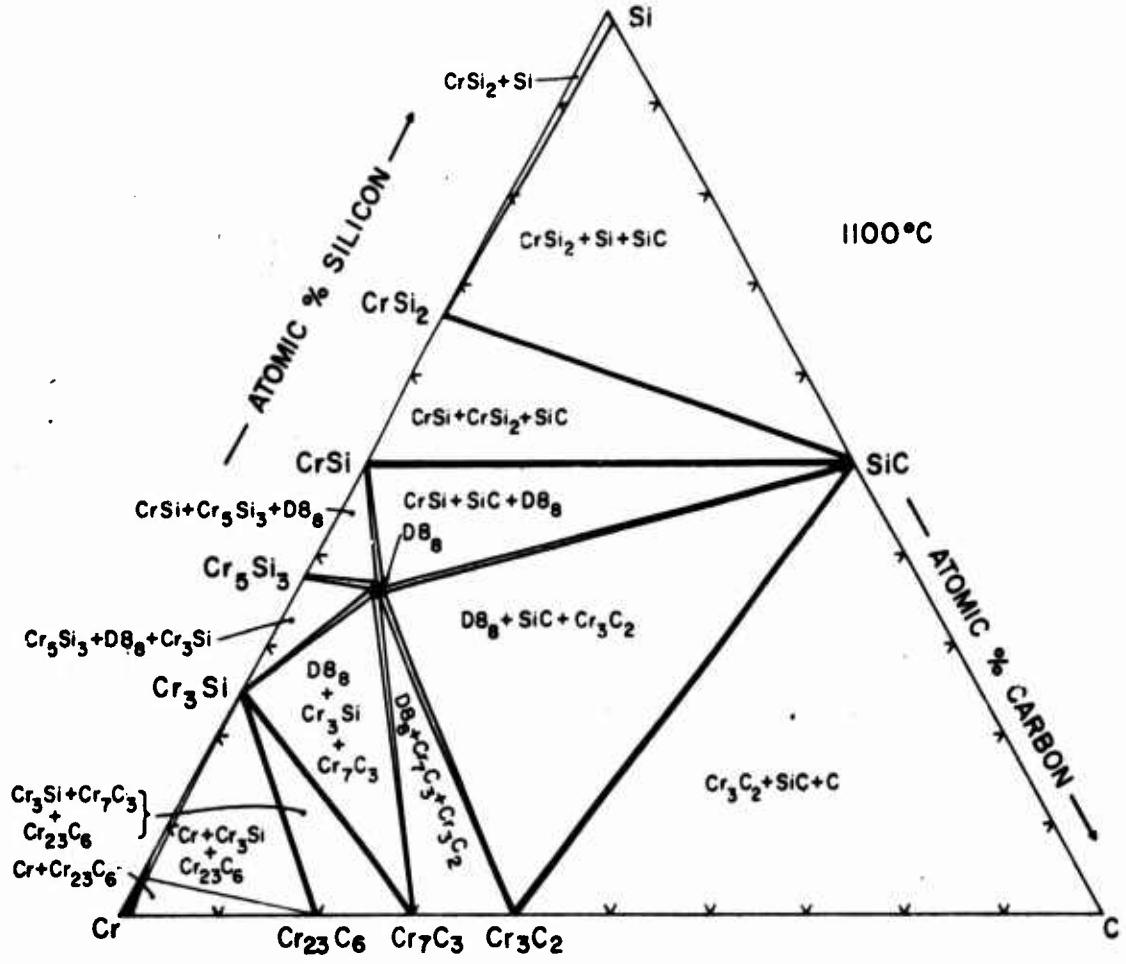

Figure 54. Cr-Si-C: Isotherm at 1100°C.

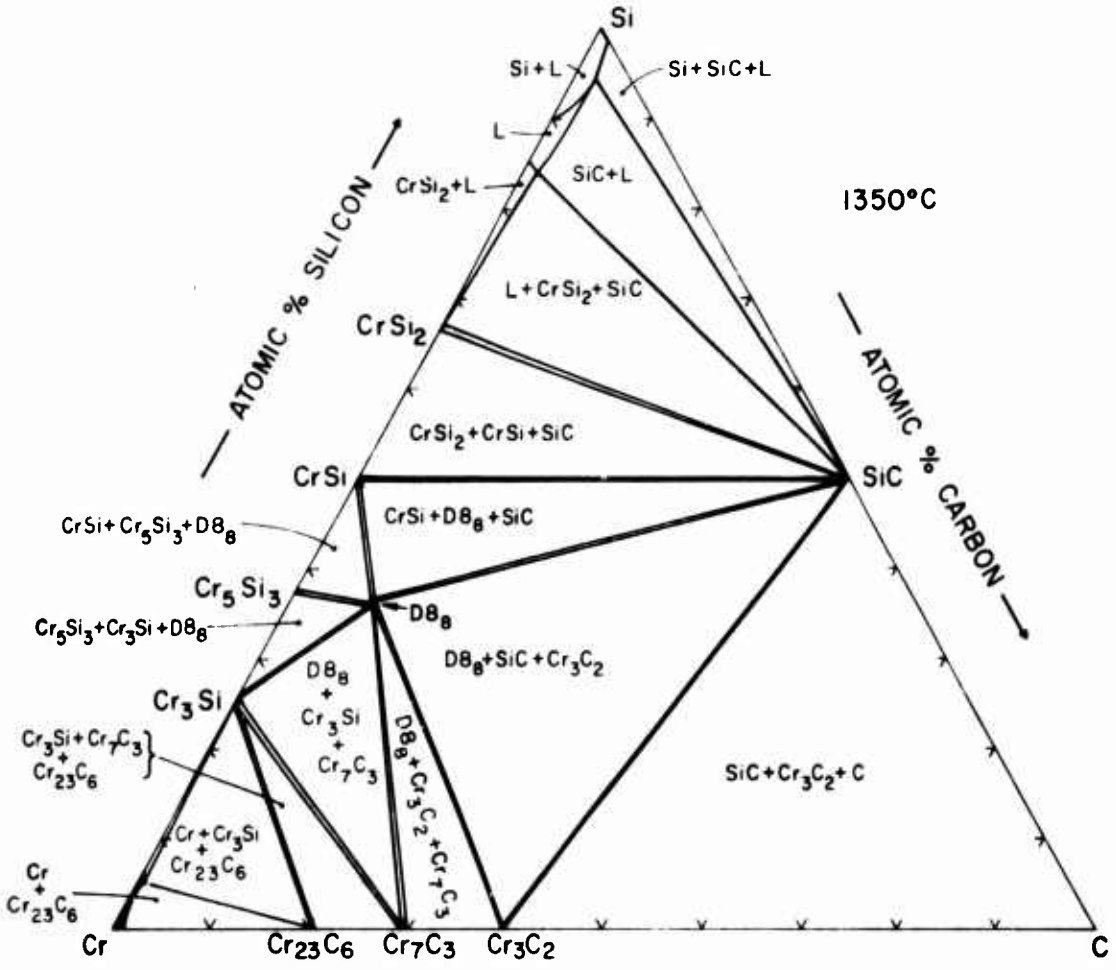

Figure 55. Cr-Si-C: Isotherm at 1350°C.

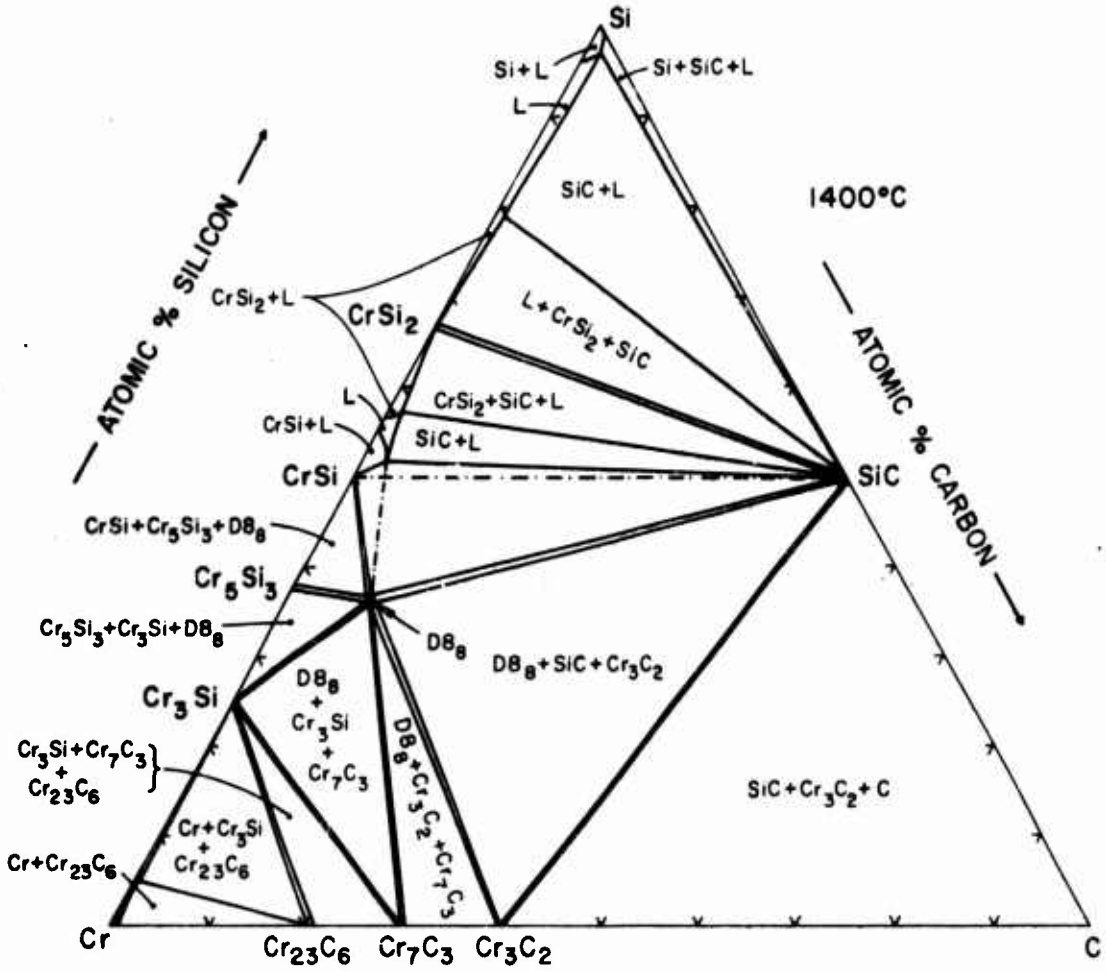

Figure 56. Cr-Si-C: Isotherm at 1400°C.

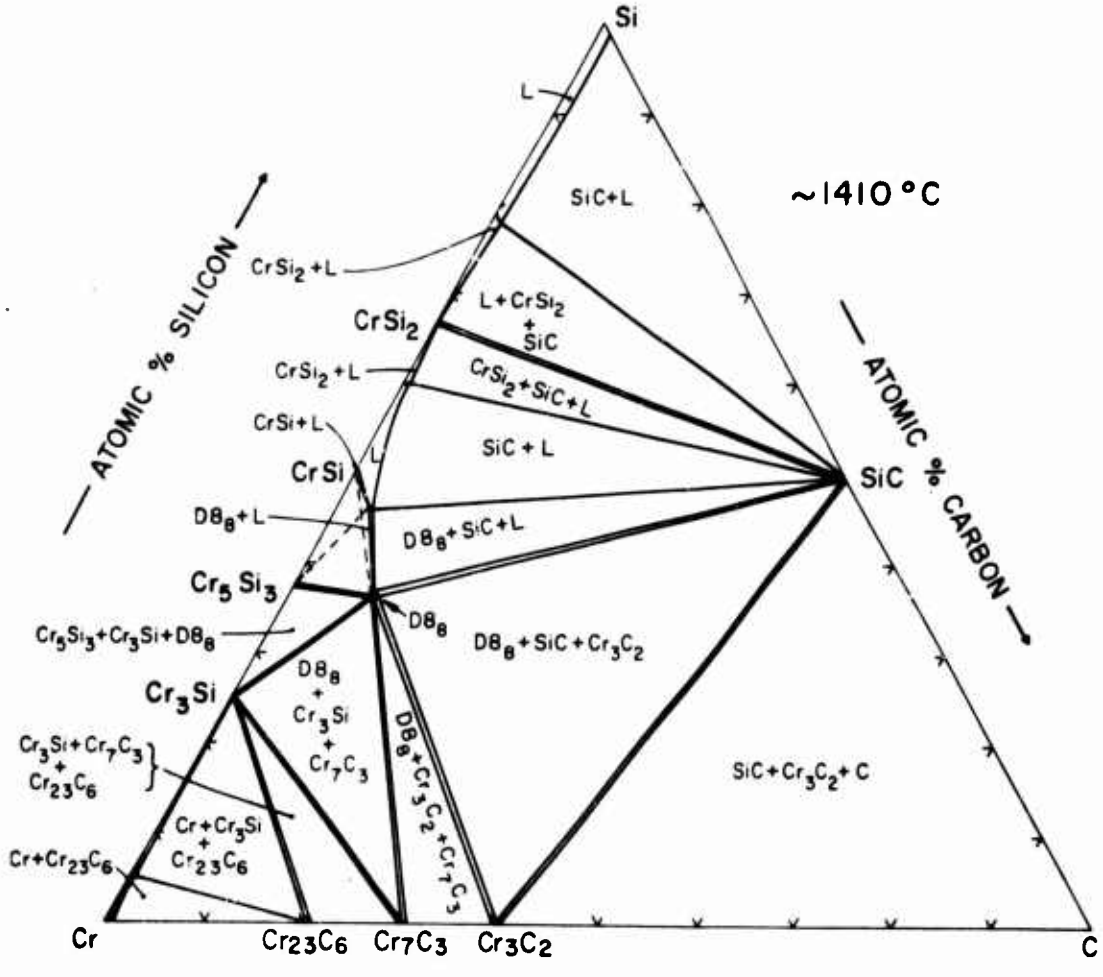

Figure 57. Cr-Si-C: Isotherm at ~1410°C.

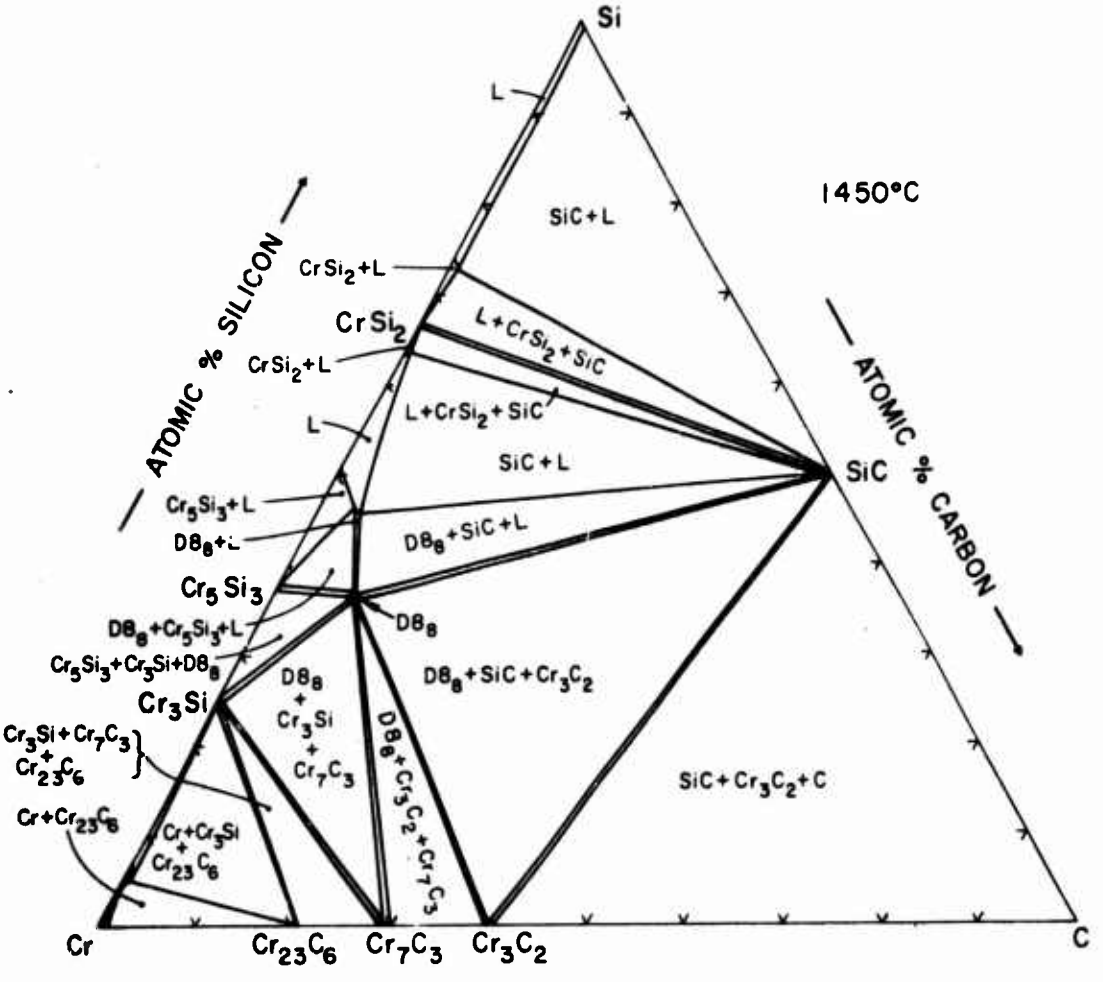

Figure 58. Cr-Si-C: Isotherm at 1450°C.

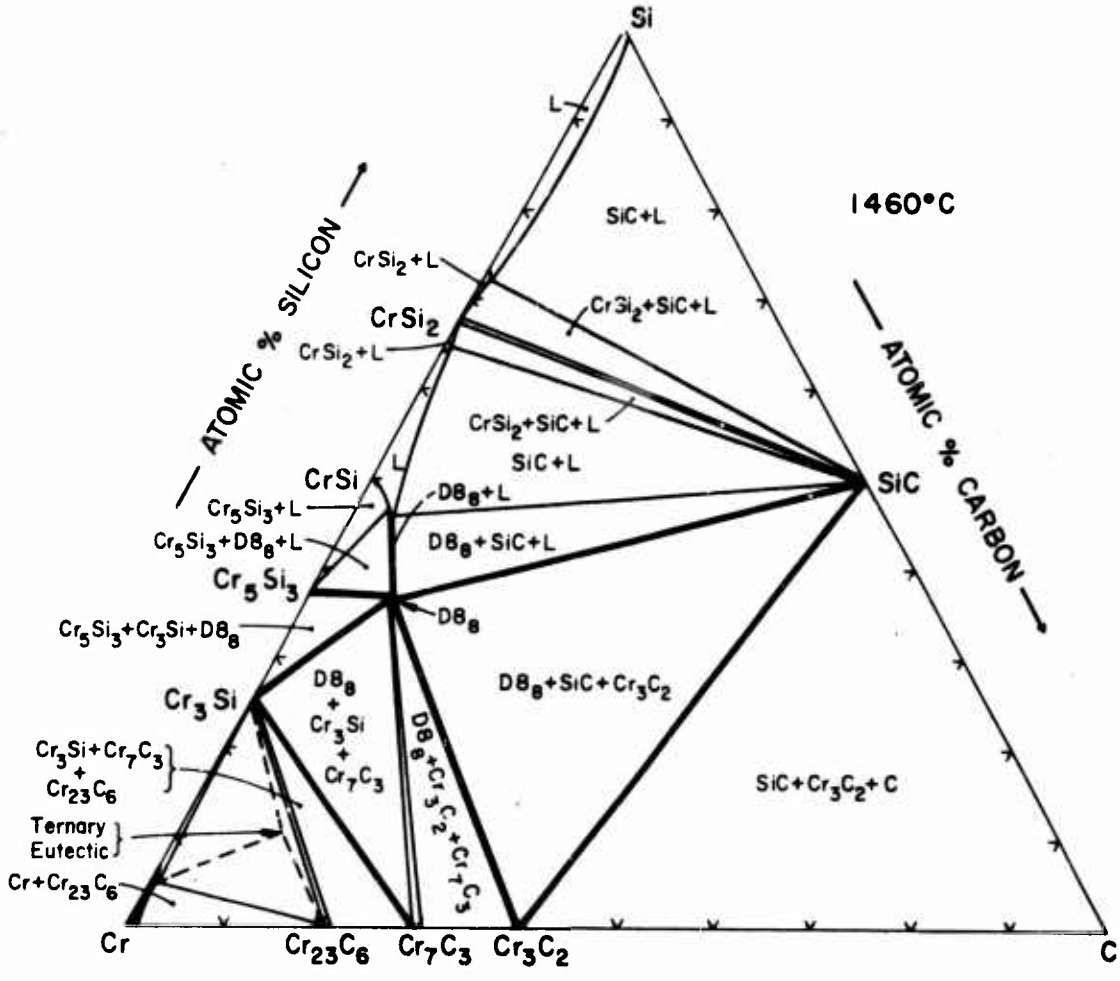

Figure 59. Cr-Si-C: Isotherm at 1460°C.

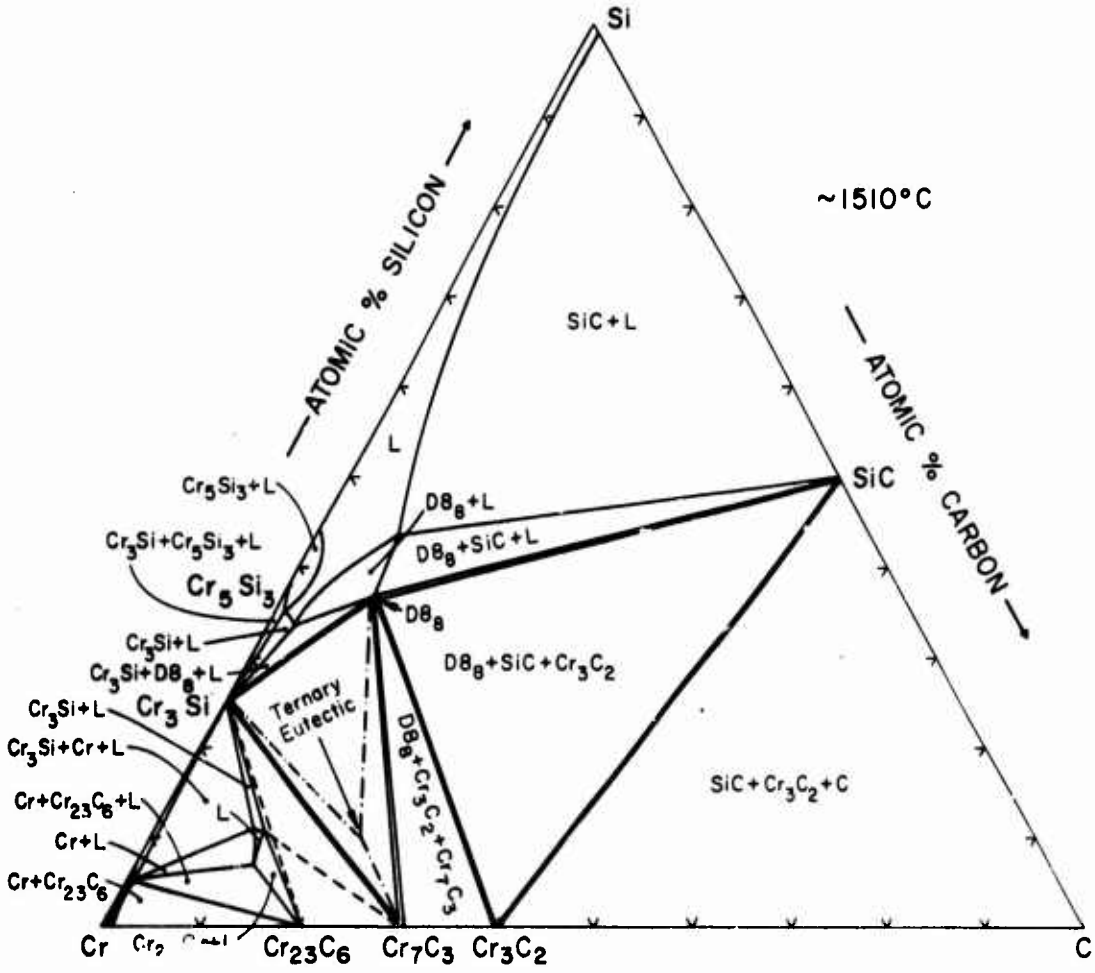

Figure 60. Cr-Si-C: Isotherm at ~1510°C.

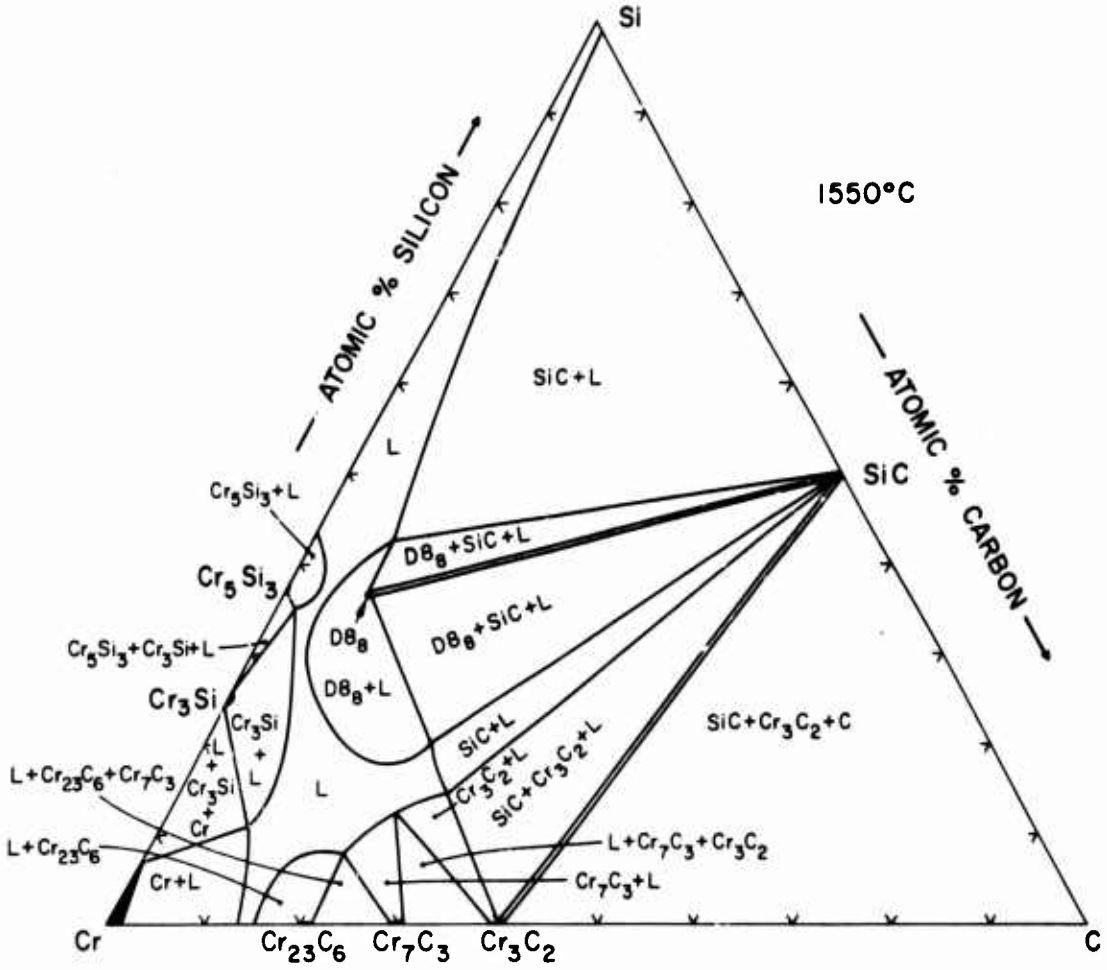

Figure 61. Cr-Si-C: Isotherm at 1550°C.

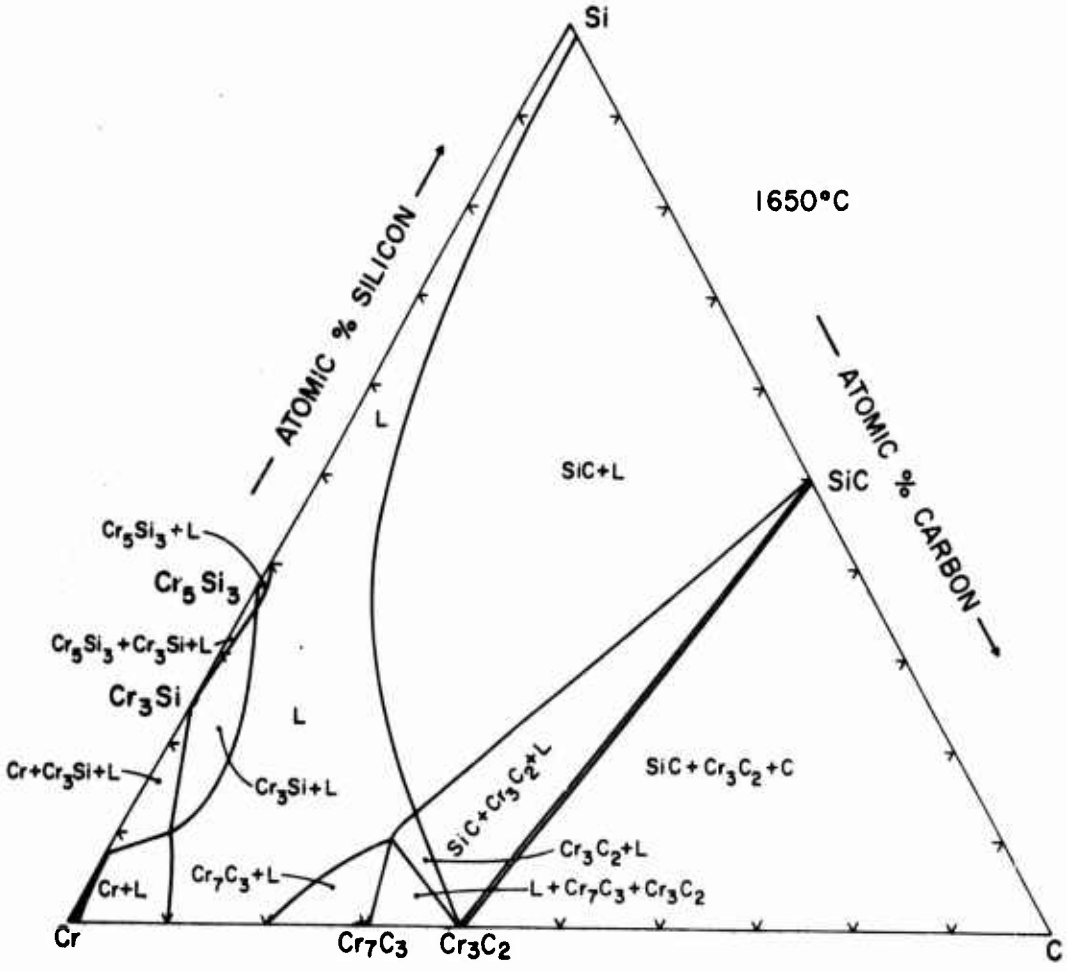

Figure 62. Cr-Si-C: Isotherm at 1650°C.

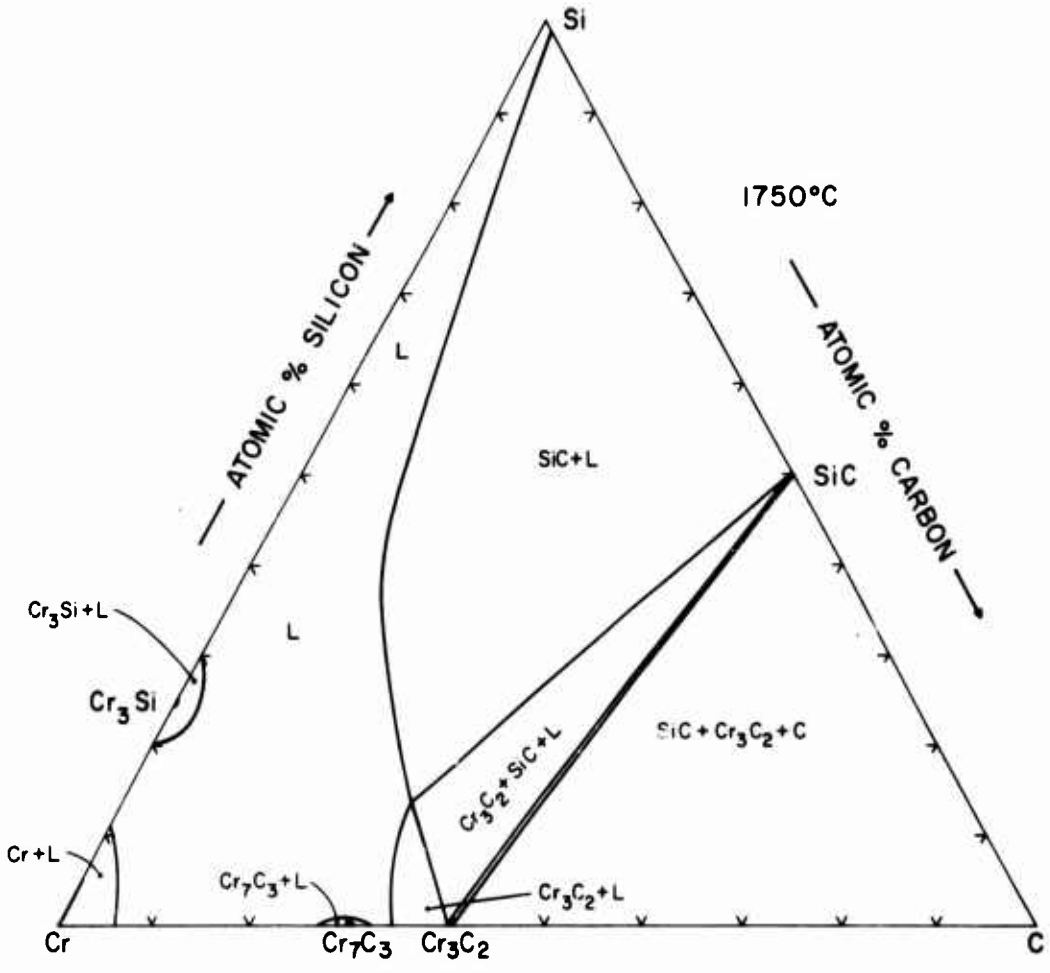

Figure 63. Cr-Si-C: Isotherm at 1750°C.

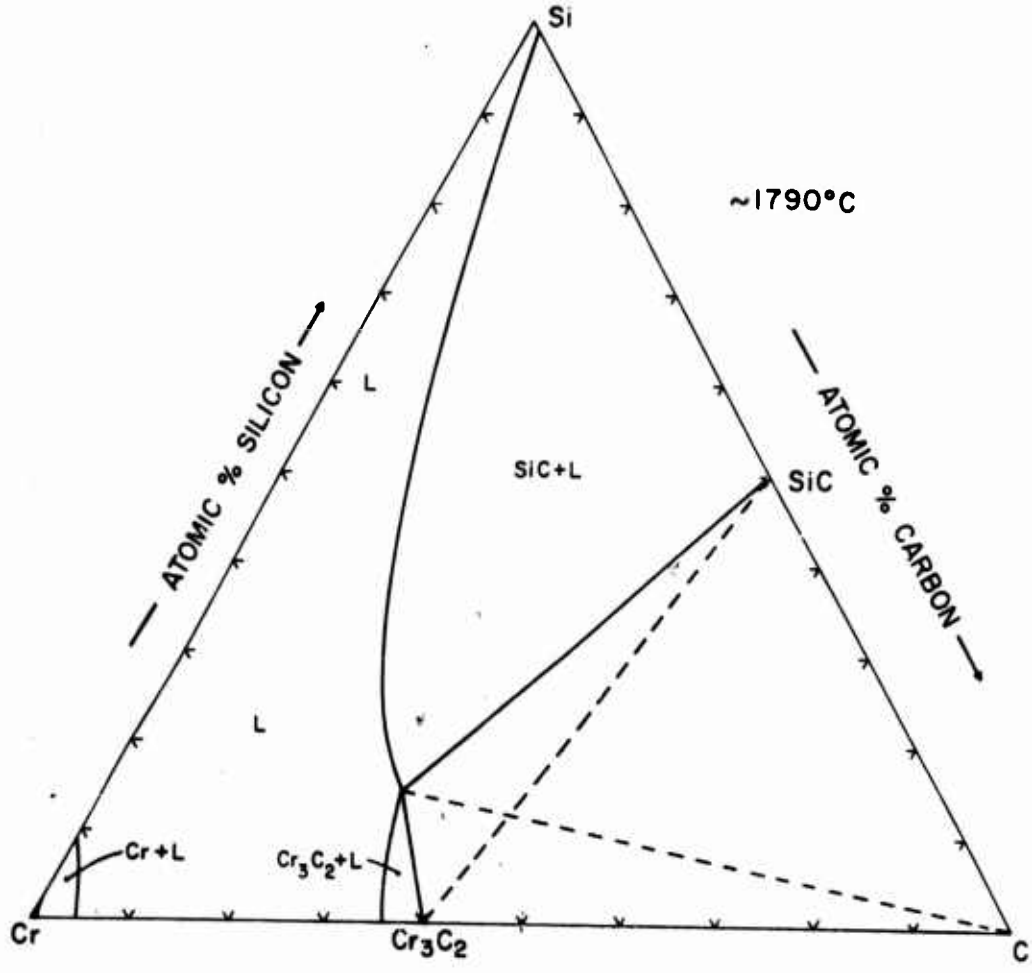

Figure 64. Cr-Si-C: Isotherm at ~1790°C.

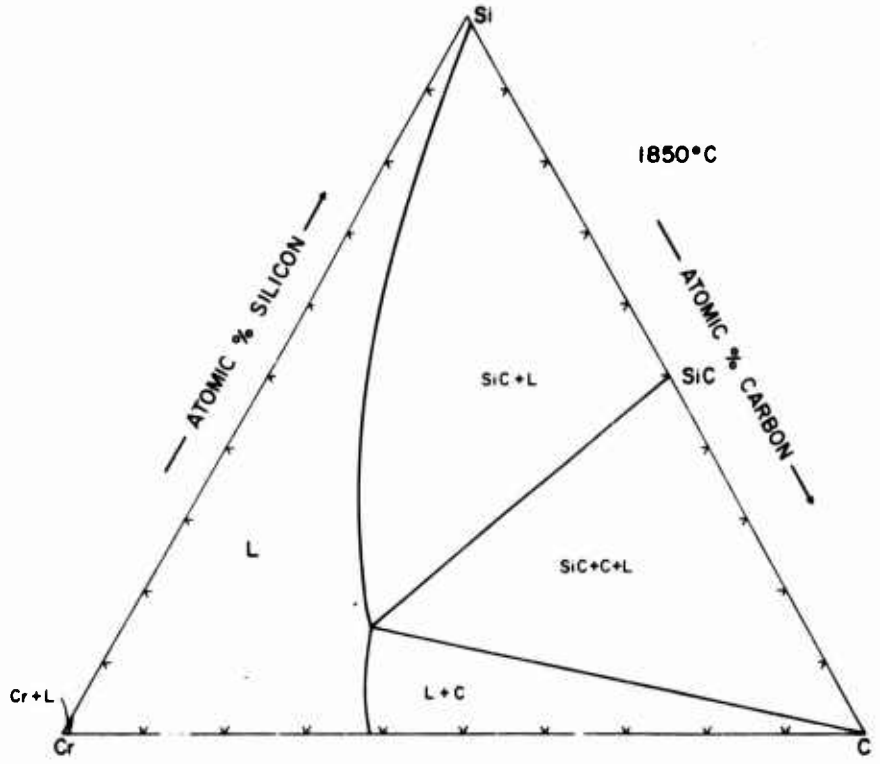

Figure 65. Cr-Si-C: Isotherm at 1850°C.

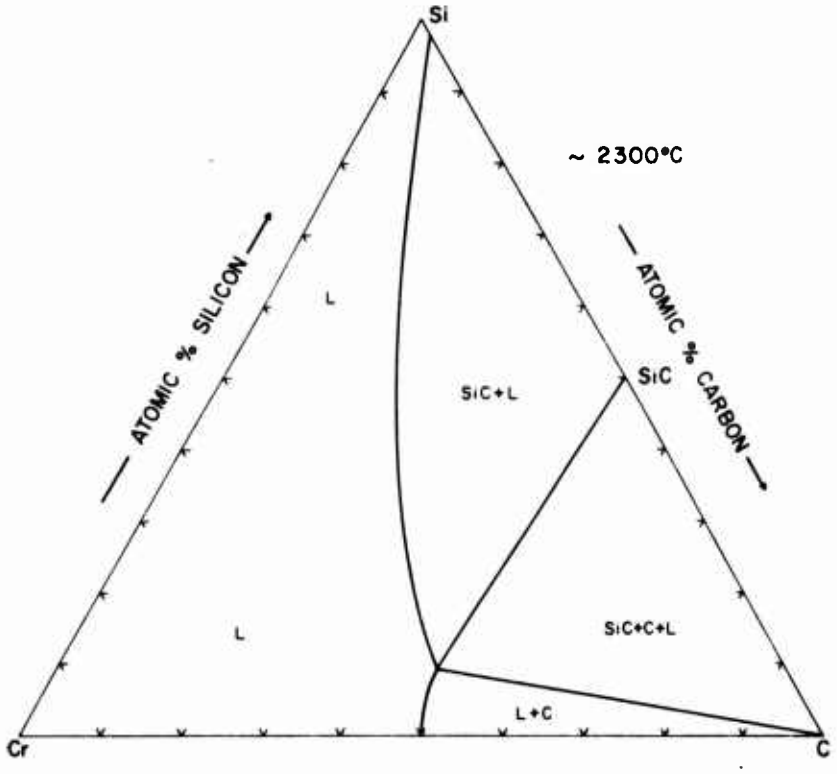

Figure 66. Cr-Si-C: Isotherm at ~2300°C.

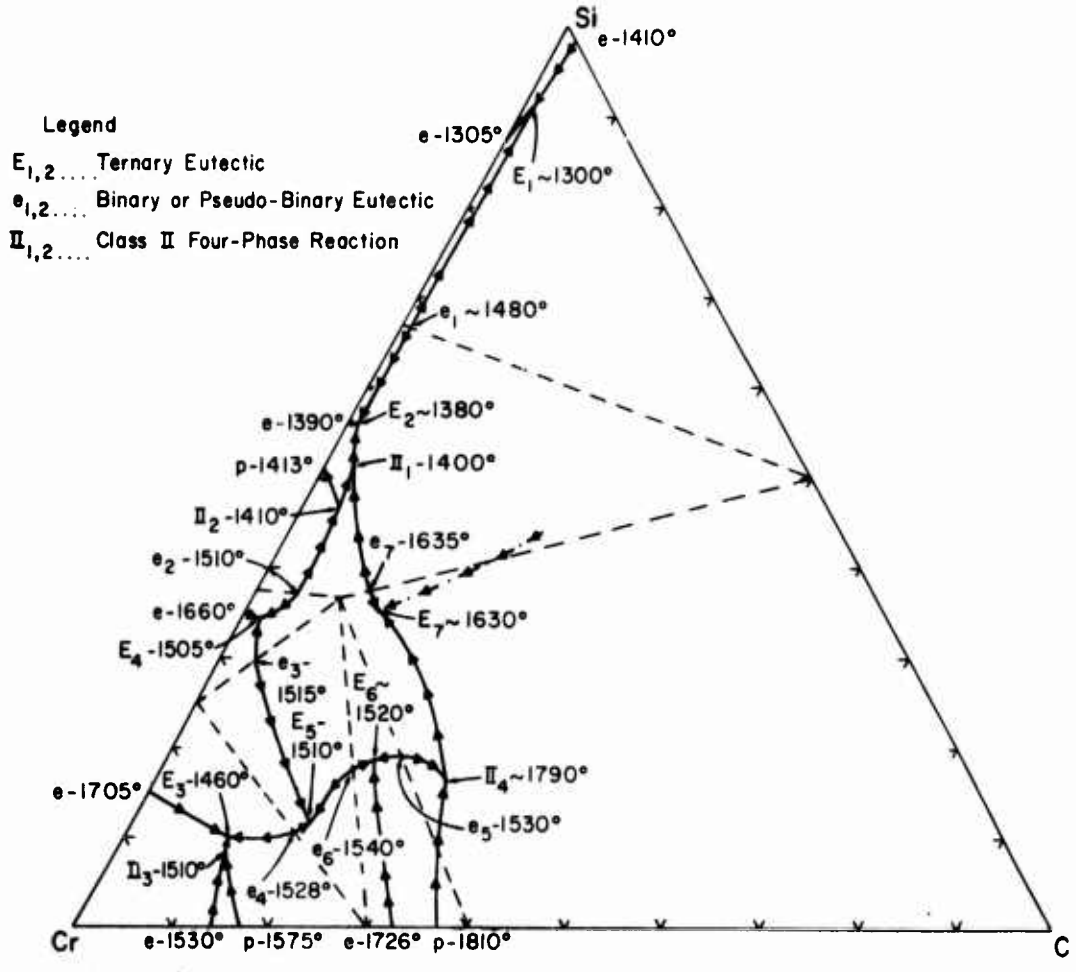

Figure 67. Cr-Si-C: Melting Trough Projections and Isothermal Reactions.

3. Qualitative Kinetic Studies on the Chromium-Silicon Carbide Interaction

Several differential thermal analysis experiments were run under special conditions to check the speed of the interaction between chromium metal and silicon carbide. A cold pressed mixture of 40 Mole % silicon carbide-rest chromium metal was shielded from the D.T.A. graphite sample holder by additional SiC powder. In the D.T.A. unit, this sample was heated at a rate of 5°C/sec. At about 1330°C, a strong exothermic reaction was observed, carrying the temperature rapidly upwards where incipient melting occurred at about 1460°C, the temperature of the ternary, metal-rich Cr_3Si-$Cr_{23}C_6$-Cr eutectic; the sample was practically completely molten at about 1530°C (Figure 68).

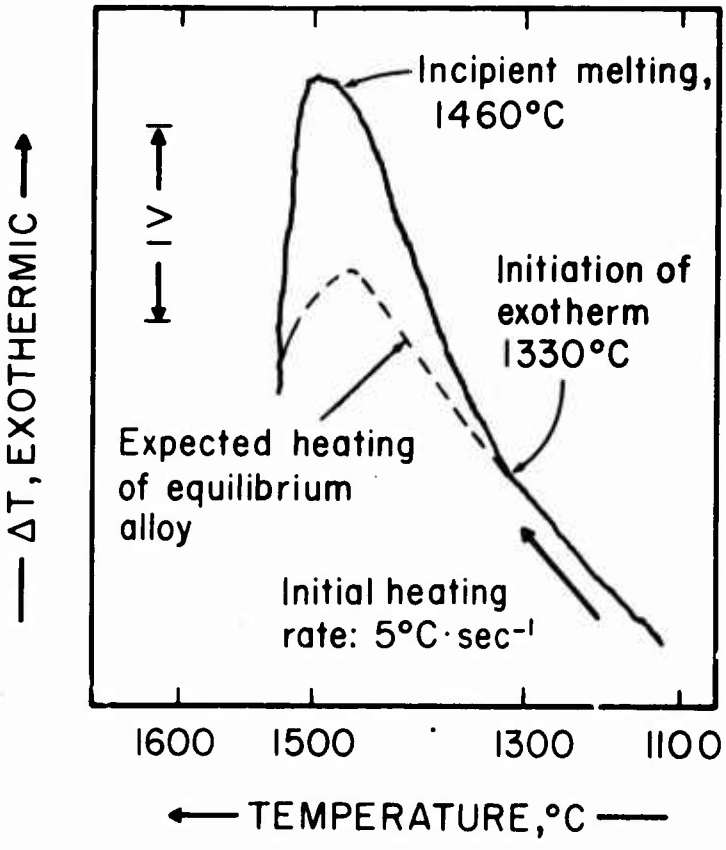

Figure 68. Cr-Si-C: 60/20/20, (40 Mole % SiC) D.T.A. Heating Thermogram Showing Exothermic Reaction to Correct Conjugate Pairs and Ternary Eutectic Melting.

These results were certainly not unexpected in view of the knowledge of the phase equilibria intersection the Cr-SiC join. The exothermic reaction resulted from the irreversible interaction of Cr and SiC to form the correct equilibria. Initial melting occurred, as expected, at or near the chromium-rich eutectic since the lowest melting eutectic along this join appears first. A Debye-Scherrer X-ray photograph of the reaction products showed the presence of $D8_8$ phase, Cr_3C_2, and Cr_7C_3 which is in perfect accord with the phase diagram.

A second experiment in the D.T.A. was performed using the same SiC-shielded Cr-SiC mixture as in the first experiment; the temperature, however, was raised slowly from room temperature to about 1250-1300°C over a period of 1 hour. The sample was held at this temperature for about 2 hours; at no time was a strong exothermic reaction observed. At the completion of the heat treatment, an X-ray of the umelted sample showed complete conversion of the chromium-silicon carbide mixture to $D8_8$ phase, Cr_3C_2, and Cr_7C_3.

The results of these qualitative kinetic experiments show that there is a definite strong interaction between chromium and silicon carbide, even in a short period of time at temperatures some 160°C below the solidus. It is quite likely that it is even possible to grow single crystals of SiC[63] from a carbon-silicon chromium melt. (SiC is in equilibrium with a chromium-rich melt, practically on the Cr-SiC join, at temperatures above about 1550°C.) It is certain, however, that no particular kinetic phenomena are present which would permit the nonequilibrium crystallization of silicon carbide in a chromium-rich metal matrix.

E. THE NICKEL-SILICON-CARBON SYSTEM

1. Solid-State Equilibria

The phase equilibria of this ternary system at temperatures below melting is considerably less complicated than the

chromium-silicon-carbon system; in the nickel-silicon-carbon system there are no ternary phases formed, and the basic ternary phase equilibria in the solid-state is simply a function of the presence of the various binary nickel silicides.

The investigation of the solid-state phase equilibria in the ternary region was complicated by the low melting behavior of the nickel silicides when compared to the high melting point of silicon carbide. Heat treating temperatures had to be chosen low enough to prevent melting of the binary nickel silicides; these temperatures were, however, not nearly high enough to permit sufficient reaction between free silicon and carbon to completely form silicon carbide in those areas of the ternary system where equilibria with SiC occurs, nor were they high enough conversely, to permit the silicon carbide to decompose in the appropriate areas—even under long time heat treatments.

Figure 11 shows the location and conditions of heat treated samples in the ternary Ni-Si-C system. Some of the heat treated samples were hot pressed from elemental powder and Ni_2Si, and some were arc melted portions of melting point samples.

By and large, however, the results of the X-ray analysis of the heat treated samples in the lower melting portion of the ternary system showed that the attainment of equilibrium was in most cases not nearly complete and very slow indeed. The X-ray patterns were multiphased showing sizeable quantities of the starting materials and but little of the equilibrium phases formed in heat treating. For these reasons, then, no figure is presented showing the qualitative X-ray evaluation of solid-state heat-treated samples. Nonetheless, however, owing to the simplicity of the ternary phase equilibria, a clarification of the solid-state equilibria was possible and is presented in an isotherm at 800°C (Figure 69).

It is seen that $NiSi_2$, NiSi, Ni_3Si_2, and δ-Ni_2Si are in equilibrium with SiC, while δ-Ni_2Si, Ni_5Si_2, and Ni_{ss} are in equilibrium with graphite.

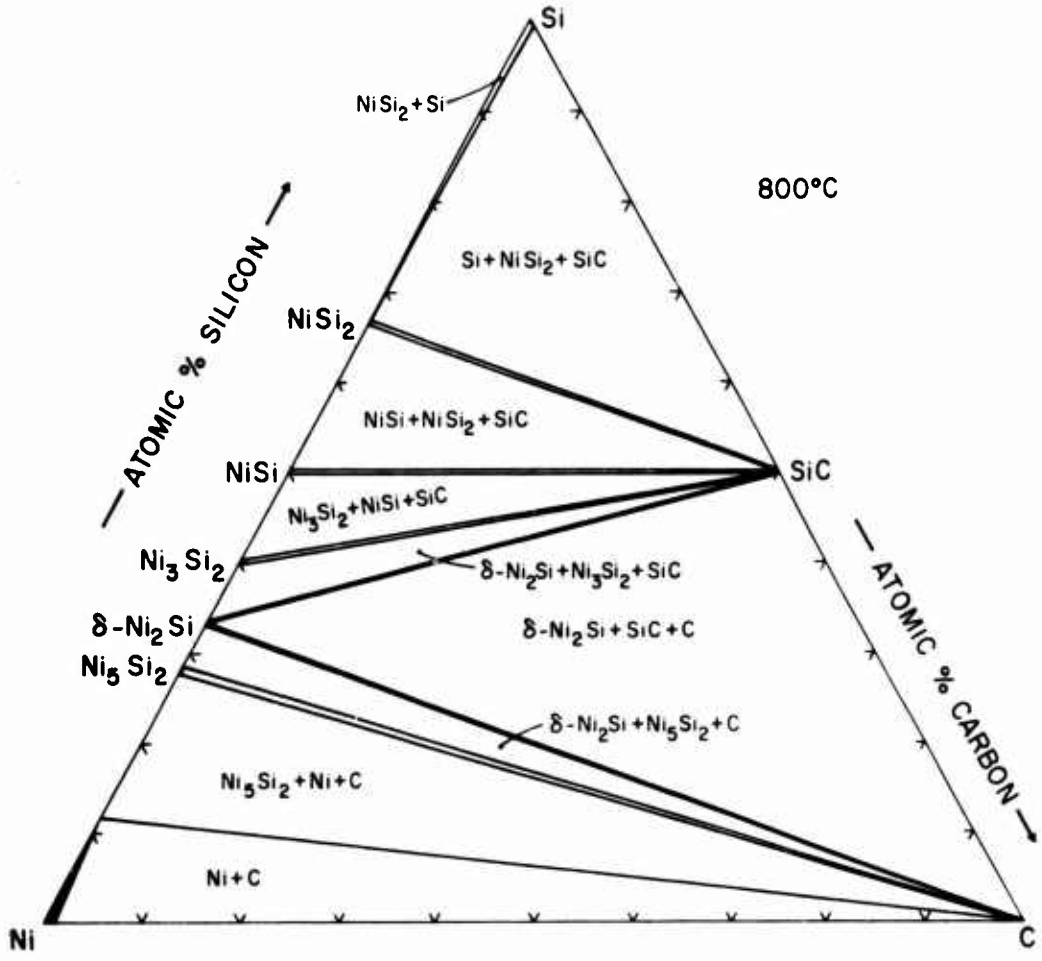

Figure 69. Ni-Si-C: Phase Equilibria at 800°C.

A comparison of all the Debye-Scherrer powder X-ray photographs of the ternary alloys showed that none of the binary silicide phases present in these ternary alloys had lattice parameter changes over the binary values; in addition, since none of the metallographic investigations yielded indications of a temperature dependent solubility, the conclusion is drawn that the nickel silicides do not take either silicon carbide or carbon into solid solution.

One interesting result of the heat treatments was observed in the region near the Ni_3Si phase. Although the rather diffuse lines on the X-ray films of melting point and arc melted samples in this region were not positively identified as belonging to the Cu_3Au structure of Ni_3Si[3][16][17], observation of the X-ray patterns of these same arc melted and melting point specimens subsequently heat treated at 950°C showed that all traces of this pattern had disappeared, and the low temperature three-phase field of Ni_{ss}-Ni_5Si_2-C was definitely established. Excluding the remote possibility of a small three-phase region β_1-Ni_3Si-Ni_5Si_2-Ni_{ss} lying close to the Ni-Si binary which would cut off the appearance of the β_1-Ni_3Si in ternary phase equilibria, it seems as though the Ni_3Si phase is not stable at lower temperatures as also is claimed by other authors[4].

The ternary isothermal section at 800°C does not, therefore, contain any equilibria with the Ni_3Si phase.

Even though only a few D.T.A. experiments were possible in this ternary system (see Section III-D), two binary nickel silicide reactions are presumed to initiate two solid-state, four-phase ternary reactions at temperatures slightly above 800°C.

At about 806°C, the binary eutectoid temperature of δ-Ni_2Si and Ni_3Si_2, a four-phase reaction is presumed to occur with the appearance of θ-Ni_2Si. The most logical description of this reaction is a Class II, four-phase reaction:

$$\theta\text{-}Ni_2Si + SiC \xrightarrow{\sim 806\,^\circ C} Ni_3Si_2 + \delta\text{-}Ni_2Si$$

Both of these Class II reactions can occur under the condition that a vanishingly small silicon carbide solubility is present in the binary nickel silicides, which is most probably the case, be it ever so small. Because of the absence of these physically measurable

solubilities in the binary silicides, a graphical representation of these four-phase reactions in ternary isotherms is not feasible and therefore not depicted. The isotherm at 850°C (Figure 93) shows the phase equilibria after the disappearance of Ni_3Si_2 and the appearance of θ-Ni_2Si.

As stated in the section on the Nickel-Silicon system, under the experimental procedures employed in these investigations, the high temperature θ form of Ni_2Si was never clearly observed in X-ray films of either binary or ternary alloys. Nonetheless, the metallography, shown in subsequent sections, shows the definite transformation structures in the Ni_2Si phase along with the presence of graphite and SiC grains. Since no interaction of either graphite or silicon carbide with the transformed Ni_2Si matrix was detected, the indicated ternary equilibria of the θ-Ni_2Si phase is certainly valid even though this θ phase itself was not retained from temperatures above its transformation and eutectoid decomposition points.

2. High Temperature Phase Equilibria

Melting point determinations and metallographic studies on arc melted alloys along with X-ray evaluation of these samples provided the means of establishing the high temperature isotherms. It must be noted, however, that the liquidus temperatures, by nature of the experimental techniques employed, are generally estimated, although in this system these liquidus temperatures were especially difficult to approximate from the collapsing behavior of the melting point samples because the segregation behavior of the low melting binary silicides described in Section III-C caused a filling of the black body hole before the collapsing temperature could be precisely recorded. Figure 70 shows the compositional location of the ternary Ni-Si-C melting point samples.

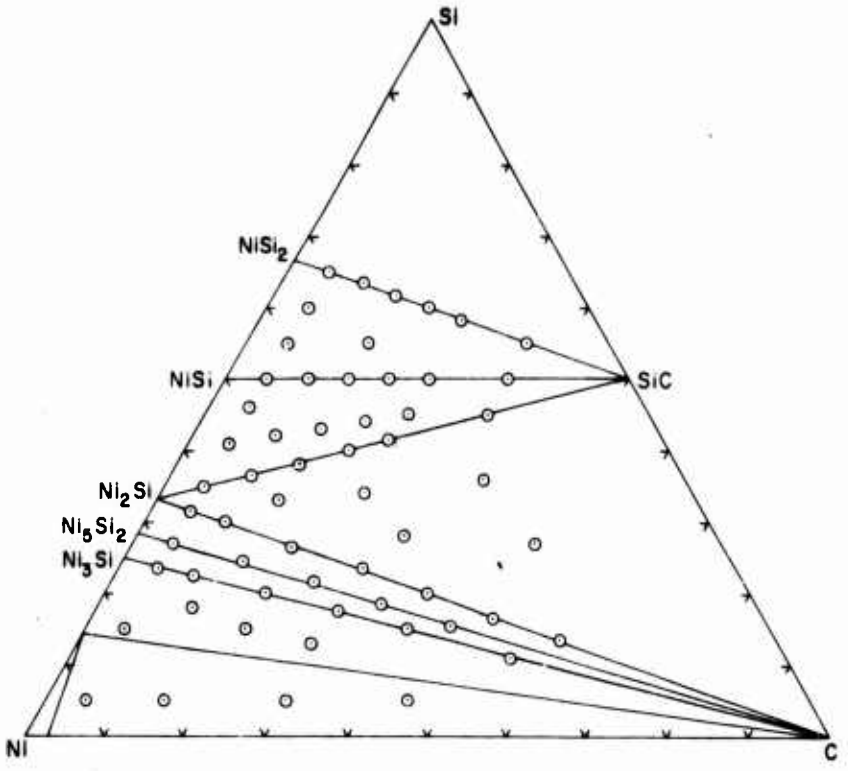

Figure 70. Ni-Si-C: Compositional Location of Melting Point Samples.

a. The Ni_2Si-C Section

Alloys along this pseudo-binary section showed eutectic melting at 1282°C. The eutectic point is located at less than 2.5 Mole % carbon. Figure 71 shows this pseudo-binary eutectic system with experimental melting points, and Figure 72 shows the typical metallographic findings along this section.

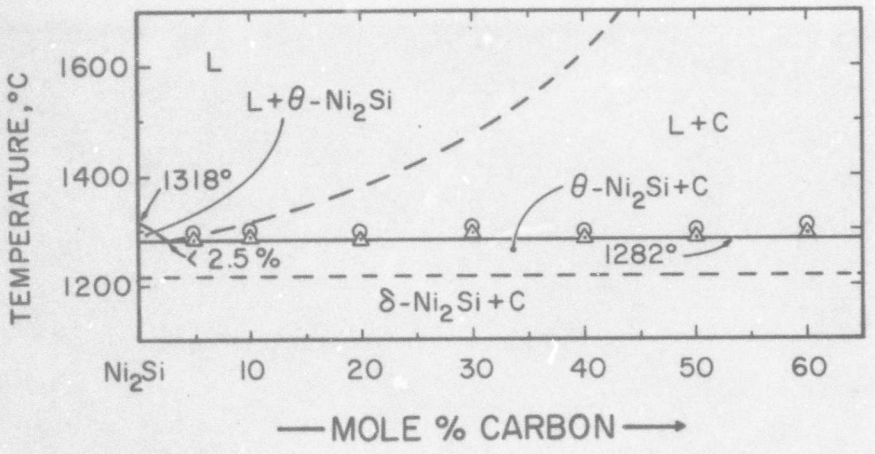

Figure 71. Ni-Si-C: The Ni_2Si-C Pseudo-Binary System.

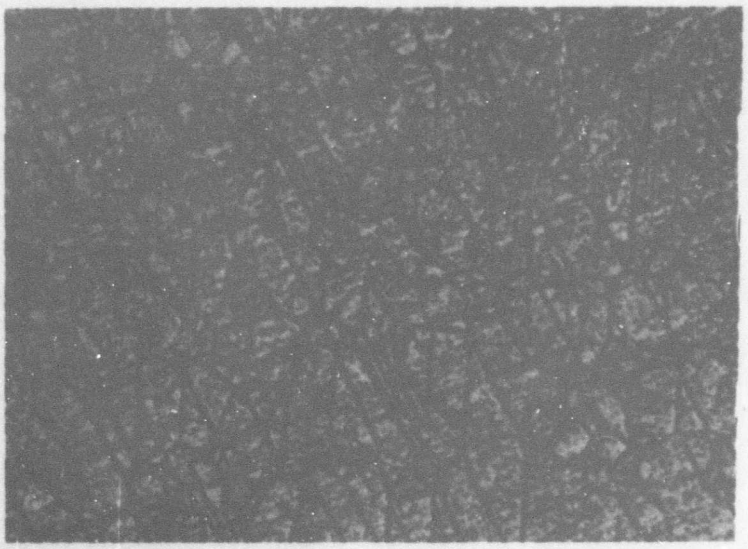

Figure 72. Ni-Si-C: 65/32/3, Photomicrograph of an Arc Melted Alloy. X475

θ-Ni_2Si (Transformed to δ)-Graphite Eutectic. Graphite Visible as Fine Black Dots.

X-ray: δ-Ni_2Si

Figure 73. Ni-Si-C: 60/30/10, Photomicrograph of an Arc Melted Alloy. X175

Primary Graphite in a Matrix of θ-Ni_2Si (Transformed to δ).

X-ray: δ-Ni_2Si + Barest Trace Graphite

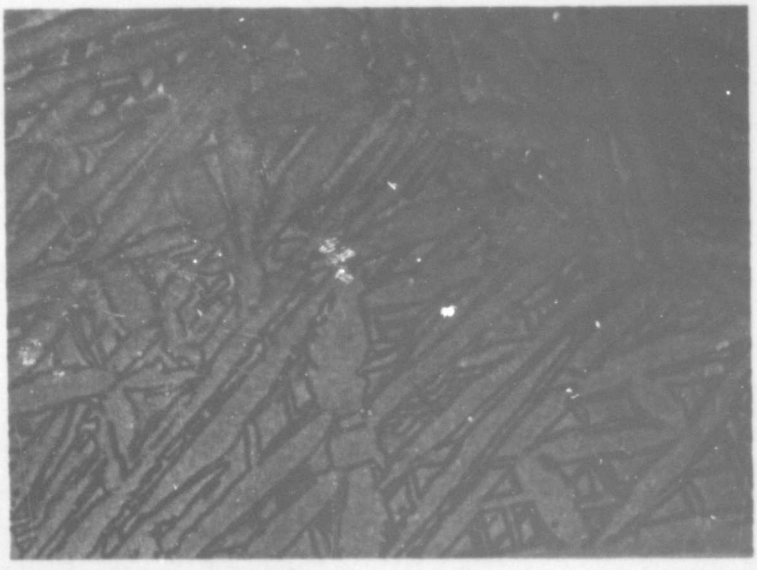

Figure 74. Ni-Si-C: 60/30/10, Photomicrograph of an Arc Melted Alloy. X760

Silicide Portion Without Primary Graphite.

$\theta \longrightarrow \delta$-$Ni_2Si$ Transformation Structure.

b. The Ni_5Si_2-C Section

The Ni_5Si_2 compound, which is in equilibrium with graphite throughout almost its full temperature range, partakes of a pseudo-binary eutectic reaction; the eutectic lies very close to the binary Ni_5Si_2 compound at about 1 Mole % carbon: the eutectic temperature is 1270°C. Figure 75 depicts the pseudo-binary eutectic system with the experimentally measured melting points; the metallographic results of alloys on or near this section showing the low graphite containing eutectic are given in Figures 76 through 78.

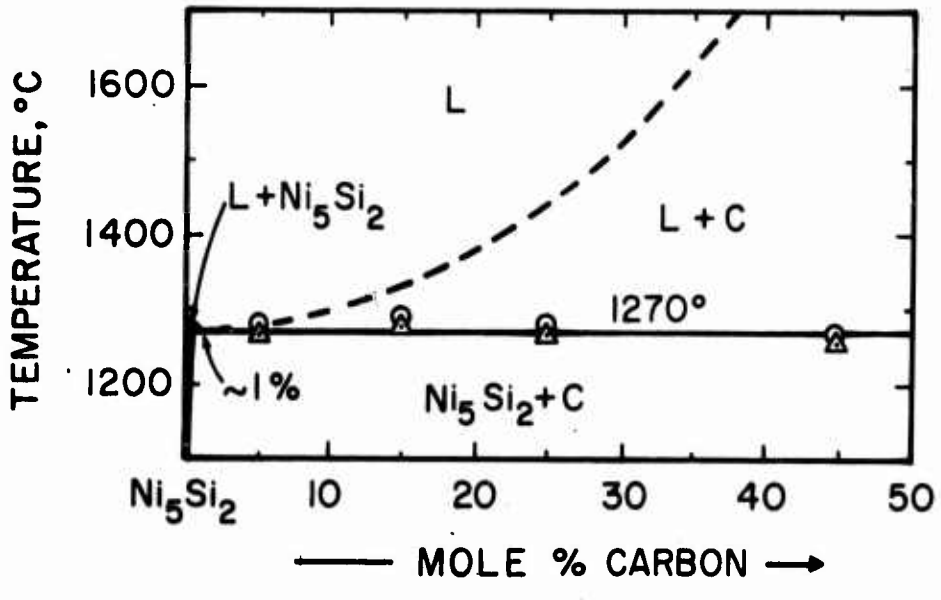

Figure 75. Ni-Si-C: The Ni_5Si_2-C Pseudo-Binary System.

Figure 76. Ni-Si-C: 69.5/28/2.5, Photomicrograph of an Arc Melted Alloy. X475

Primary Ni_5Si_2 with some Amount of Ni_5Si_2-C Eutectic on Grain Boundaries. Small Amounts of White Phase are δ-Ni_2Si.

X-ray: Ni_5Si_2

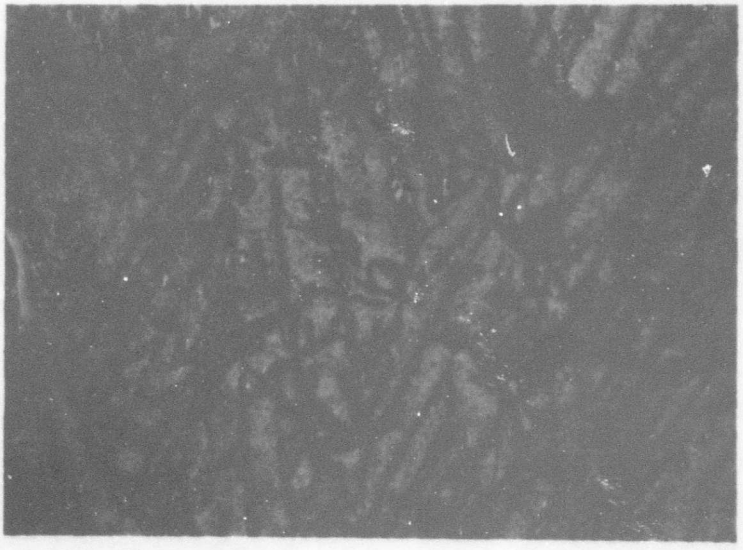

Figure 77. Ni-Si-C: 68.5/27.5/4, Photomicrograph of an Arc Melted Alloy. X150

Co-crystallized Graphite and Ni_5Si_2 in Ni_5Si_2-C Eutectic Matrix with Small Amounts of Annealed θ (Transformed)-Ni_2Si-Ni_5Si_2 Eutectic on Grain Boundaries.

X-ray: Ni_5Si_2

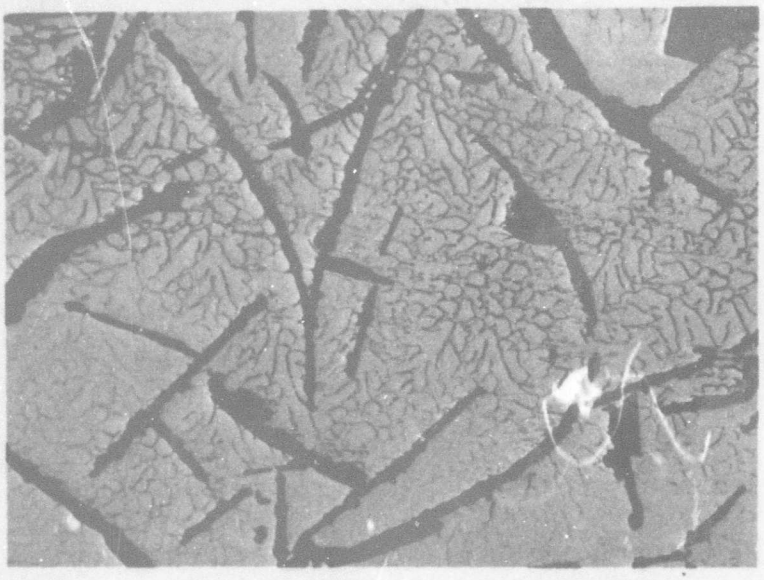

Figure 78. Ni-Si-C: 61/24/15, Photomicrograph of an Arc Melted Alloy. X160

Co-crystallized Graphite Spears and Ni_5Si_2 (Larger White Grains) with Annealed Ni_5Si_2-θ (Transformed)-Ni_2Si Eutectic Between Grains.

X-ray: Ni_5Si_2 + Trace Graphite and Trace $\theta \longrightarrow \delta$ Transformed Ni_2Si

c. The Ni-C-Ni_3Si Region

In the metal-rich portion of the ternary system a ternary eutectic among nickel, graphite, and Ni_3Si was found at a composition of about $Ni_{78}Si_{19}C_3$; the melting temperature of this ternary eutectic as determined from Pirani melting point specimens is close to 1145°C. The location of this ternary eutectic which is described by a Class I reaction:

$$\text{Liquid} \xrightarrow{\sim 1145°C} Ni_{ss} + Ni_3Si + \text{Graphite}$$

is shown in Figures 97 and 103. The microstructures of alloys near this ternary eutectic and also near the Ni-C eutectic trough (Figure 103) are shown in Figures 79 through 82.

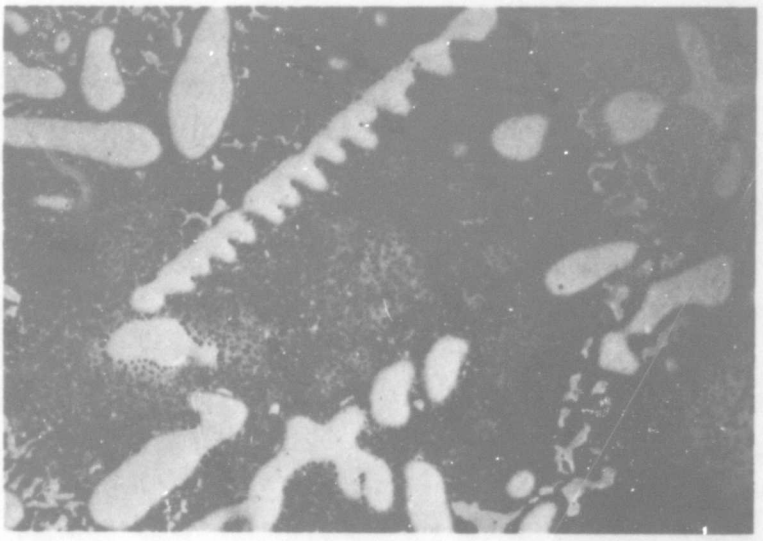

Figure 79. Ni-Si-C: 80/15/5, Photomicrograph of an Arc Melted Alloy. X600

Primary Ni_{ss}-Dendrites in a Ternary Eutectic Matrix of Ni_{ss}, Ni_3Si, and Graphite.

X-ray: Ni_{ss} + Ni_3Si (Diffuse, Probably Decomposing to Ni_{ss} and Ni_5Si_2) Graphite Undetected

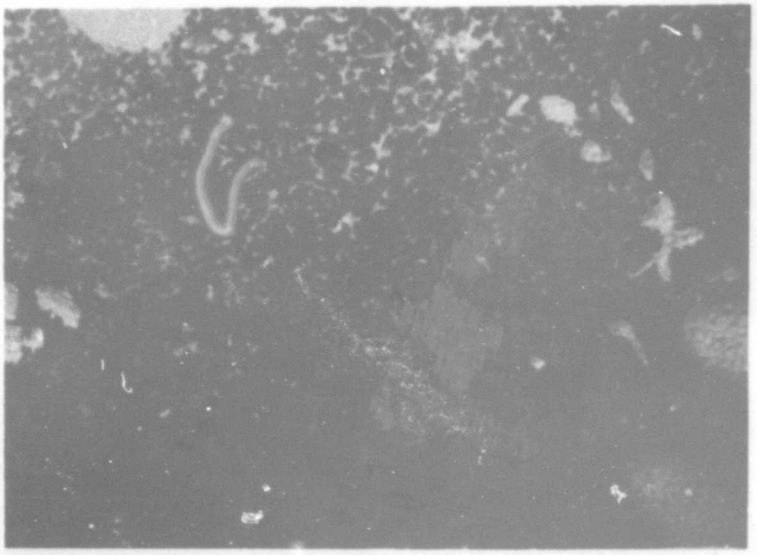

Figure 80. Ni-Si-C: 80/15/5, Photomicrograph of an Arc Melted Alloy. X2500

Enlarged View of Ternary Ni_{ss}-Ni_3Si-Graphite Eutectic Portion with some Ni_{ss} Primary Grains.

X-ray: Ni_{ss} + Ni_3Si (Diffuse, Probably Decomposing to Ni_{ss} and Ni_5Si_2) Graphite Undetected.

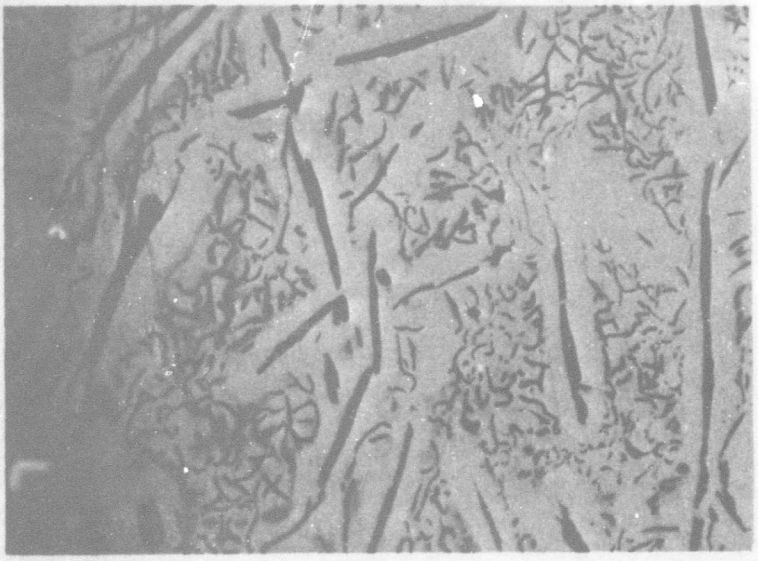

Figure 81. Ni-Si-C: 80/5/15, Photomicrograph of an Arc Melted Alloy. X440

Primary Graphite in Ni_{ss}-Graphite Eutectic—Note Partial Divorcing and Agglomeration Tendency of Graphite.

X-ray: Ni_{ss} + Little Graphite

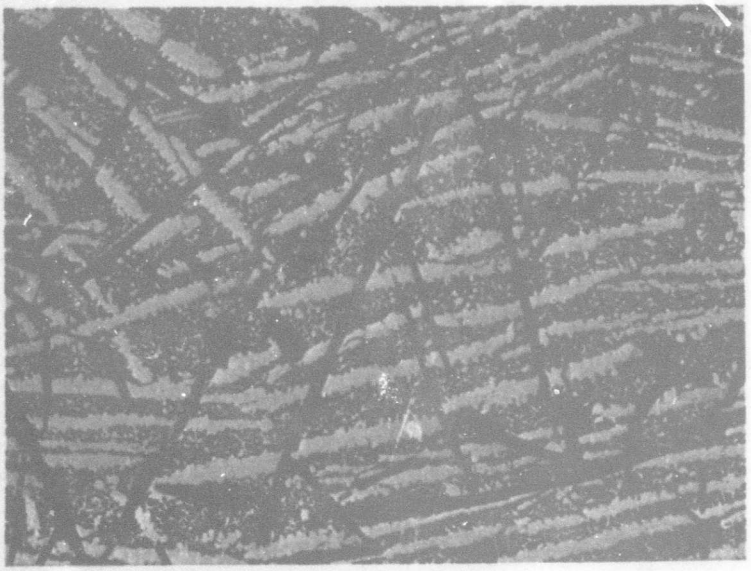

Figure 82. Ni-Si-C: 70/18/12, Photomicrograph of an Arc Melted Alloy. X95

Co-crystallized Graphite and Ni_{ss} in Eutectic Matrix of Ni_{ss}-Ni_3Si.

X-ray: Ni_{ss} + Little Graphite, Ni_3Si, Ni_5Si_2. (From Transformation of Ni_3Si to Ni_{ss} and Ni_5Si_2)

Two other four-phase reactions are presumed to occur in this region of the ternary system; they could not, however, be confirmed because of the limited range of the high temperature D.T.A. equipment employed.

Under the assumption that the Ni_3Si phase is stable only in a small temperature range and decomposes in a eutectoid reaction as stated by other authors[2][4][67] and appears to be indicated in these investigations; a Class II, four-phase reaction is the best choice for describing the disappearance of the Ni_3Si phase and its equilibrium with graphite (under the assignment of a very slight graphite solubility to Ni_3Si) at some temperature near 1120°C:

$$Ni_3Si + \text{Graphite} \xrightarrow{\sim 1120^\circ C} Ni_{ss} + Ni_5Si_2$$

Since this reaction based on unconfirmed reports in the open literature, it is not indicated in the isothermal sections.

The third, four-phase reaction occurring in this region involves the disappearance of the Ni_3Si from ternary equilibria prior to its peritectic melting at about 1160°C, a temperature slightly below the binary peritectic isotherm of this phase (1165°C). The Class II reaction is:

$$\text{Liquid} + Ni_5Si_2 \xrightarrow{\sim 1160^\circ C} Ni_3Si + \text{Graphite}$$

This four-phase reaction is depicted in a Ni-Si-C isotherm at ~1160°C (Figure 98) and in the melting trough projection (Figure 103). The metallographic evidence of this four-phase reaction is shown in Figure 83 below.

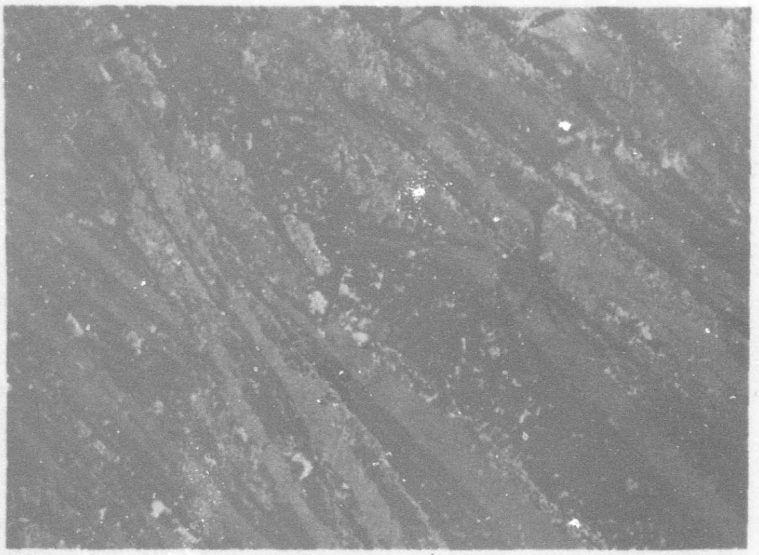

Figure 83. Ni-Si-C: 71/24/5, Photomicrograph of an Arc Melted Alloy. Polarized Light X190

Four-Phase Reaction Mixture: Graphite, Ni_3Si, Ni_5Si_2, and Nickel.

Graphite (Black Streamers) and Ni_5Si_2 (Smooth Grey) in Rest Eutectic Matrix of Ni-Ni_3Si. Peritectic Walls (Speckled, Darker Grey) of Ni_3Si Surrounding Ni_5Si_2 Grains.

X-ray: Ni_5Si_2 (Diffuse) + Some Ni_{ss} + Some Ni_3Si (Diffuse); Graphite Undetected

d. The Ni_2Si-SiC-Si Region

Aside from the melting point results which showed that all ternary alloys had low melting points corresponding for all practical purposes to the melting temperatures of the binary nickel-silicon system, metallographic studies showed the primary or co-crystallization of silicon carbide superimposed on the matrices of the nickel-silicon alloys. In this manner, almost all of the reported characteristics of the nickel-silicon constitution diagram were verified.

e. The Ni_2Si-Ni_3Si_2-NiSi-SiC Region

The temperature dependent solubility boundary on the nickel-rich side of the θ-Ni_2Si phase, the eutectoid decomposition of the θ-Ni_2Si phase, and the eutectic between NiSi and θ-Ni_2Si were well documented while establishing the ternary equilibria of these phases with graphite and silicon-carbide. The following metallographic pictures show not only the ternary equilibria, but also portray the binary nickel-silicon reactions.

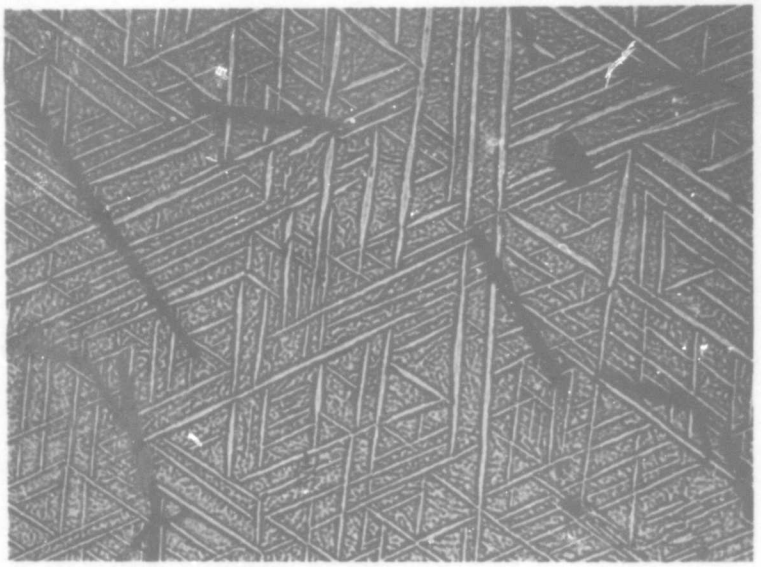

Figure 84. Ni-Si-C: 60/35/5, Photomicrograph of an Arc Melted Alloy. X600

Primary Graphite in an Originally θ-Ni_2Si Matrix.

Matrix shows Pro-eutectoid Ordered Precipitations of δ-Ni_2Si (White Spears) in Background of Rippled θ-$Ni_2Si \longrightarrow \delta$-$Ni_2Si + Ni_3Si_2$ Eutectoid Structure.

X-ray: δ-Ni_2Si+Ni_3Si_2

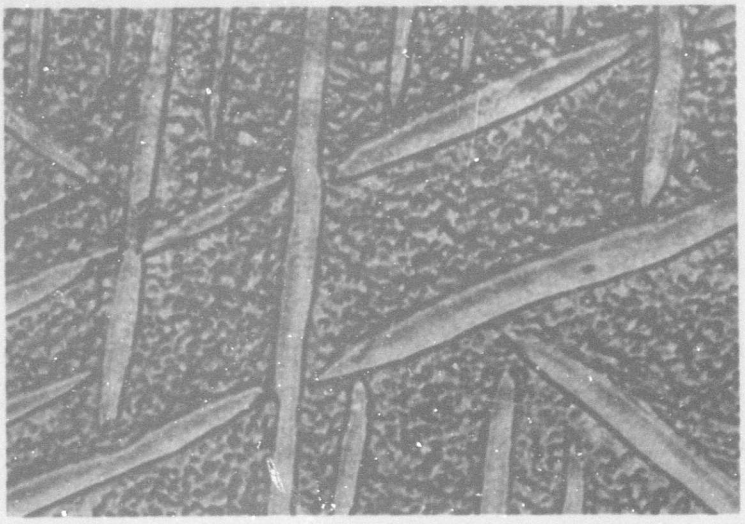

Figure 85. Ni-Si-C: 60/35/5, Photomicrograph of an Arc Melted Alloy. X2500

Nickel-Silicon Binary Portion: Pro-eutectoid Ordered δ-Ni_2Si Precipitates in Matrix of Rippled θ-Ni_2Si ⟶ δ-Ni_2Si + Ni_3Si_2 Eutectoid Structure.

X-ray: δ-Ni_2Si + Ni_3Si_2

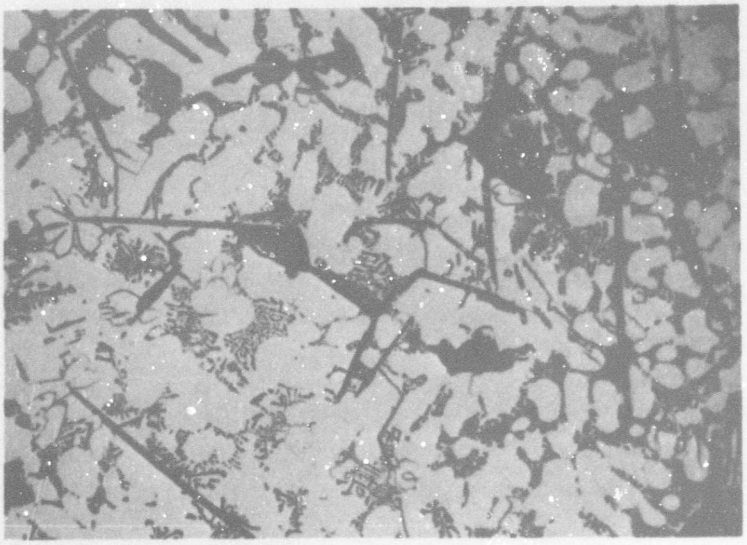

Figure 86. Ni-Si-C: 53.5/36.5/10, Photomicrograph of an Arc Melted Alloy. X600

Co-crystallized θ-Ni_2Si (White Grains) and Graphite Spears with θ-Ni_2Si-NiSi Eutectic on Grain Boundaries.

θ-Ni_2Si in Both White Grains and Eutectic Transformed to δ-Ni_2Si, NiSi, and Ni_3Si_2 by Eutectoid and Peritectoid Reactions Which are not Resolved.

X-ray: Ni_3Si_2 + δ-Ni_2Si + Little NiSi.

Figure 87. Ni-Si-C: 53.5/36.5/10, Photomicrograph of an Arc Melted Alloy. X2000

Co-crystallized θ-Ni_2Si (Grey) and Graphite (Heavy-Dark Spears) with θ-Ni_2Si-NiSi Eutectic on Grain Boundaries.

θ-Ni_2Si in Both Grey Grains and in Eutectic Shows Rippled θ-$Ni_2Si \longrightarrow \delta$-$Ni_2Si + Ni_3Si_2$ Eutectoid Structure.

X-ray: Ni_3Si_2 + δ-Ni_2Si + Little NiSi

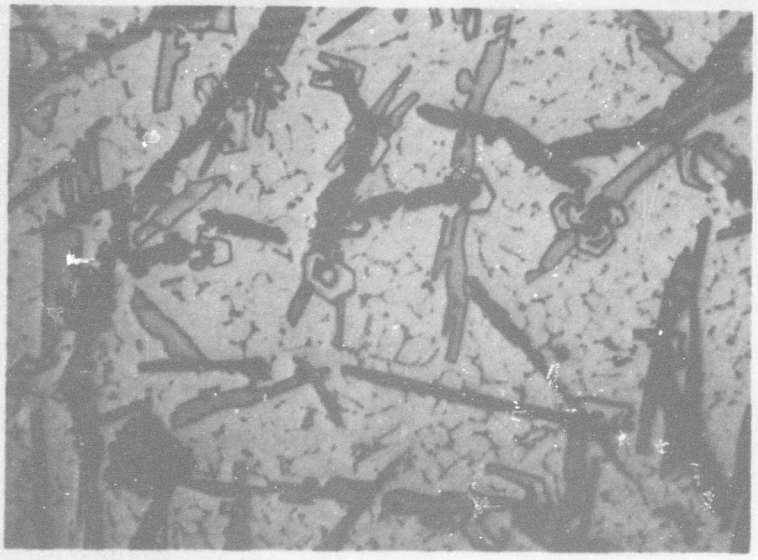

Figure 88. Ni-Si-C: 47/38/15, Photomicrograph of an Arc Melted Alloy. X60

Co-crystallized Graphite (Black Spears), Silicon Carbide (Grey Grains) and θ-Ni_2Si with θ-Ni_2Si-NiSi Eutectic on Grain Boundaries of θ-Ni_2Si Grains.

Eutectoid Decomposition of θ-Ni_2Si to δ-Ni_2Si and Ni_3Si_2 as well as Peritectoid Formation of Ni_3Si_2 from θ-Ni_2Si and NiSi Unresolved.

X-ray: Ni_3Si_2 + NiSi + Traces of Graphite and SiC

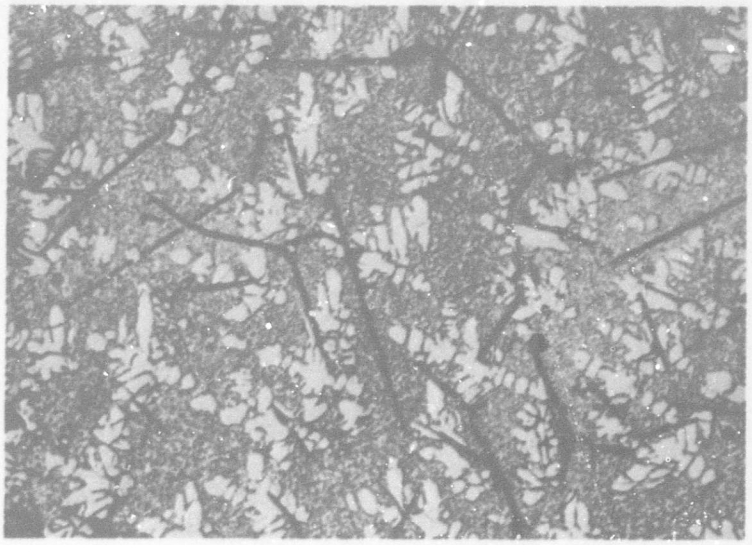

Figure 89. Ni-Si-C: 49/46/5, Photomicrograph of an Arc Melted Alloy. X160

Co-crystallized SiC (Dark Spears) and NiSi (White Grains) in Matrix of NiSi-θ-Ni_2Si (Transformed) Eutectic. Peritectoid Formation of Ni_3Si_2 from θ-Ni_2Si and NiSi not Resolved.

X-ray: Ni_3Si_2 + NiSi

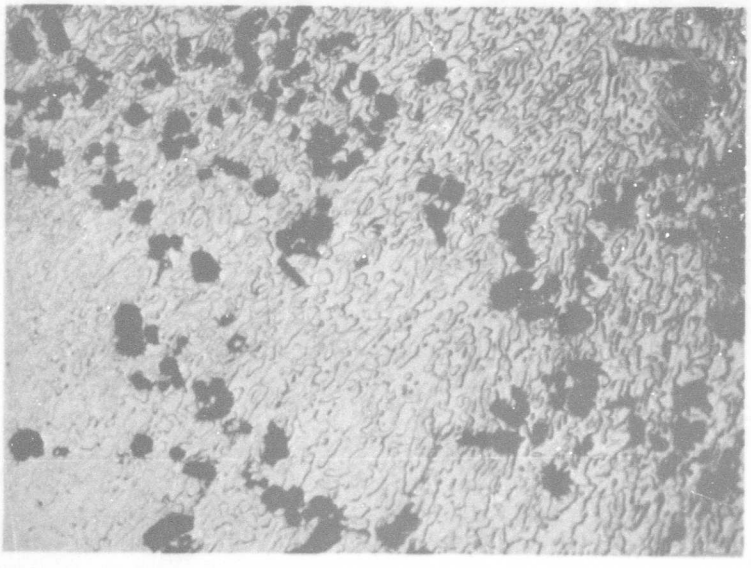

Figure 90. Ni-Si-C: 40/55/5, Photomicrograph of an Arc Melted Alloy. X600

Primary Silicon Carbide (Black Grains) in an Annealed $NiSi_2$-NiSi Eutectic Matrix.

X-ray: $NiSi_2$ + NiSi

f. The $NiSi_2$-SiC-Si Region

In this section of the ternary system a four-phase reaction involving the disappearance of the $NiSi_2$-SiC solid-state equilibrium with increasing temperature is present. The Class II, four-phase reaction is shown in Figures 95 and 103 and is described by:

$$\text{Liquid} + \text{Si} \xrightarrow{\sim 993^\circ C} NiSi_2 + SiC$$

The photomicrograph of the four-phase reaction mixture is shown in the following figure.

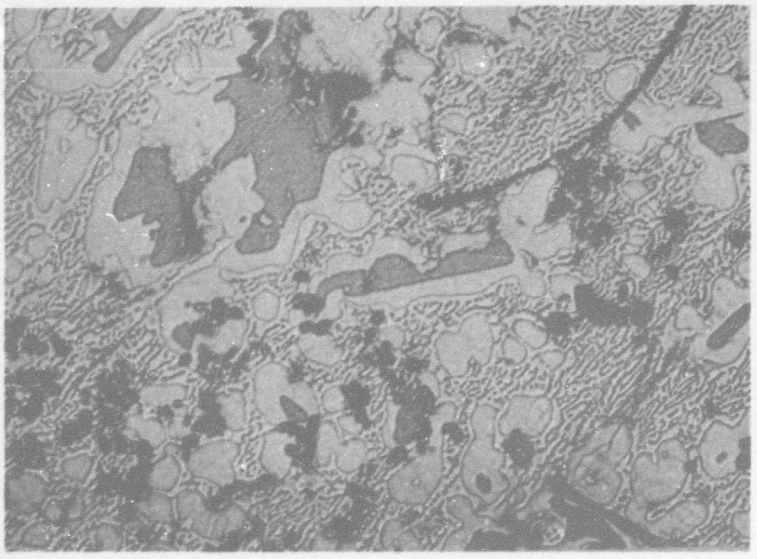

Figure 91. Ni-Si-C: 35/60/5, Photomicrograph of an Arc Melted Alloy X480

Co-crystallized Silicon Carbide (Black Grains and Spears) and Silicon (Grey) in a Partially Agglomerated $NiSi_2$-NiSi Eutectic Matrix. Peritectic Formation of $NiSi_2$: Note Walls of $NiSi_2$ (White) Surrounding Silicon Grains (Grey).

X-ray: $NiSi_2$ + Little Si + Little NiSi

g. Other Four-Phase Reactions in the Nickel-Silicon Carbon System

As stated in one of the Cr-Si-C sections of this report (see Section IV-D-2-n), there are certain four-phase reactions, which, for the reasons presented previously, are very difficult to detect and experimentally confirm; such is the case in the Nickel-Silicon-Carbon system. There are four such four-phase reactions, all belonging to the Class I ternary eutectic grouping. These reactions are indicated in Figure 103 and listed in Table XXIV; it must be stated that these reactions probably lie even closer to the nickel-silicon binary than pictorial clarity permits.

Table XXIV. Undetected Probable Four-Phase Reactions in the Nickel-Silicon-Carbon System.

Reaction	Class	Approximate Temperature °C	Remarks
$L \longrightarrow Ni_5Si_2 + \theta\text{-}Ni_2Si + C$	I	1260	Ternary Eutectic
$L \longrightarrow \theta\text{-}Ni_2Si + SiC + C$	I	1280	Ternary Eutectic
$L \longrightarrow \theta\text{-}Ni_2Si + NiSi + SiC$	I	964	Ternary Eutectic
$L \longrightarrow NiSi + NiSi_2 + SiC$	I	966	Ternary Eutectic

In addition, again for the same reasons noted in Section IV-D-2-n, the following pseudo-binary eutectic reactions must occur in the ternary region even though the respective eutectic points are located so exceptionally close to the nickel silicon binary side that they escape detection.

$$\text{Liquid} \xrightarrow{\sim 1300^\circ C} \theta\text{-}Ni_2Si + SiC$$

and

$$\text{Liquid} \xrightarrow{\sim 992^\circ C} NiSi + SiC.$$

h. Assembly of the Phase Diagram

Again, as in the case of the Cr-Si-C system, all the experimental information, including the proposed, undetected four-phase reactions was used in drawing the isotherms of the Nickel-Silicon-Carbon ternary system presented in Figures 92 through 102. These isotherms were used, in turn, to prepare the three dimensional space model (Figure 4). As a final presentation, a melting trough projection including the pseudo-binary eutectics and four-phase reactions in the ternary system is given (Figure 103). One trough arm of the probable ternary eutectic among θ-Ni_2Si, SiC, and graphite is drawn dashed to indicate other four-phase reactions at much higher temperatures toward the silicon-carbon side.

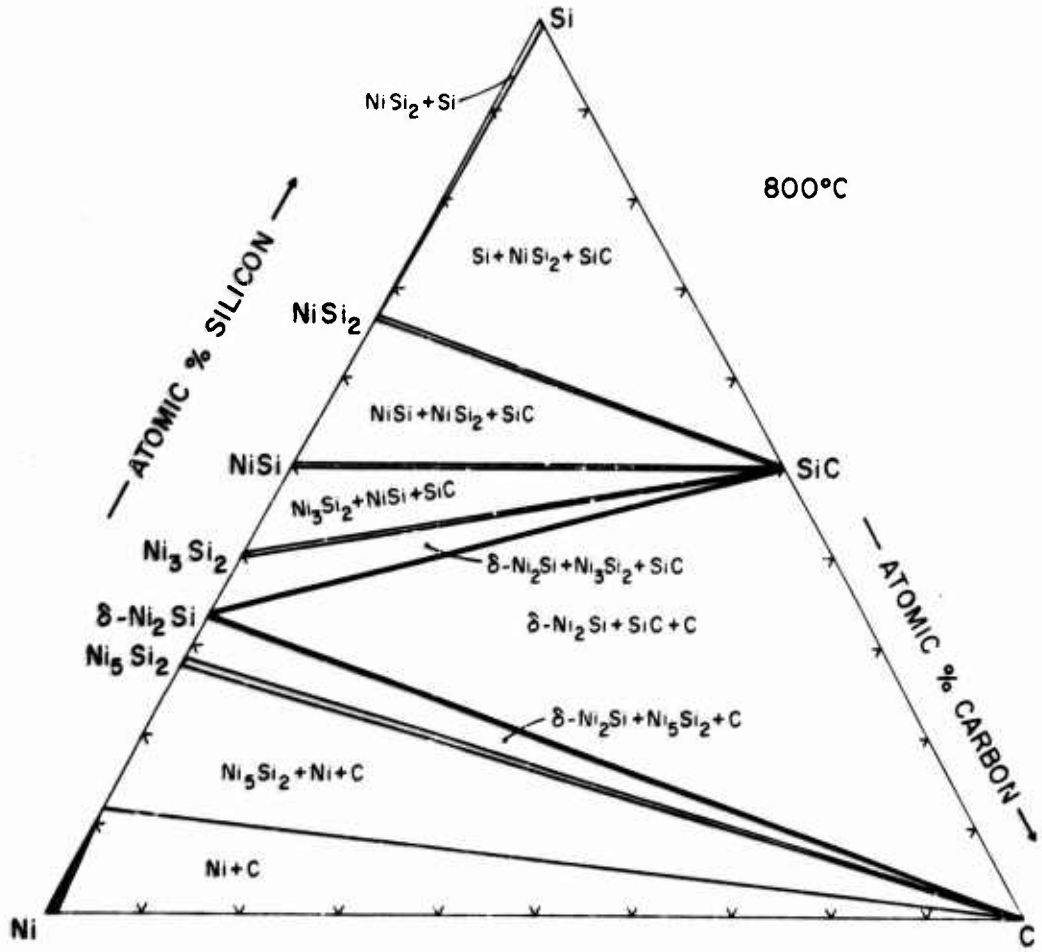

Figure 92. Ni-Si-C: Isotherm at 800°C.

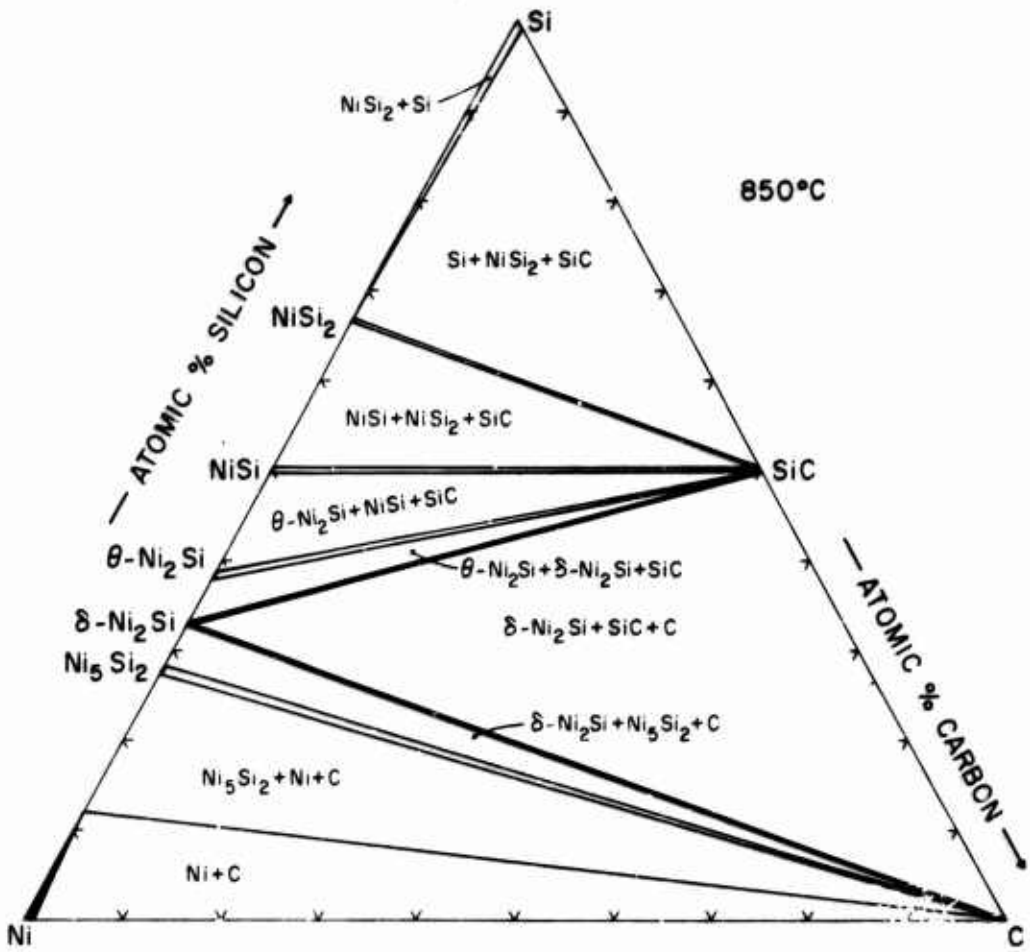

Figure 93. Ni-Si-C: Isotherm at 850°C.

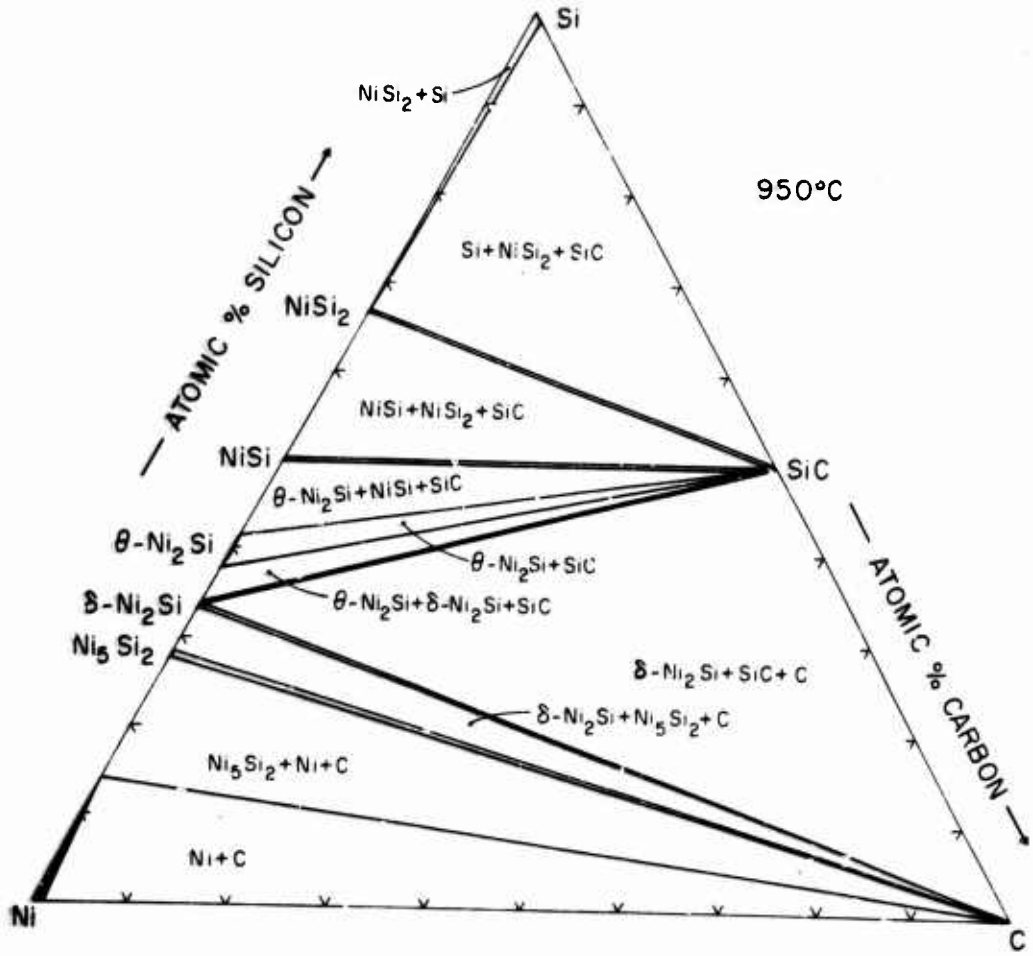

Figure 94. Ni-Si-C: Isotherm at 950°C.

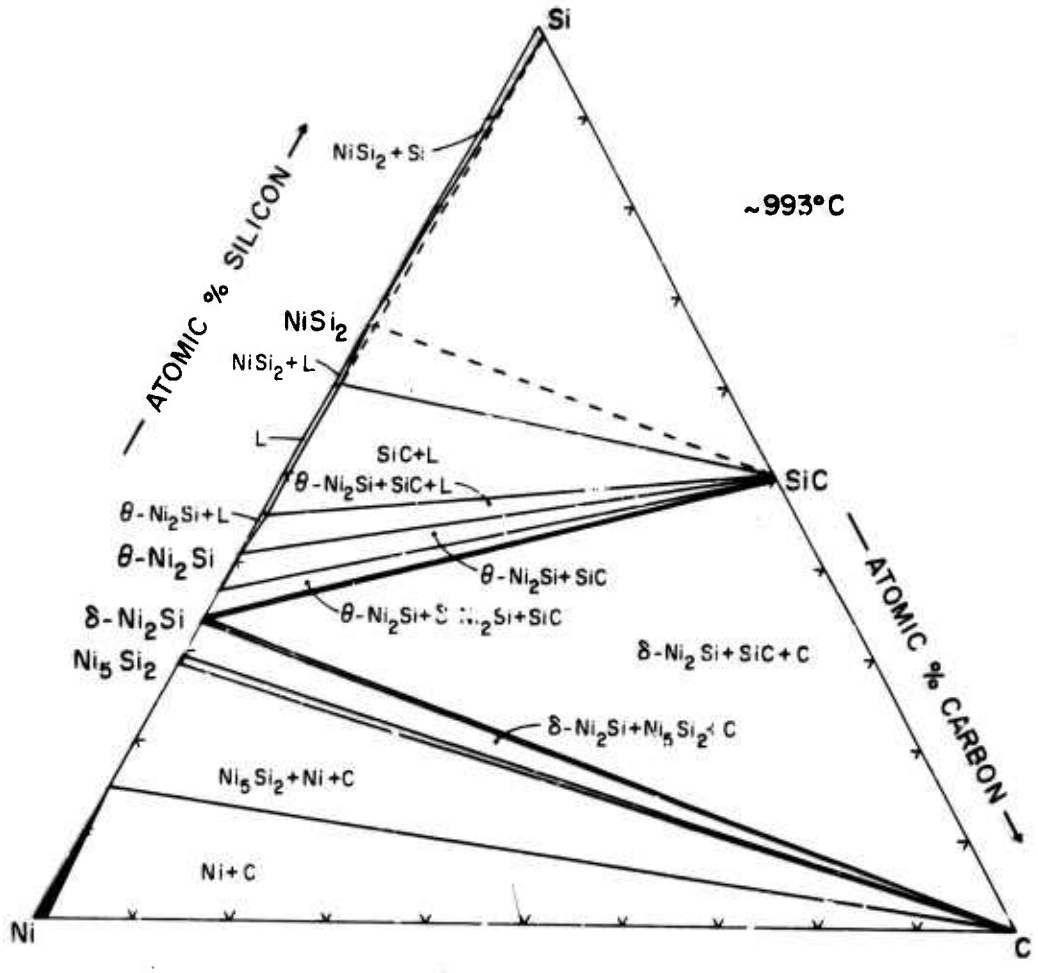

Figure 95. Ni-Si-C: Isotherm at ~993°C.

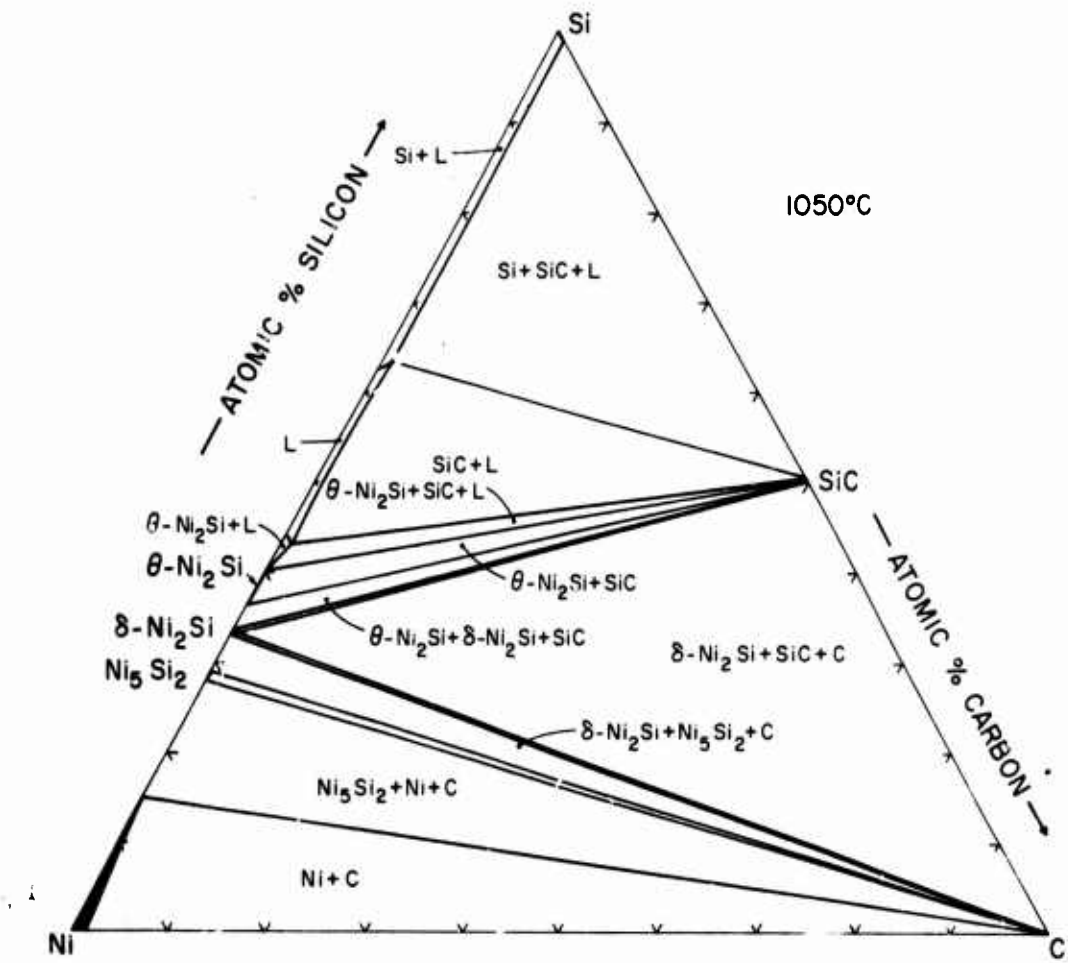

Figure 96. Ni-Si-C: Isotherm at 1050°C.

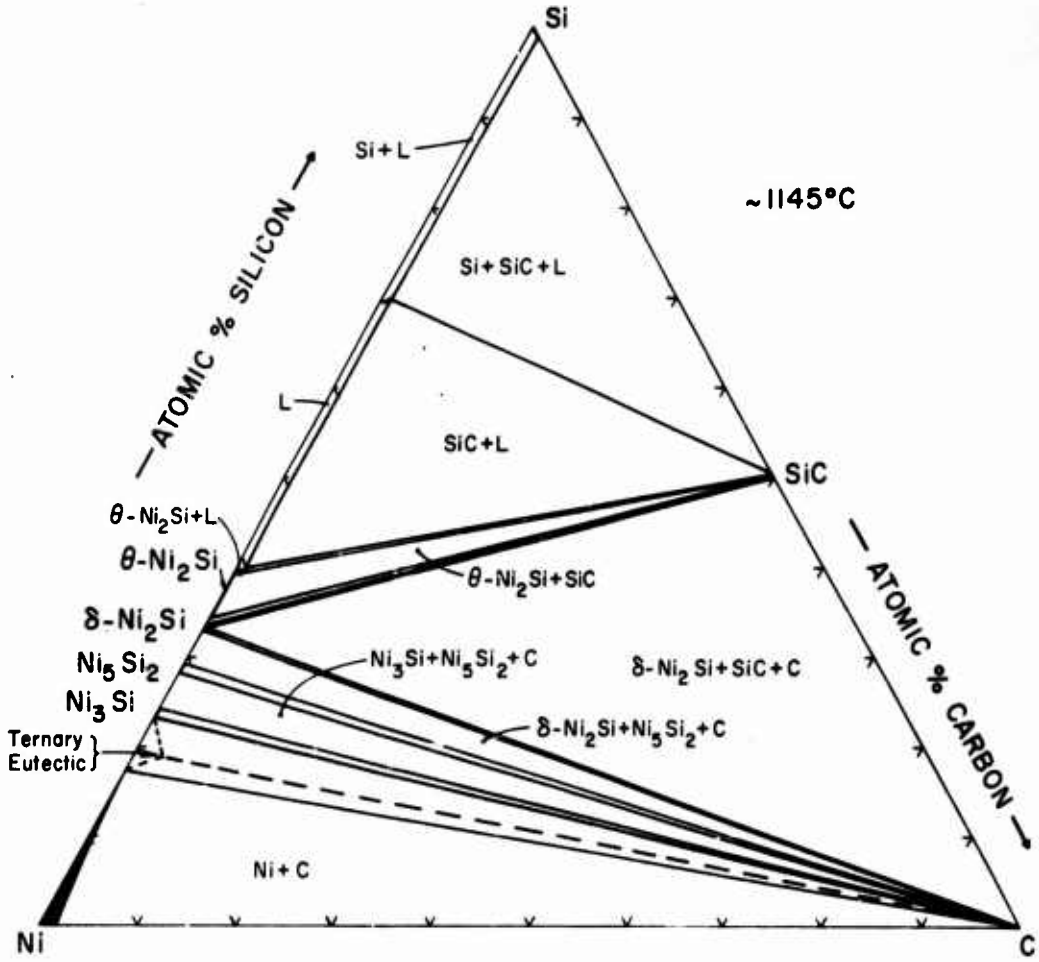

Figure 97. Ni-Si-C: Isotherm at ~1145°C.

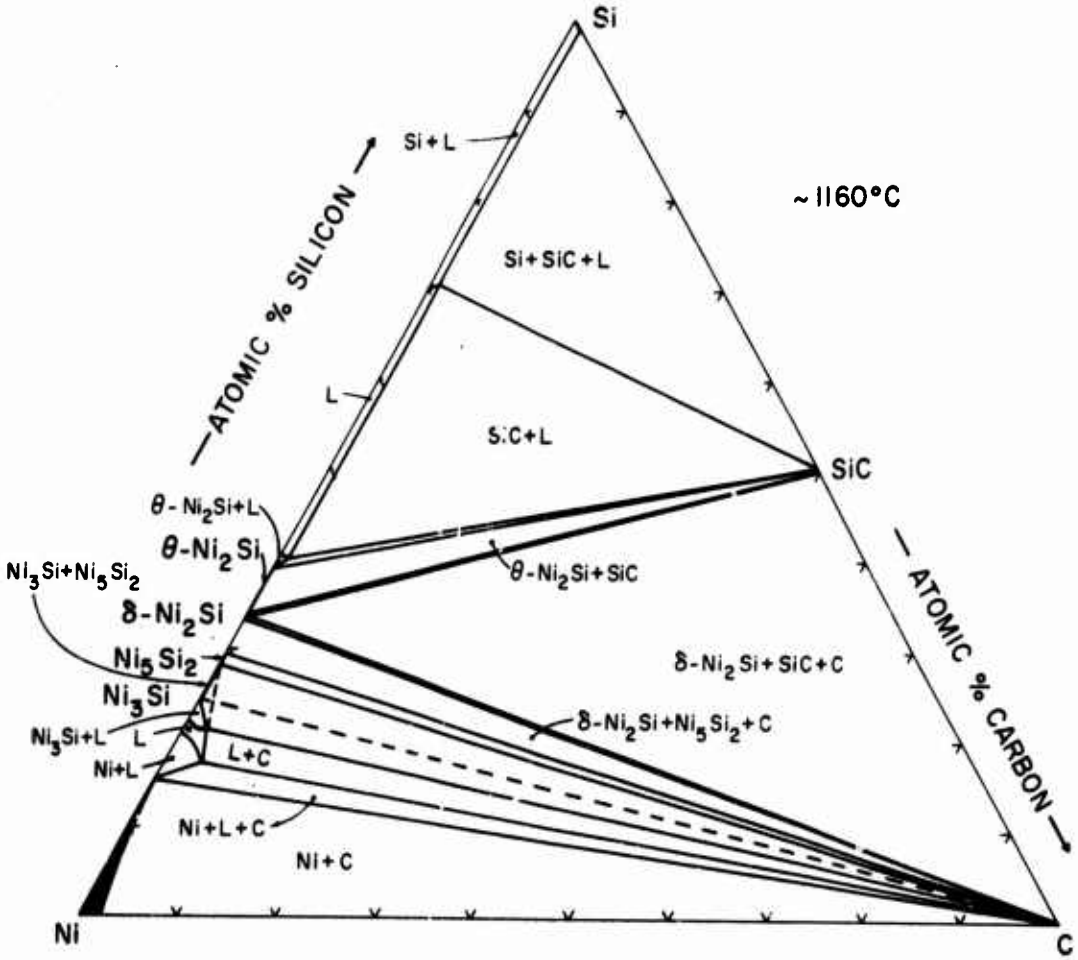

Figure 98. Ni-Si-C: Isotherm at ~1160°C.

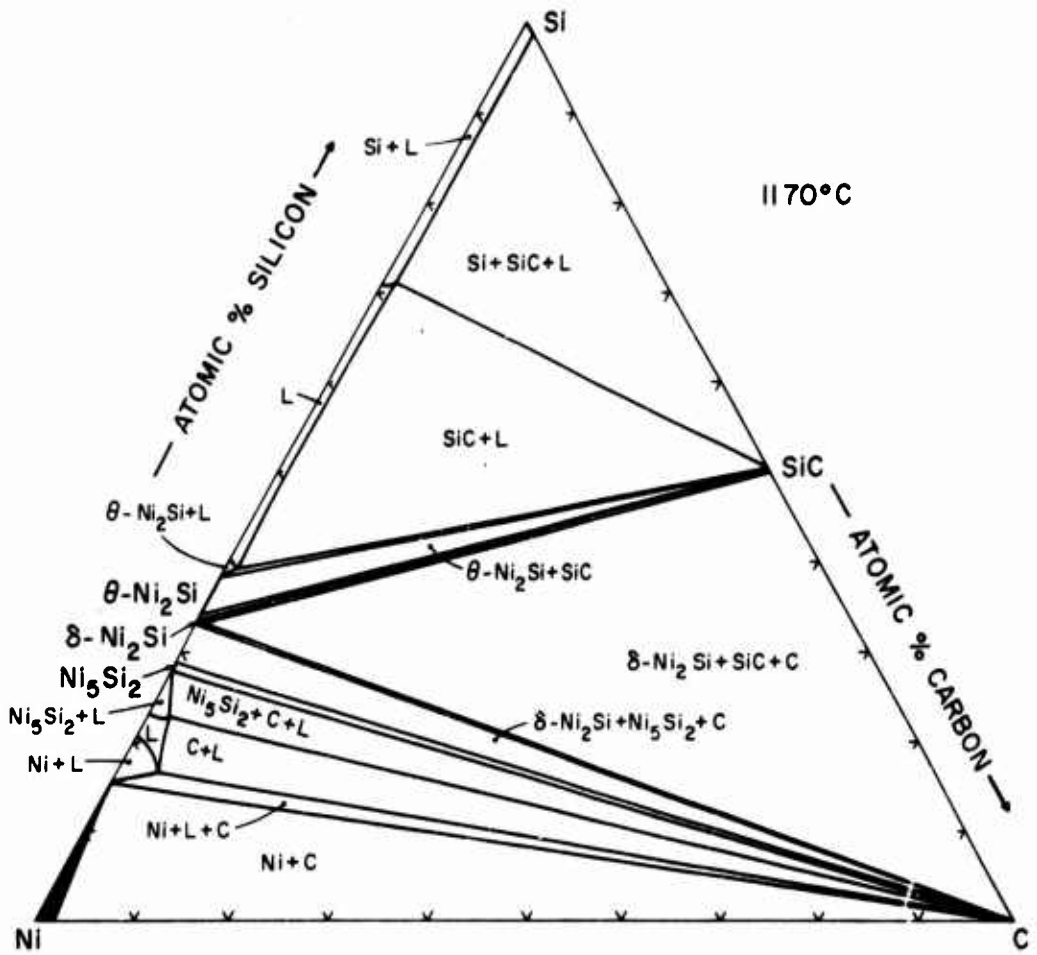

Figure 99. Ni-Si-C: Isotherm at 1170°C.

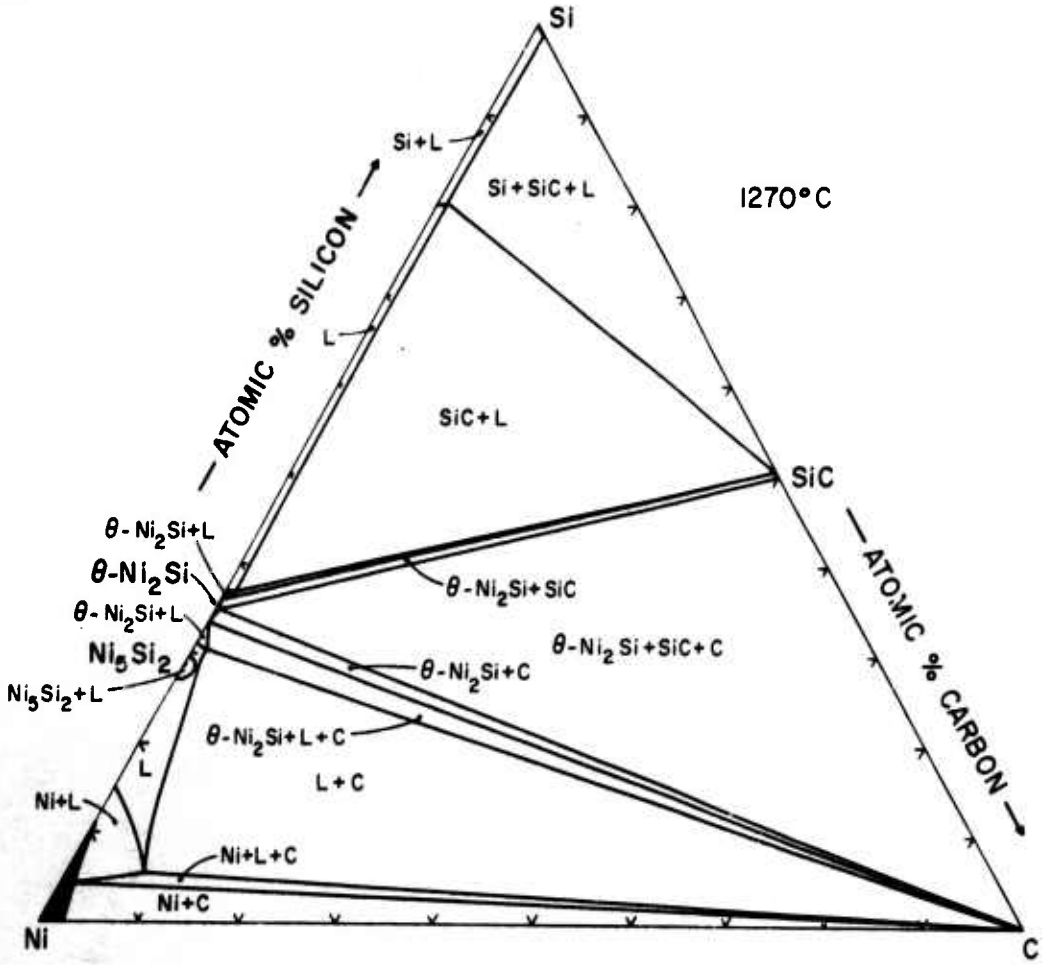

Figure 100. Ni-Si-C: Isotherm at 1270°C.

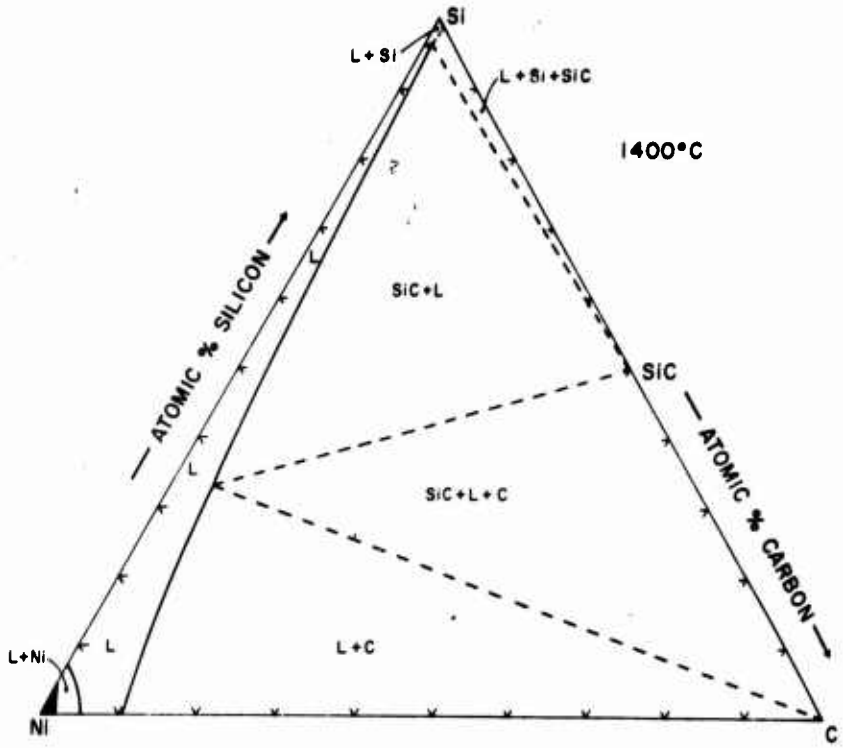

Figure 101. Ni-Si-C: Isotherm at 1400°C.

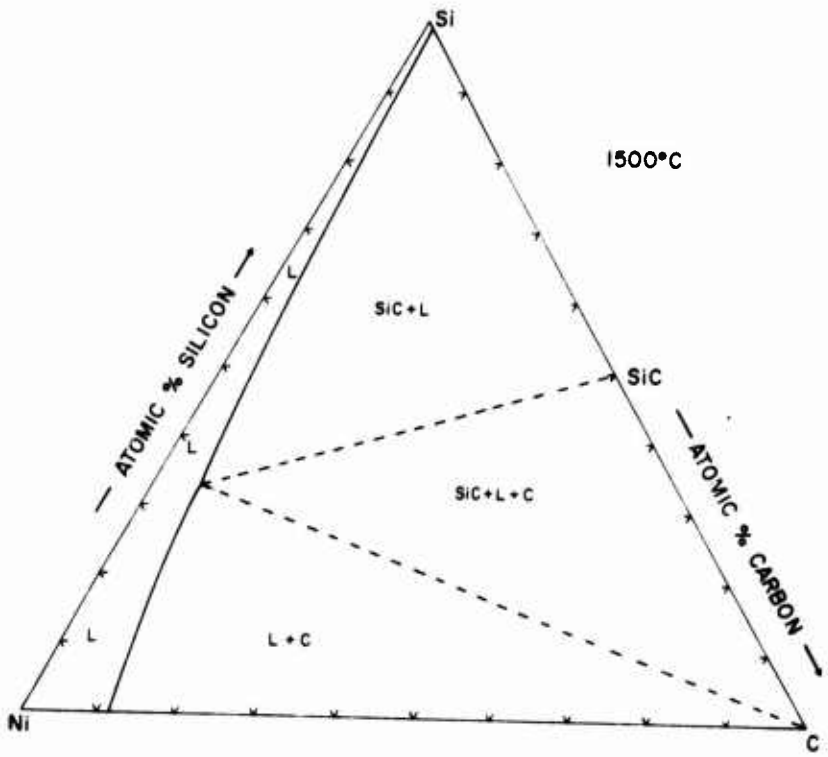

Figure 102. Ni-Si-C: Isotherm at 1500°C.

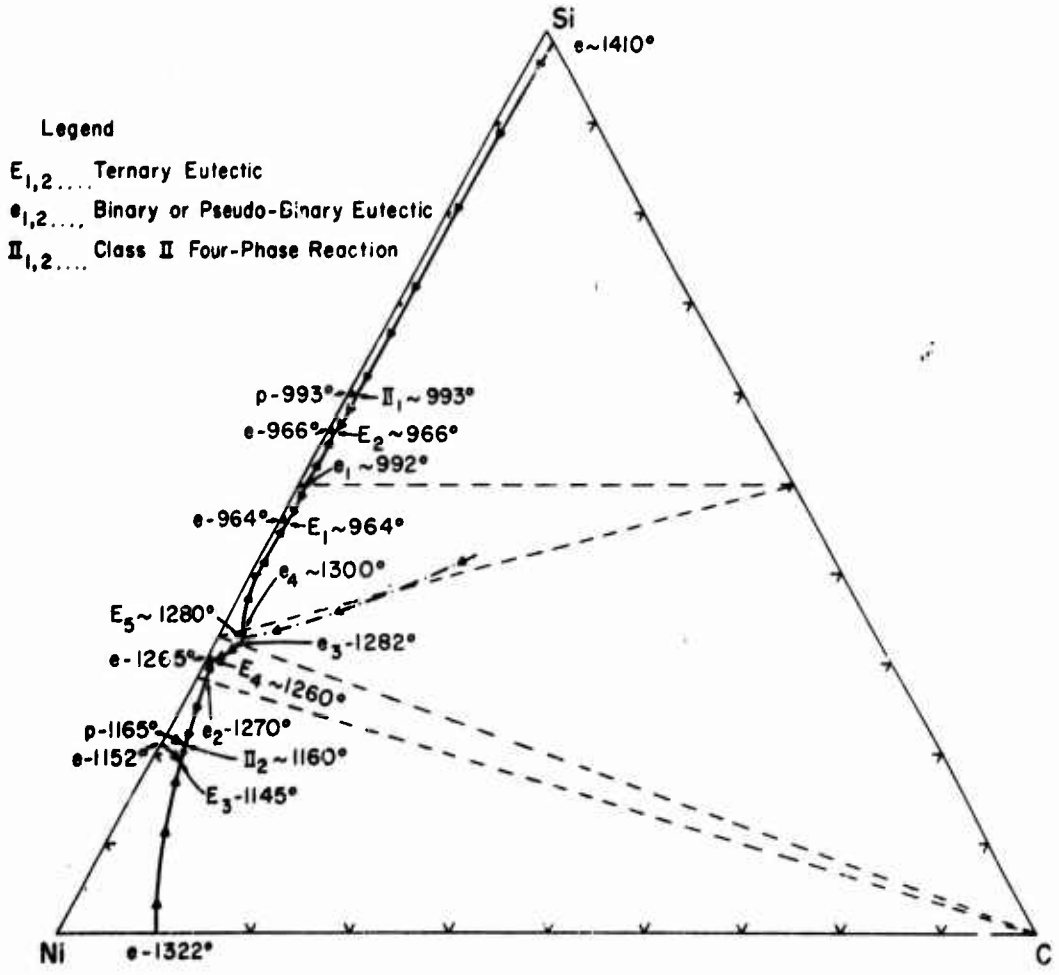

Figure 103. Ni-Si-C: Melting Trough Projections and Isothermal Reactions.

3. Qualitative Kinetic Studies on the Nickel-Silicon Carbide Interaction

Analogous to the experiments performed in the Cr-Si-C system, nickel and silicon carbide powder in a 58/42 Mole ratio were cold compacted and shielded from graphite interaction by additional SiC powder and placed in the Differential Thermal Analysis apparatus to check the interaction between nickel and silicon carbide.

The sample was heated at about 5°/sec. from room temperature; as in the combination with chromium, a strong exothermic reaction, initiating at about 1000°C, carried the temperature

rapidly upwards where melting occurred at about 1200°C as indicated by the D.T.A. trace in Figure 104.

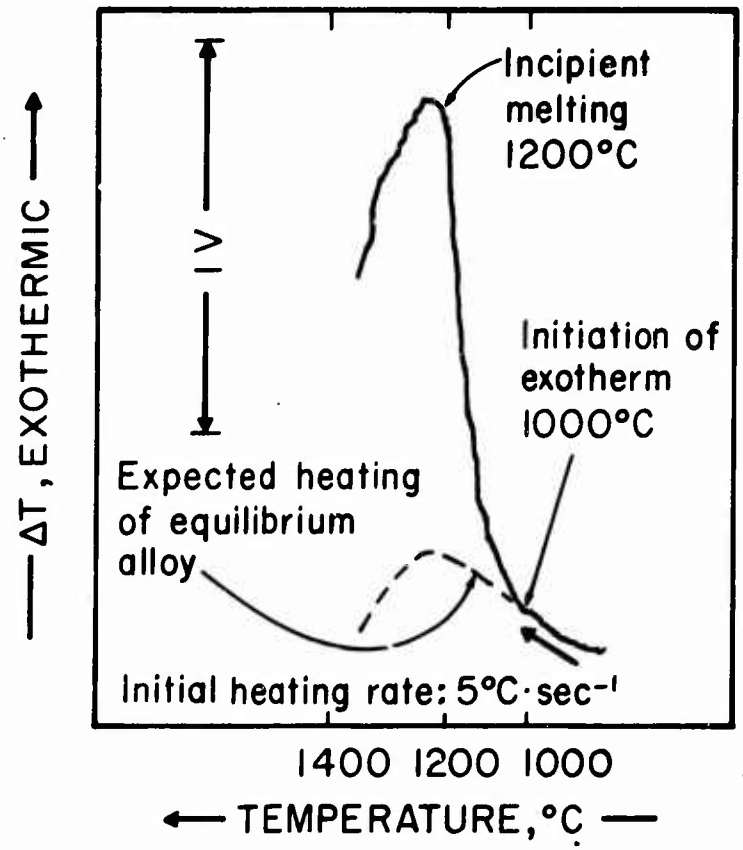

Figure 104. Ni-Si-C: D.T.A. Heating Thermogram of a Ni-SiC (58/42 Mole %) Mixture Showing an Exothermic Reaction to Correct Conjugate Pairs and Subsequent Melting.

The exothermic reaction was caused by the Ni-SiC interaction to form the correct nickel-silicide-graphite equilibria as shown by the Ni-Si-C isothermal sections. Melting occurred at the lowest melting (~1200°C) composition on the Ni-SiC join, the Ni-C eutectic trough in the nickel-rich portion of the ternary.

A second experiment with this nickel-silicon carbide mixture was performed; the mixture was heated slowly to 1100°C and held at this temperature for one hour. At no time was an exothermic reaction observed. An X-ray of this heat treated alloy showed practically complete conversion to Ni_5Si_2, Ni_{ss}, and graphite, with but traces of unreacted SiC remaining.

Again, similar to the conclusions drawn in the analogous Cr-SiC experiment, there is a strong interaction tendency between Ni and SiC, even at temperatures about 200°C below solidus on the Ni-SiC join; by the same token, it is obvious to see that by the nature of the melting troughs and phase equilibria in the Nickel-Silicon-Carbon system, no particular kinetic phenomena are present which would permit the crystallization of silicon carbide in a nickel metal matrix.

V. DISCUSSION AND RECOMMENDATIONS

The basic reasons underlying the investigation of the ternary systems Cr-Si-C and Ni-Si-C are two-fold. Silicon carbide, as a semiconductor, could have many important electronic applications, even at high temperatures, if the appropriate high temperature chemical compatibility of this compound with other materials were established. Silicon carbide, in addition, has several unique physical and mechanical properties which make it attractive as a possible fiber reinforcing candidate for the strengthening of metal matrix composite bodies. Two such metals and their alloys, chromium and nickel, have been selected to have their chemical compatibility with silicon carbide investigated. Chromium and nickel form the basis of several high temperature alloys which perform quite well in oxidizing environments by nature of the inherent oxidation resistance of these two metals. It is desirable, however, to increase the strength of these metals and their alloys by fabricating a metal-silicon carbide fiber-metal matrix composite, providing of course, that chemical compatibility between these components is present in the temperature range of interest.

The most desirable means of fabrication of such a composite body would involve the casting of the metal or metal alloy into or onto a suitably designed silicon carbide fiber or whisker matrix, or even directly casting a slurry of the silicon carbide—molten metal alloy. These investigations have shown, however, that the direct fabrication of a chromium or nickel and most certainly a chromium-nickel base alloy in contact with silicon carbide from a molten state is not possible. Even though silicon carbide in equilibrium with a chromium or nickel-rich melt containing sizeable quantities of carbon and silicon, the solidification processes which take place do not yield a predominately metal-rich product, but rather a combination of chromium silicides and carbides, or in the case of nickel, nickel silicides and graphite.

These investigations have shown that the exothermic reaction between chromium and silicon carbide as well as between nickel and silicon carbide occurs at about 1330° and 1000°C respectively. This reaction is a function of particle size and intimate union of the mixtures, of course, but it may well be possible to employ powder metallurgical fabrication techniques at lower temperatures where the kinetics of the metal-silicon carbide interactions are less favorable; although it must be said that the low temperatures which would be employed do not favor the densification of the metal matrix. It is recommended, then, that the low ($< \sim 900$°C for Cr-Si-C and $< \sim 800$°C for Ni-SiC) temperature diffusion and reaction kinetics of the chromium-silicon carbide and nickel-silicon carbide combinations be studied in some detail to determine not only the feasible upper limit of application of such composite bodies, but also to ascertain whether or not powder metallurgical techniques are possible as fabrication methods for such composite bodies.

It is further recommended that detailed investigations be conducted with the promising concept of coating silicon carbide fibers with refractory carbides of the 4a group metals and using the coated silicon carbide in melts of chromium and/or nickel to achieve the desired fiber strengthening of the nickel-chromium base alloys by direct casting. It is known that the monocarbides of the 4a group metals, TiC, ZrC, and HfC are in equilibrium with silicon carbide at high temperatures; it is further established[68] that chromium and most probably nickel are in chemical and thermodynamic equilibrium with the carbides of the 4a group metals. Therefore, these carbides, which are in equilibrium with both SiC and chromium, and probably nickel, present themselves as interesting diffusion–interaction barriers between chromium/nickel and silicon carbide.

REFERENCES

1. M. Hansen: Constitution of Binary Alloys, McGraw-Hill, New York 1958, p. 1039.

2. K. Iwase and M. Okamoto: "Science Repts Tohoku Imp. Univ., K. Honda Anniv. Vol." (1936) 777.

3. A. Osawa and M. Okamoto: "Science Repts Tohoku Imp. Univ. 27 (1939) 326.

4. K. Ruttewit and G. Masing: Zeitschrift f. Metallknde 3 (March 1940) 52.

5. K. Schubert and H. Pfisterer: Zeitschrift f. Metallknde 41 (1950) 433.

6. H. Pfisterer and K. Schubert: Naturwiss. 5 (1950) 112.

7. K. Toman: Acta Cryst. 4 (1951) 462.

8. G. Pilstrom: Acta Chemica Scand. 15 (1961) 893.

9. K. Toman: Acta Cryst. 5 (1952) 329.

10. A. Wittmann, K. Burger, and H. Nowotny: Mh. Chem. 92 (1961) 961.

11. B. Boren: Ackiv, Kemi, min., geol: 11A No. 11 (1933) 22.

12. W. Guertter, Handbuch der Metallographie, Vol. I, part 2, p. 676, Verlagsbuchhandlung Gebrueder Borntraeger, Berlin, 1917.

13. O. Dahl and N. Schwartz: Metallwirtschaft, 11 (1932) 277.

14. O. Dahl: Z. Metallknde, 24 (1932) 277.

15. V. Marian: Ann. Phys. 7 (1937) 459.

16. M. Okamoto: Nippon Kinzoku Gakkai-Shi 2 (1938) 544.

17. N. F. Lashko: Doklady Akad. Nauk. SSSR. 81 (1951) 605.

18. G. Saini, I. Calvert, and J. Taylor: Canad. J. Chem. 42 (1964) 1511.

19. W. Klement: Canad. J. Phys. 40 (1962) 1397.

20. A. Westgren, G. Phragmen, and T. Negresco: J. Iron Steel Inst. 117 (1928) 386.

REFERENCES (cont'd)

21. E. Friemann and F. Saurwald: Z. anorg. Chem. 203 (1931) 64.

22. K. Hatsuta: Kinzoku-no-Kenkyu 8 (1931) 81.

23. D. Bloom and N. Grant: Trans. AIME 188 (1950) 41.

24. A. Westgren: Jernkontorets Ann. 117 (1933) 501.

25. V. Arkharov, I. Kvater, and S. T. Kiselev: Isvest. Akad. Nauk, SSSR. (Tekh.) (1947) 749.

26. A. G. Allten, J. Chow, and A. Simon: Trans. ASM 46 (1954) 948.

27. A. Westgren and G. Phragmen: Svensk Vetenskaps Akad. Handl. 2 (1925) No. 5.

28. A. Westgren: Jernkontorets Ann. 119 (1935) 231.

29. K. Hellbom and A. Westgren: Svensk. Kem. Tidskr. 45 (1933) 141.

30. H. Moissan: Compt. rend. 119 (1894) 185.

31. T. Murakami: Science Repts. Tohoku Univ. 7 (1918) 263.

32. E. Rudy: Unpublished Work: To be published in a compendium appearing under Air Force Contract No. AF33(615)-1249 (March 1968).

33. W. Hempel: Z. angew, Chem. 17 (1904) 300.

34. E. Heyn: Stahl und Eisen 26 (1906) 1390.

35. N. Kurnakow and S. F. Zemczuzmy: Z. anorg. Chem. 54 (1907) 151.

36. K. Friederich and A. Leroux: Metallurgie 7 (1910) 10.

37. O. Ruff and W. Bormann: Z. anorg. Chem. 88 (1914) 386.

38. T. Kase: Science Repts. Tohoku Univ. 14 (1925) 187.

REFERENCES (Cont'd)

39. H. Morrogh and W. J. Williams: J. Iron Steel Inst. 155 (1947) 341.

40. O. Ruff and W. Martin: Metallurgie 9 (1912) 143.

41. O. Ruff and E. Gersten: Z. anorg. Chem. 88 (1914) 393.

42. ibid cit. ref. 1 pg. 374.

43. E. Briner and R. Senglet: J. chem. phys. 13 (1915) 351.

44. G. Meyer and F. Scheffer: J. Am. Chem. Soc. 75 (1953) 486.

45. S. Oketani et al: Met. Abstr. 23 (1956) 444.

46. L. Hofer, E. Cohn, and W. Peebles: J. Phys. and Colloid Chem. 54 (1950) 1161.

47. B. Jacobson and A. Westgren: Z. physik. Chem. B20 (1933) 361.

48. R. Bernier: Ann. Chem. (Paris) 6 (1951) 104.

49. T. Mishima: "World Eng. Congr. Tokyo, Paper 716 (1929).

50. J. Lander, H. Kern, and A. Beach: J. Appl. Phys. 23 (1952) 1305.

51. S. Nagakura: J. Phys. Soc. Japan 12 (1957) 482.

52. R. A. Sidorenko: Fiz. Metal, i Metalloved., 8 (1959) 595.

53. ibid. cit. ref. 1 pg. 378.

54. N. Thibault: Amer. Min. 29 (1944) 249 and 327.

55. H. Nowotny, E. Parthe, R. Kieffer, and F. Benesovsky: Mh. Chem. 85 (1954) 255.

56. O. Ruff: Trans. Electrochem. Soc. 68 (1935) 87.

57. R. Scarce and G. Slack: J. Chem. Phys. 30 (1959) 1551.

REFERENCES (Cont'd)

58. R. Dolloff: WADD-TR-60-143, Part I (1960).

59. E. Gugel, P. Ettmayer, and A. Schmidt: Ber. Dtsch. Keram. Ges. 45 (1968) 359.

60. I. S. Brokhin and V. F. Funke: Hard Metals Production Technology and Research in the USSR (1964) 212 Pergamon Press, Oxford.

61. W. Knippenberg: Phillips Res. Rept. 18 (1963) 161.

62. E. Parthe, H. Schachner, and H. Nowotny: Mh. Chem. 86 (1955) 182.

63. L. B. Griffiths and A. I. Mlavsky: J. Electrochem. Soc. III (1964) 805.

64. E. Rudy and G. Progulski: Technical Report AFML-TR-65-2, Part III, Vol. II.

65. E. Rudy, St. Windisch, and Y. A. Chang: Technical Report AFML-TR-65-2, Part I, Vol. I.

66. H. D. Heetderks, E. Rudy, and T. Eckert: Technical Report AFML-TR-65-2, Part III, Vol. I.

67. A. Forsyth and R. McDowdell, Trans. AIME, 137 (1940) 373.

68. Unpublished Results from the Aerojet-General's Material Research Laboratory (1965-1968).

Metal Matrix Composites - Distribution List - Located at Wright-Patterson AFB, Ohio

REPORT NUMBER: AFML-TR-68-63 Volume II

TITLE: Phase Compatibility Studies on Nickel-Chromium-Silicon-Carbon Base Alloys Volume II: The Chromium-Silicon-Carbon and Nickel-Silicon-Carbon Systems

AFML (MAM) - 2 cys
Wright-Patterson AFB, Ohio 45433

AFML (MAMS/Branch Office) - 25 cys
Wright-Patterson AFB, Ohio 45433

AFML (MAMP/Mr. I. Perlmutter)
Wright-Patterson AFB, Ohio 45433

AFML (MAMD)
Wright-Patterson AFB, Ohio 45433

AFML (MAMC)
Wright-Patterson AFB, Ohio 45433

AFML (MAYE, Dr. Tanner) - 2 cys
Wright-Patterson AFB, Ohio 45433

AFML (MAAM, Library)
Wright-Patterson AFB, Ohio 45433

AFML (MAN) - 6 cys
Wright-Patterson AFB, Ohio 45433

AFML (MAC)
Wright-Patterson AFB, Ohio 45433

AFML (MAT)
Wright-Patterson AFB, Ohio 45433

AFML (MANN)
Wright-Patterson AFB, Ohio 45433

AFFDL (FDT)
Wright-Patterson AFB, Ohio 45433

ASD (ASEP)
Wright-Patterson AFB, Ohio 45433

SEG (SEPI)
Wright-Patterson AFB, Ohio 45433

SEG (SEPS)
Wright-Patterson AFB, Ohio 45433

AFAPL (APT)
Wright-Patterson AFB, Ohio 45433

AFAPL (API) - 3 cys
Wright-Patterson AFB, Ohio 45433

AFAPL (APFT)
Wright-Patterson AFB, Ohio 45433

AFAL (AVTM)
Wright-Patterson AFB, Ohio 45433

AFML (MAY)
Wright-Patterson AFB, Ohio 45433

DDC (TISIA) - 20 cys
Bldg 5
3010 Duke Street
Alexandria, Virginia 22314

Air University Library
Maxwell AFB, Alabama 36112

Hq USAF (AFXSAI)
Air Battle Analysis Center
Deputy Director of Plans for War Plans
Directorate of Plans, DCS/P&O
Washington, D. C. 20330

Chief of Naval Material
Navy Department
Washington, D. C. 20360

Security Classification

DOCUMENT CONTPOL DATA - R & D

(Security classification of title, body of abstract and indexing annotation must be entered when the overall report is classified)

1. ORIGINATING ACTIVITY *(Corporate author)*
Materials Research Laboratory
Aerojet-General Corporation
Sacramento, California

2a. REPORT SECURITY CLASSIFICATION
Unclassified

2b. GROUP
N/A

3. REPORT TITLE
Phase Compatibility Studies on Nickel-Chromium-Silicon-Carbon Base Alloys Volume II. The Chromium-Silicon-Carbon and Nickel-Silicon Carbon System

4. DESCRIPTIVE NOTES *(Type of report and inclusive dates)*

5. AUTHOR(S) *(First name, middle initial, last name)*
Charles E. Brukl

6. REPORT DATE
January 1969

7a. TOTAL NO. OF PAGES
134

7b. NO. OF REFS
68

8a. CONTRACT OR GRANT NO.
AF 33(615)-67-C-1286

b. PROJECT NO.
7353

c.
735306

d.

9a. ORIGINATOR'S REPORT NUMBER(S)
AFML-TR-68-63, Vol. II

9b. OTHER REPORT NO(S) *(Any other numbers that may be assigned this report)*
N/A

10. DISTRIBUTION STATEMENT This document is subject to special export controls, and each transmittal to foreign nationals may be made only with prior approval of the Metals and Ceramics Division (MAMS), Air Force Materials Laboratory, Wright-Patterson AFB, Ohio 45433.

11. SUPPLEMENTARY NOTES

12. SPONSORING MILITARY ACTIVITY
AFML (MAMC)
Wright-Patterson AFB, Ohio 45433

13. ABSTRACT

The high temperature phase equilibria of the Cr-Si-C and Ni-Si-C ternary systems have been investigated by means of melting point, differential thermal analytical, X-ray, and metallographic techniques. Cursory investigations were also made in the Ni-Si and Ni-C binary systems.

In the Cr-Si-C system, a ternary D8$_8$-type phase, which forms two-phase equilibria with most of the other respective binary phases is present. The high temperature phase equilibria include eleven, four-phase reactions of which seven are ternary eutectics. Seven pseudo-binary eutectics also occur.

The Ni-Si-C system has simple solid-state equilibria governed by the occurring binary phases. The high temperature phase equilibria of this system include seven four-phase reactions of which five are ternary eutectics and four pseudo-binary eutectics.

Isothermal sections into the melting range as well as three-dimensional space models are presented for both ternary systems.

This document is subject to special export controls, and each transmittal to foreign governments or foreign nationals may be made only with prior approval of the Metals and Ceramics Division (MAMS), Air Force Materials Laboratory, Wright-Patterson AFB, Ohio 45433. The distribution of this report is limited because the protection of technology relating to critical materials is restricted by the Export Control Act.

DD FORM 1 NOV 65 1473

Unclassified
Security Classification

14. KEY WORDS	LINK A		LINK B		LINK C	
	ROLE	WT	ROLE	WT	ROLE	WT
Ternary Phase Equilibria						
Chromium-Silicon-Carbon Alloys						
Nickel-Silicon-Carbon Alloys						
Nickel-Silicon Alloys						
Nickel-Carbon Alloys						